87

SYNTHESIS, CHARACTERISATION AND CHEMISTRY OF *N*-ALKYL- AND *N,N*-DIALKYL-*N'*-ACYLTHIOUREA PLATINUM(II) AND PALLADIUM(II) COMPLEXES

A thesis submitted to the

UNIVERSITY OF CAPE TOWN

in fulfilment of the requirements for the degree of

MASTER OF SCIENCE

by

YALI WANG

B.Sc.

(Taiyuan University of Technology, People's Republic of China)

Department of Chemistry

University of Cape Town

Rondebosch 7701

South Africa

March 1997

ACKNOWLEDGEMENTS

I would sincerely like to thank:

My supervisor, Professor Klaus R. Koch, for his constant enthusiasm and motivation

Professor Roger Hunter for the valuable comments

Dr. Krassi Dimitrikova for her assistance with the NMR spectra

Dr. Anita Coetzee for determining the crystal structure addressed in this work

Mr. Chungpu Wu for sketching the apparatus

Mrs. Elizabeth Wilson for her constant support

Mr. William Hendriks for his friendly assistance in the laboratory

To all the staff and students of Chemistry Department, especially to Mr. Jörn Miller, Mr. Darren Handforth, Ms. Claire Lawrence and Ms. Yushan Wu who have spent a lot of time to proof reading this thesis.

The University of Cape Town for financial assistance.

I also wish to thank my husband, Xiaolong Yin, for his fruitful discussions and valuable comments; and my daughter, Wenjing Yin, for her understanding and support.

ABSTRACT

N-(*n*-butyl)-*N*-methyl-*N'*-benzoylthiourea and *N*-(*n*-butyl)-*N*-methyl-*N'*-naphthoyl-thiourea (HL) have been synthesised and characterised. These ligands react with K_2PtCl_4 to yield neutral square planar *cis*- [Pt(L-*O*,*S*)$_2$] complexes. These complexes exist as mixture of *EE*, *EZ* and *ZZ* isomers.

Reaction of *N*-(*n*-propyl)-*N'*-benzoylthiourea (H_2L^1) with K_2MX_4 (M = Pt, Pd; X = Cl, Br, I) gives a series of complexes [M(H_2L^1-*S*)$_2X_2$]. The tendency to form *trans*-isomers increases when M is substituted from Pt to Pd, and X is varied from Cl to I. The results reveal that an unrecrystallised complex [Pt(H_2L^1)$_2Cl_2$] is mainly *cis*-isomer, but isomerises into a *cis-trans* mixture to reach equilibrium in solution. The equilibrium constants for the *cis*- ⇔ *trans*- mixture was measured in six solvents, being the smallest in polar nitromethane and the largest in nonpolar benzene. Particularly, the rate of isomerisation of *cis*- to *trans*- isomer of this complex has been studied in detail in chloroform-d_3 by ^{1}H NMR spectroscopy. It was found that the isomerisation reaction is second order relative to the concentration of *cis*-[Pt(H_2L^1)$_2Cl_2$] complex. The results of these kinetic studies show that the *cis*- ⇔ *trans*- isomerisation is an autocatalysed reaction. There are two postulated mechanisms in which two molecules of *cis*-[Pt(H_2L^1)$_2Cl_2$] are in collision forming a chloro-bridged dimer, in which either the ligand or the chloride is lost. The unbound ligand H_2L or Cl^- catalyse the isomerisation process. A study of thermodynamics of the isomerisation has been undertaken in three solvents, i.e. DMF, chloroform and benzene. From the enthalpy and entropy values, it is clear that the *cis*- isomer is enthalpy favoured, and the change of entropy favours *trans*- isomer form.

Some novel metallomesogens [Pt(H_2L')$_2I_2$] (H_2L' = modified *N*-acylthioureas) have been synthesised, characterised and investigated. These mesogenic phases have been identified to be smectic phases, with the aid of polarising optical microscopy and confirmed by differential scanning calorimetry studies.

The determination of crystal structure of $[Pd(H_2L^1)_2Br_2]$ indicates that *two* intramolecular hydrogen bonds make this molecular forming a rod-like square-planar structure.

CONTENTS

CHAPTER 1

Introduction

INTRODUCTION

N,N-dialkyl-*N'*-acylthioureas and *N*-alkyl-*N'*-acylthioureas as ligands for the platinum group metals have recently attracted much attention. Although these molecules were first prepared by Neucki in 1873[1], some aspects of their coordination chemistry towards first-row transition metals have been investigated only recent years by the group of Beyer and Hoyer[2]. *N,N*-dialkyl-*N'*-acylthioureas have been studied as selective agents for platinum group metals[3-4], as well as for the trace enrichment and chromatographic separation of these metals[5]. These compounds are potential *O* and *S* donor bidentate ligands, that can coordinate metal ions with the loss of a proton from the acyl-substituted nitrogens. X-ray crystal studies have revealed that *N*-benzoylthioureas form *bis*, square-planar complexes of *cis*- configuration[6-11]. However, depending on the nature of the substituent groups, *N*-acylthioureas may also act as unidentate *S* donor atom ligands. The determination of the crystal structure[12] of bis(*N*-(*n*-propyl)-*N'*-benzoylthiourea)dichloroplatinum(II) indicates that *N*-(*n*-propyl)-*N'*-benzoylthiourea acts with Pt(II) as a unidentate ligand forming a strong *S*-bonded complex. Thus, *N,N*-dialkyl-*N'*-acylthioureas and *N*-alkyl-*N'*-acylthioureas can display different coordination chemistry to metals. Furthermore, the potential liquid-crystalline properties of *N*-alkyl-*N'*-acylthioureas have also been studied[13].

Therefore, we have become interested in the study of these *N*-acylthioureas. The easy synthesis of the *N*-alkyl(dialkyl)-*N'*-acylthioureas and their complexes, *especially* platinum complex (Figure 1.1), and the stability of the complexes formed prompted us to further study their coordination chemistry and to investigate their potential applications as new materials. South Africa contributes to more than half of the Platinum production in the world, so that studying the coordination chemistry of platinum and palladium complexes of *N*-acylthiourea could be of industrial value.

Figure 1.1 Schematic representation of the platinum complexes of *N*-alkyl-*N*'-acylthioureas (a) and *N,N*-dialkyl-*N*'-acylthioureas (b).

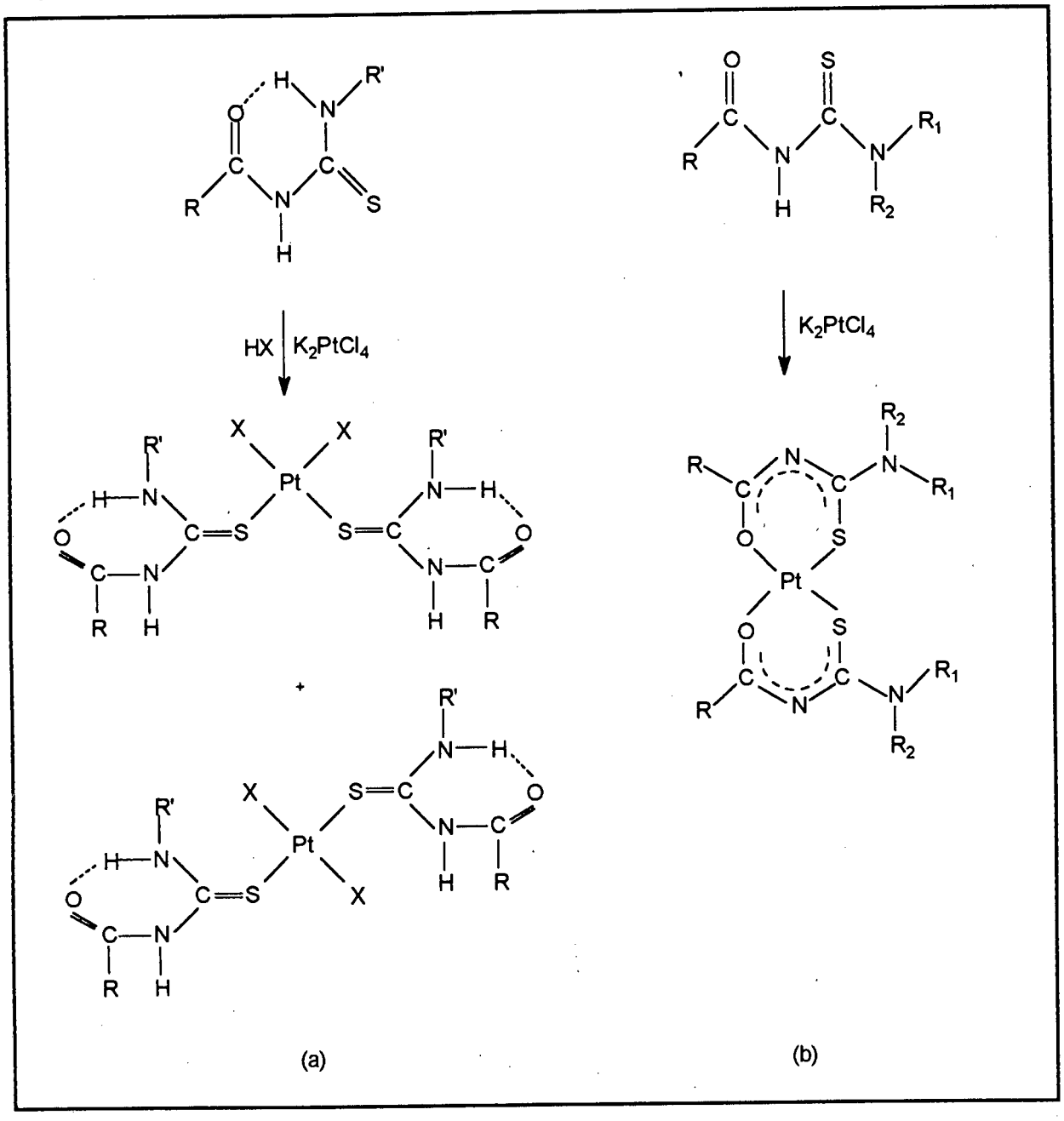

Accordingly, the isomerism of platinum complexes of *N,N*-dialkyl-*N*'-acylthioureas has been studied and is described in Chapter 2. The synthesis of $[Pt(H_2L)_2X_2]$ has been examined with a view to understanding the distribution of *cis/trans* isomers. The rate of isomerisation of bis(*N*-(*n*-propyl)-*N*'-benzoylthiourea)dichloroplatinum(II) has been studied in detail, and the kinetics and mechanism of the isomerisation have been investigated in Chapter 3. A series of new platinum and palladium containing metallomesogens involving *N*-alkyl-*N*'-acylthiourea ligands have been synthesised and

characterised as described in Chapter 4. The determination of crystal structure of bis(*N*-(*n*-propyl)-*N'*-benzoylthiourea)dibromopalladium(II) is described in Chapter 5.

References

1. K. Neucki, *Ber. Dtsch. Chem. Ges.*, 1873, **6**, 598.
2. L. Beyer, E. Hoyer, J. Liebscher and H. Hartmann, *Z. Chem.*, 1981, **21**, 81.
3. K.-H. König, M. Schuster, G. Schneeweiss and B. Steinbrech, *Fresenius'Z. Anal. Chem.*, 1985, **325**, 621.
4. P. vest, M. Schuster and K.-H. König, *Fresenius'Z. Anal. Chem.*, 1989, **335**, 759.
5. M. Schuster, *Fresenius'Z. Anal. Chem.*, 1992, **342**, 791.
6. R. Richter, L. Beyer and J. Kaiser, *Z. Anorg. Allg. Chem.*, 1980, **461**, 67.
7. P. Knuuttilla, H. Knuuttilla, H. Hennig, and L. Beyer, *Acta Chem. Scnd., Ser.A*, 1982, **36**, 541.
8. A. Irving, K. R. Koch and M. Matoetoe, *Inorg. Chem. Acta*, 1993, **206**, 193.
9. G. Fitzl, L. beyer, J. Sieler, R. Richter, J. Kaiser and E. Hoyer, *Z. Anorg. Allg. Chem.*, 1977, **433**, 237.
10. J. Sieler, R. Richter, E. Hoyer, L. Beyer, O. Lindqvist and L. Andersen, *Z. Anorg. Allg. Chem.*, 1990, **580**, 167.
11. W. Bensch and M. Schuster, *Z. Anorg. Allg. Chem.*, 1992, **615**, 93.
12. K. R. Koch and S. Bourne, *J. Chem. Soc. Dalton Trans.*, 1993, 2071.
13. T. Grimmbacher, *Ph.D thesis*, University of Cape Town, 1995.

CHAPTER 2

Synthesis, Characterisation And Isomerism Of Bis(*N*-(*n*-butyl)-*N*-methyl-*N*'-acylthioureato)platinum(II) Complexes

2.1 Introduction

N,N-dialkyl-*N'*-benzoylthioureas (HL) have recently attracted interest because of their potential use as highly selective reagent for the liquid-liquid extraction[1-2], preconcentration and separation[3] of the platinum group metals. The relative ease of synthesis of their metal complexes, and the high stability of the products, potentially gives rise to many investigations.

Irving and Koch[4] have reported that *N,N*-dibutyl-*N'*-benzoylthiourea coordinates to platinum(II) forming a square planar *cis*-bis(*N,N*-dibutyl-*N'*-benzoylthioureato)-platinum(II) complex [Pt(L-*S,O*)$_2$]. They have also found that both the acylthiourea ligand and the complex display restricted rotation about the thioamide C-N bond, this being a partial double bond. This property has also been found by Beyer's group in similar compounds[5]. Hence we were interested to see whether this *E,Z* isomerism is carried through in the coordination chemistry of unsymmetricllly substituted *N,N*-dialkyl-*N'*-acylthioureas as ligands. Considering the unsymmetrical and C-N partial double-bond character of this type of ligands, additional configurational *E/Z* isomerism is possible in both the ligands and the resultant complexes. This means that the complexes could have *E,E* and *E,Z* and *Z,Z* configurations. Thus, in this chapter, *N-(n*-butyl)-*N*-methyl-*N'*-benzoylthiourea and *N-(n*-butyl)-*N*-methyl-*N'*-naphthoyl-thiourea and their platinum (II) complexes are synthesised and studied.

2.2 Results and discussion

2.2.1 Preparation and characterisation of ligands (*1* - *2*)

The ligand *N-(n*-butyl)-*N*-methyl-*N'*-benzoylthiourea *1* and ligand *N-(n*-butyl)-*N*-methyl-*N'*-naphthoylthiourea *2* have been prepared according to the method reported by Douglass and Dains[6], as shown in Figure 2.1, and characterised by C, H and N analysis and ^{1}H NMR spectroscopy. The characterisation data are given in Table 2.1.

Figure 2.1 The reaction steps of formation of ligands and schematic representation for ligand *1* and *2*.

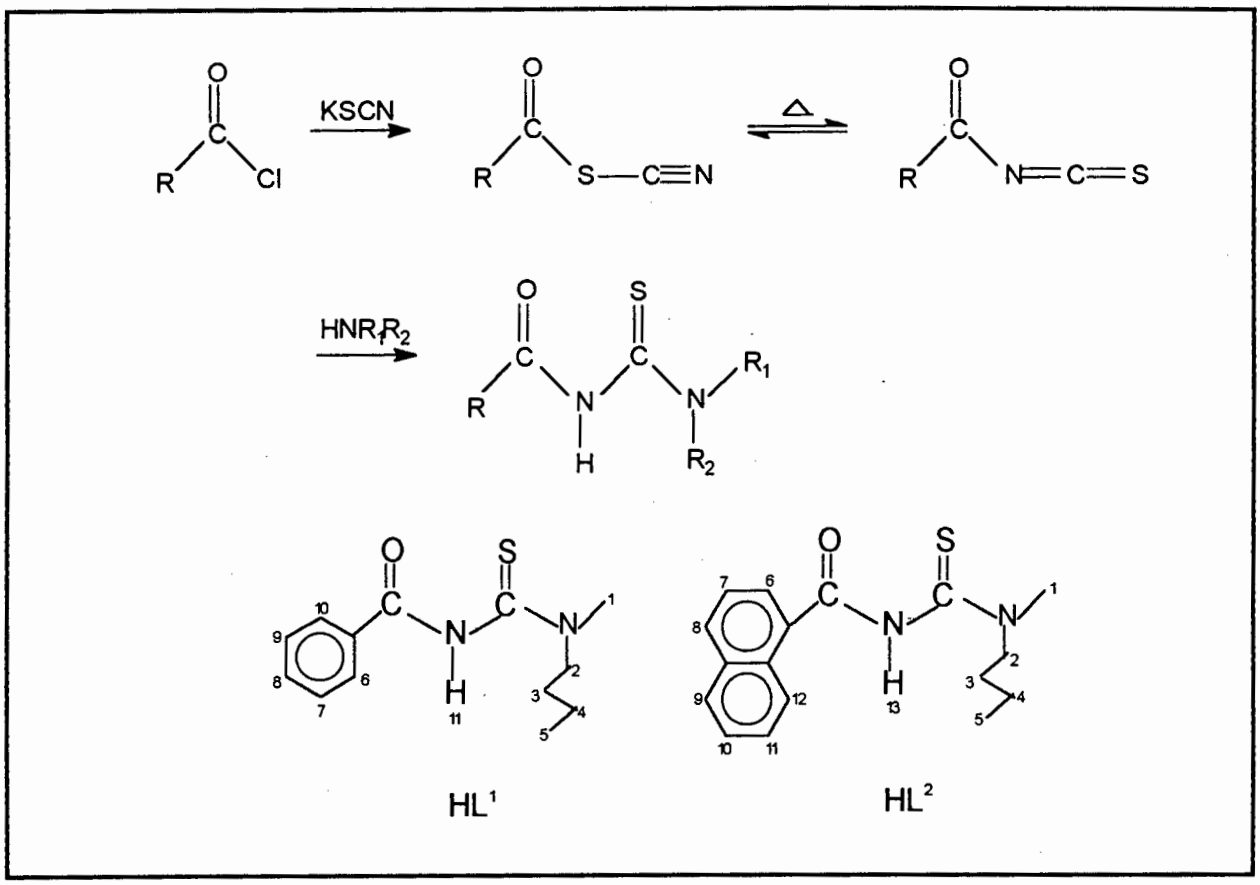

Table 2.1 Characterisation data of ligands.

ligand	yield (%)	m.p.(°C)	C. H. N. analysis (%)
1	81.7	76-77	*calc*: 62.37, 7.25, 11.19
			obs: 62.76, 7.48, 11.48
2	79.8	122-124	*calc*: 67.96, 6.71, 9.33
			obs: 68.14, 6.87, 9.46

In view of the partial double-bond character of the alkyl-substituted thiourea C-N bond, two resonance structures (a) and (b) are possible (Figure 2.2). Accordingly, ligand *1* and *2* should result in configurational isomerism which would induce different proton resonances about each alkyl group separately in the ^{1}H NMR spectrum.

Figure 2.2 Resonance structures of a thioamide C-N bond due to the electron delocalisation between the nitrogen lone pair and the thiocarbonyl sulphur atom[7].

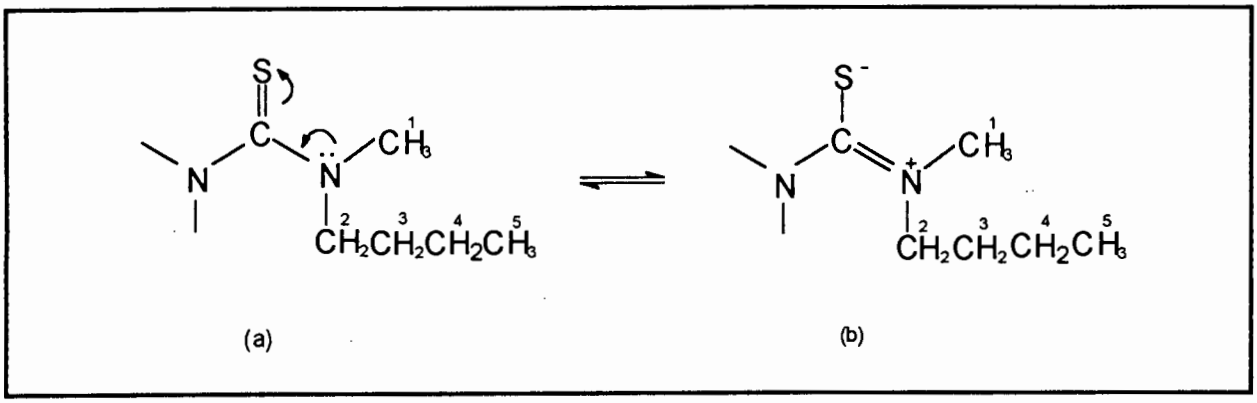

^{1}H NMR study

The ^{1}H NMR spectrum of ligand ***1*** (Figure 2.3a) shows two sets of *N*-CH_3 (H^1) and *N*-(CH_2)C_3H_7 (H^2) signals: at 3.174 and 3.391 ppm (singlets) and at 3.921 and 3.530 ppm (triplets), of relative intensity 71% : 29%, respectively. The singlets at 3.391 ppm and triplets at 3.530 ppm are assigned as *E* isomer (minor) on the basis of the expected magnetic anisotropy of the adjacent thiocarbonyl group, which is likely to deshield the closest nuclei coplanar with this group, as has been observed in carbonyl-containing compounds[7]. Thus, the 3.391 ppm H^1 resonance of the *E* isomer is down field relative to the corresponding H^1 resonance for the major *Z* isomer. Whereas, the 3.530 ppm H^2 resonance of the *E* isomer is high field relative to the corresponding H^2 resonance for the *Z* isomer, which is consistent with the chemical shift trends of the H^3, H^4 and H^5 resonances respectively. The ^{1}H NMR spectrum of ligand ***2*** (see Figure 2.3b) also shows two sets of alkyl signals separately. The detailed ^{1}H assignments and chemical shift data are given in Table 2.2a for ***1*** and 2.2b for ***2***.

Table 2.2a ^{1}H chemical shift data and assignments for ***1*** in chloroform-d_3 at 25 °C.

isomer	H^{11}	H^6/H^{10}	H^8	H^7/H^9	H^2	H^1	H^3	H^4	H^5
Z,Z + *E,Z* (65%)	8.617	7.794	7.532	7.426	3.921	3.174	1.747	1.415	0.950
E,E + *E,Z* (35%)	8.617	7.794	7.532	7.426	3.530	3.391	1.625	1.250	0.871

Figure 2.3 Part of the ^{1}H NMR spectra of ***1*** and ***2*** in chloroform-d_3 at 25 °C.

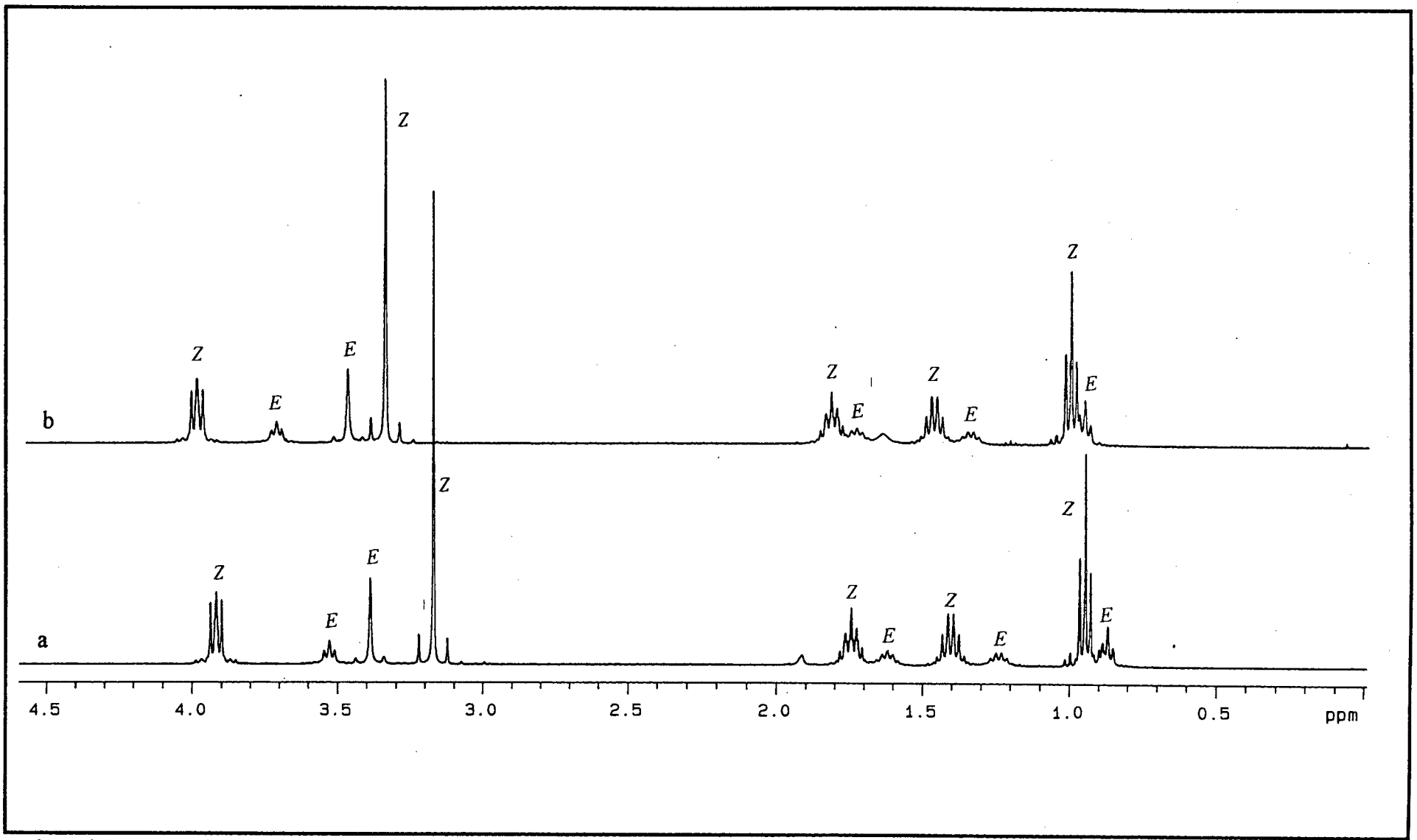

*a. ligand **1**.* *b. ligand **2**.*

Table 2.2b ^{1}H chemical shift data and assignments for ligand *2* in chloroform-d_3 at 25 °C.

isomer	H^{12}	H^{13}	H^{6}	H^{8}	H^{9}	H^{7}	H^{10}
Z,Z + *E,Z* (60%)	8.437	8.379	7.978	7.874	7.764	7.573	7.573
E,E + *E,Z* (40%)	8.437	8.379	7.978	7.874	7.764	7.573	7.573
isomer	H^{11}	H^{2}	H^{1}	H^{3}	H^{4}	H^{5}	
Z,Z + *E,Z* (60%)	7.477	3.974	3.330	1.810	1.468	0.997	
E,E + *E,Z* (40%)	7.477	3.702	3.457	1.723	1.344	0.949	

2.2.2 Preparation and characterisation of complexes (*3* - *4*)

Generally, *N,N*-dialkyl-*N'*-acylthioureas coordinate to platinum(II) forming square planar complexes, the schematic representative structures are given in Figure 2.4.

Figure 2.4 The representation of complexes formed.

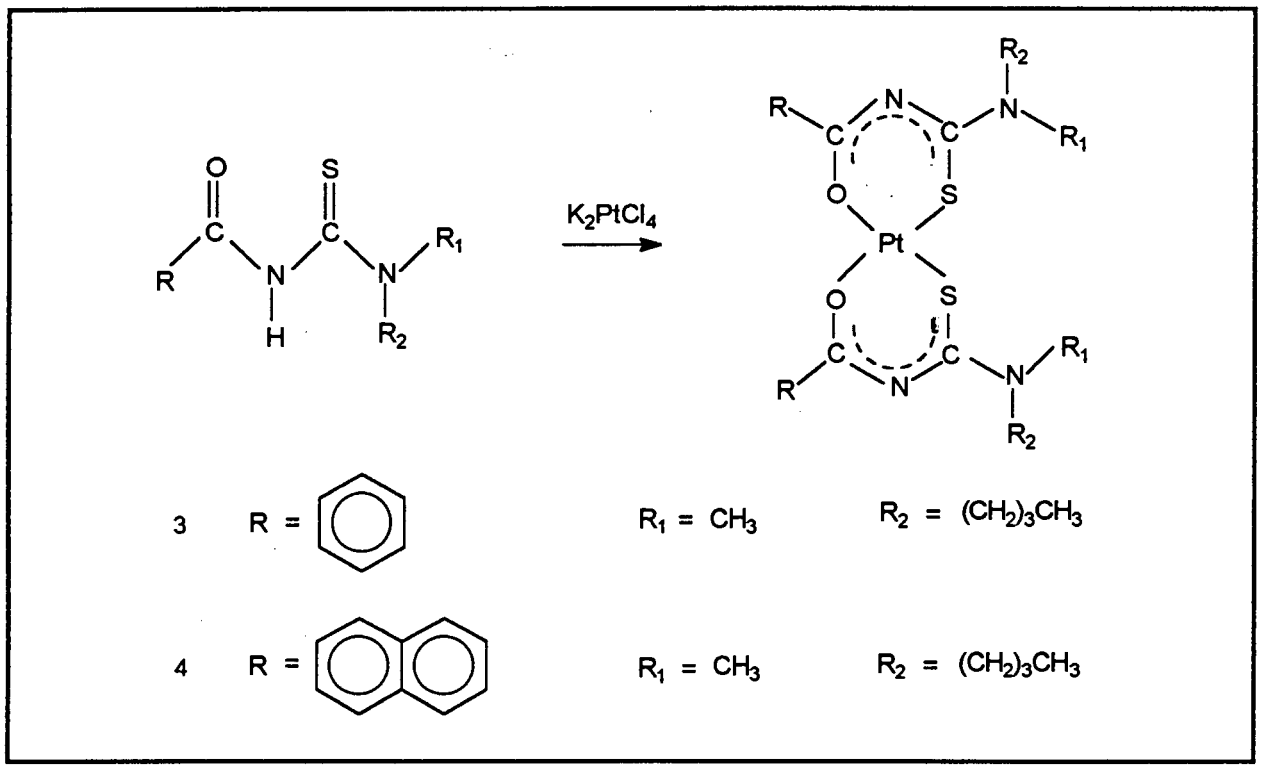

The *cis*-bis(*N*-(*n*-butyl)-*N*-methyl-*N'*-benzoylthioureato)platinum(II) ***3*** and *cis*-bis(*N*-(*n*-butyl)-*N*-methyl-*N'*-naphthoylthioureato)platinum(II) ***4*** have been synthesised in 1,4-dioxane or acetonitrile solution respectively, giving the same products, according to the method reported by Koch *et al*[8]. These complexes are satisfactorily characterised by C,H and N elemental analysis and ^{1}H NMR spectroscopy. The characterisation data are presented in Table 2.3.

Table 2.3 Characterisation data for complex ***3*** - ***4***.

complex	solvent	yield (%)	m.p.(°C)	C. H. N. analysis (%)
3	1,4-dioxane	83.7	159-160	*calc*: 45.01, 4.94, 8.08
				obs: 45.15, 4.99, 8.13
3	acetonitrile	94.5	159-160	*calc*: 45.01, 4.94, 8.08
				obs: 45.16, 4.94, 8.16
4	1,4-dioxane	68.5	153-155	*calc*. 51.44, 4.82, 7.06
				obs. 51.42, 5.00, 7.21
4	acetonitrile	87.1	153-155	*calc*. 51.44, 4.82, 7.06
				obs. 51.17, 4.78, 7.06

We have found that ligand *N*-(*n*-butyl)-*N*-methyl-*N'*-benzoylthiourea reacts with K_2PtCl_4 always forming a *cis*- complex which is identified by comparing the ^{1}H NMR spectrum with that reported[4, 9]. The ligand *N*-(*n*-butyl)-*N*-methyl-*N'*-naphthoylthiourea reacts with K_2PtCl_4 also forming a *cis*- complex which is identified by comparing the ^{1}H NMR spectrum with that of a similar complex bis(*n*-dibutyl-*N'*-naphthoylthioureato)platinum(II) [Pt(L^3)$_2$] reported by Koch *et al*[8]. The ^{1}H NMR spectrum of the aromatic region for complex ***4*** and [Pt(L^3)$_2$] are given in Figure 2.5.

Figure 2.5 ^{1}H NMR spectra of the aromatic region for ***4*** and $[Pt(L^3)_2]$ in chloroform-d_3 at 25°C.

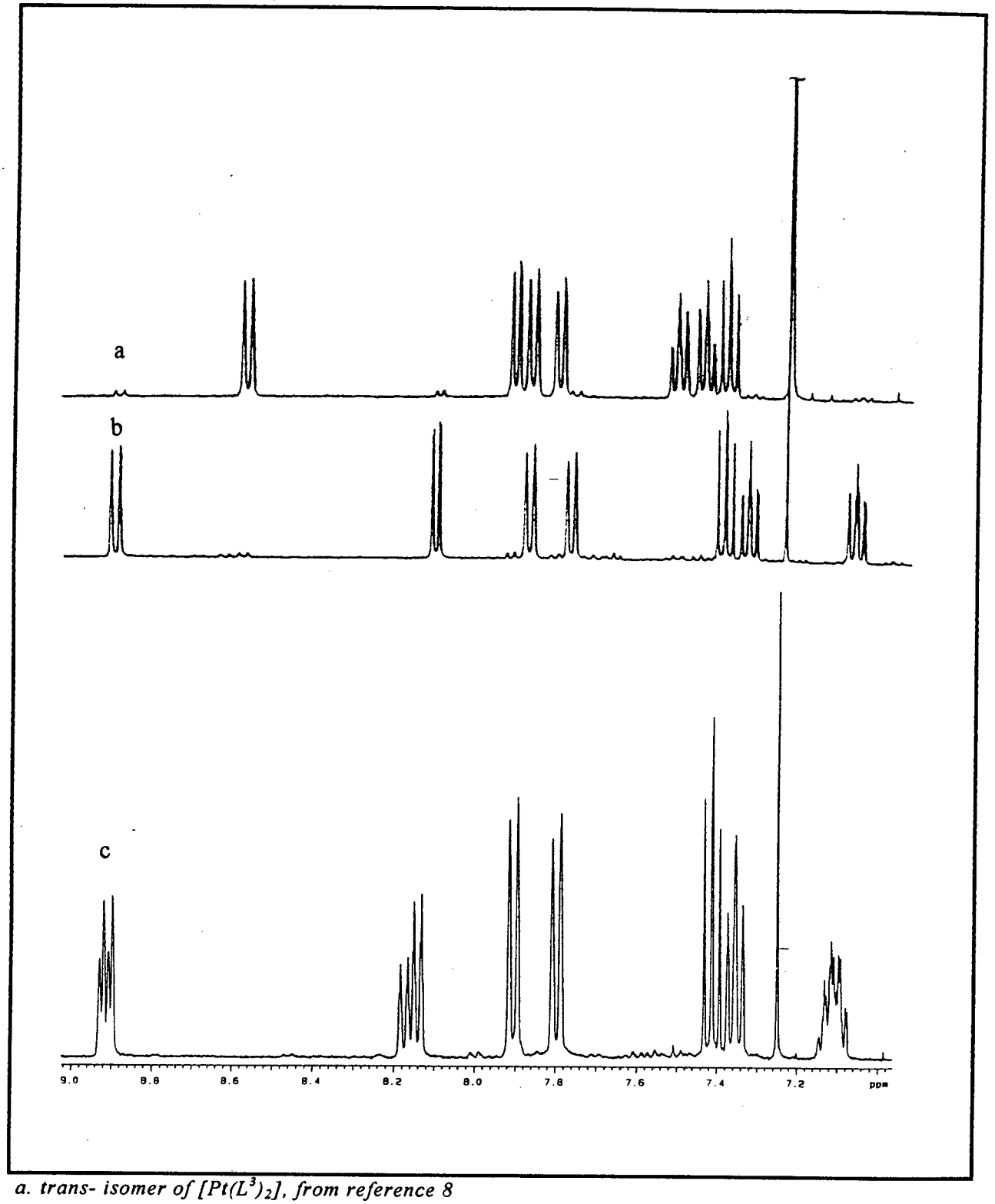

a. trans- isomer of $[Pt(L^3)_2]$, from reference 8

b. cis- isomer of $[Pt(L^3)_2]$, from reference 8

c. cis- $[Pt(L^2)_2]$ 4

Nevertheless, considering the restricted rotation about the thioamide C-N bond, it is possible to get *three* different configurations about complex ***3*** and ***4*** (Figure 2.6 and 2.7). So that the ^{1}H NMR spectra of ***3*** and ***4*** are further investigated to ascertain whether these three isomers practically exist.

Figure 2.6 The representative configurational isomers of complex ***3***.

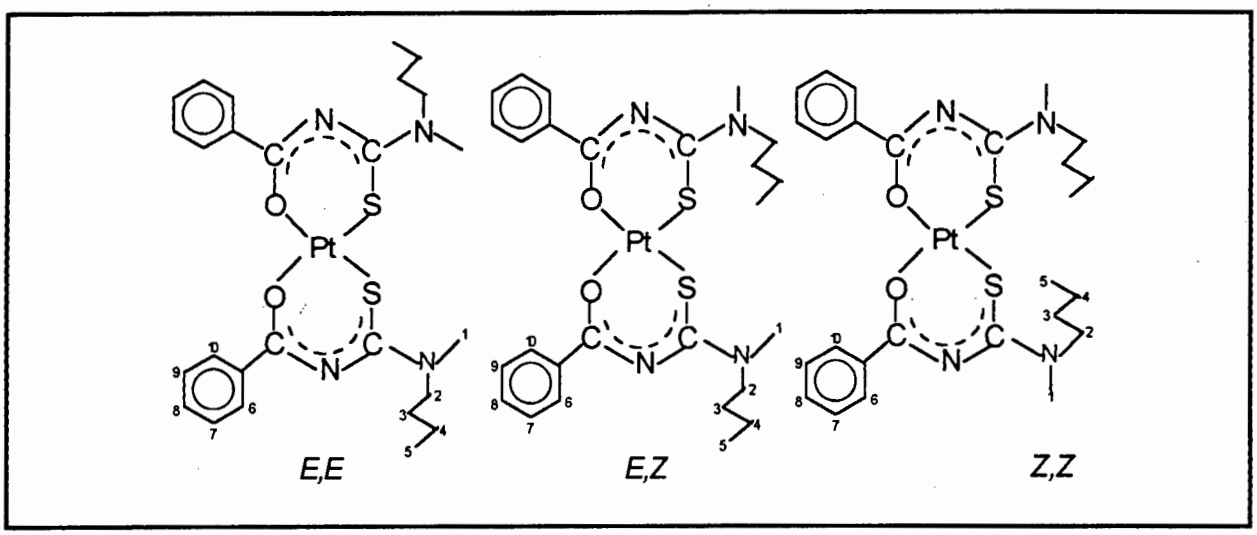

Figure 2.7 The representative configutational isomers of complex ***4***.

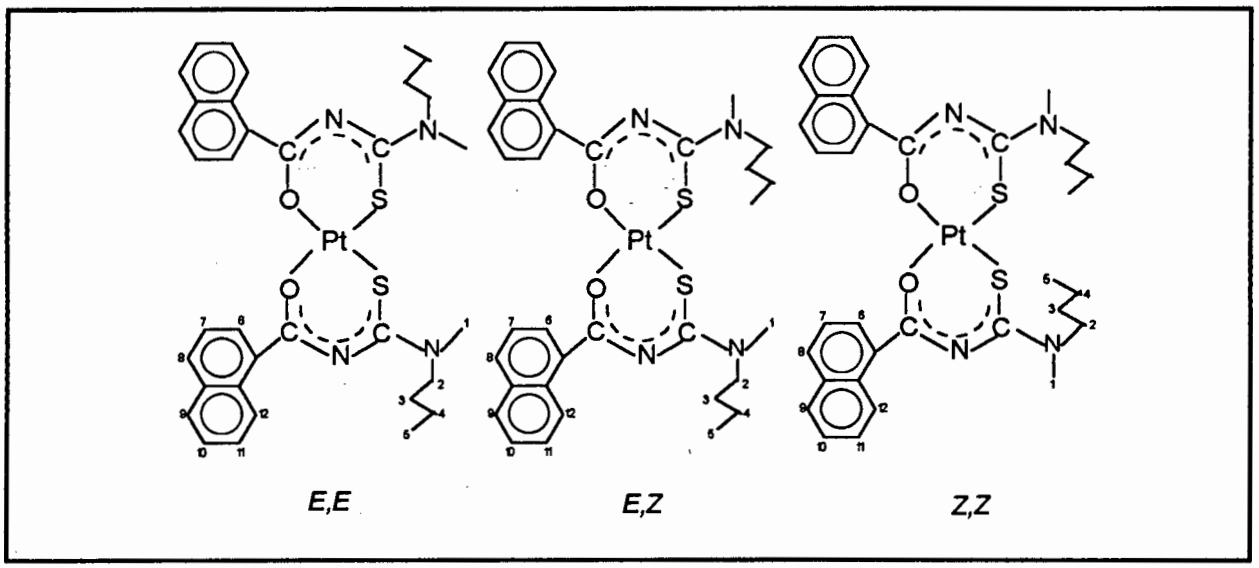

^{1}H NMR study

The ^{1}H NMR spectra of ***3*** and ***4*** indicate that for each of these complexes more than two complex isomers are present in each solution. The representative part of ^{1}H NMR spectra of ***3*** and ***4*** are given in Figure 2.8. Evidently these compounds consist of a mixture of the *cis*-[Pt(*E,E*-L)$_2$], *cis*-[Pt(*E,Z*-L)$_2$] and *cis*-[Pt(*Z,Z*-L)$_2$] (L = L^1 or L^2) complexes respectively, with the *E,E* isomer assigned to the smallest component, although this is not readily apparent from the ^{1}H NMR spectrum.

For complex ***3***, the 3.348 ppm H^1 resonance of the *E* isomer (minor) is down field relative to the corresponding H^1 resonance of the *Z* isomer. The 3.744 ppm H^2 resonance of the *E* isomer is high field relative to the corresponding H^2 resonance of the *Z* isomer, which is consistent with corresponding ligand ***1***. Interestingly, the H^3, H^4 and H^5 resonances of the *E* isomer are down field relative to the corresponding H^3, H^4 and H^5 resonances of the *Z* isomer respectively. This trend is different from corresponding ligand ***1***.

For complex ***4***, the 3.781 ppm H^2 resonance of the *E* isomer is found at high field relative to the corresponding H^2 resonance of the *Z* isomer, which is consistent with uncomplexed ligand ***2*** and similar as complex ***3***. The H^3, H^4 and H^5 resonances of the *E* isomer are down field relative to the corresponding H^3, H^4 and H^5 resonances of the *Z* isomer respectively, which is consistent with similar complex ***3***, but is different from the corresponding ligand ***2***. More interestingly, the 3.297 ppm H^1 resonance of the *E* isomer is high field relative to the corresponding H^1 resonance of the *Z* isomer, which is different from both corresponding ligand and similar complex ***3***. The reason for these phenomena observed is not clear. The ^{1}H chemical shift data and assignments for ***3*** are given in Table 2.4a, for ***4*** in Table 2.4b.

Figure 2.8 Part of the ^{1}H NMR spectra of ***3*** and ***4*** in chloroform-d_3 at 25 °C.

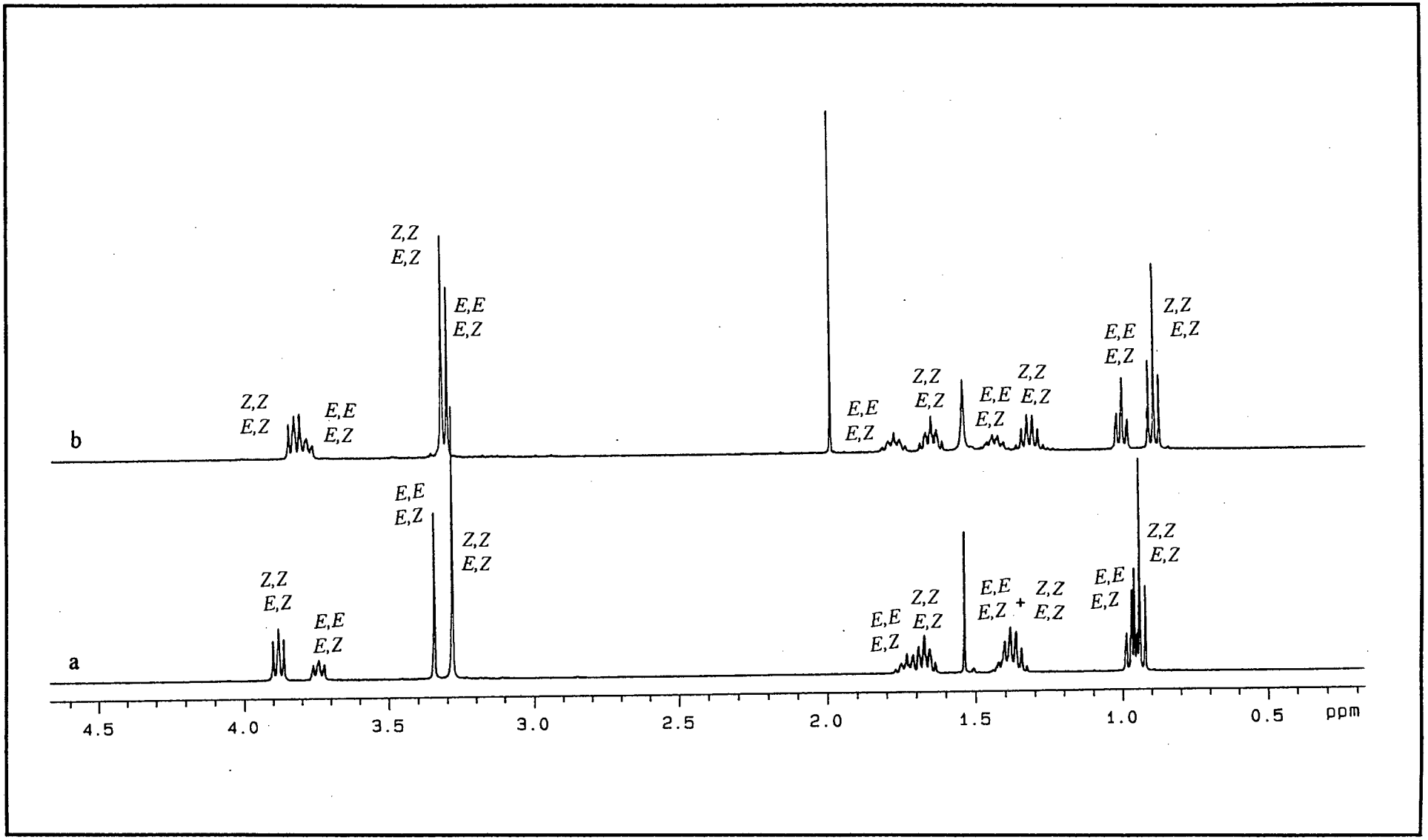

a. complex 3. *b. complex 4.*

Table 2.4a ^{1}H chemical shift data and assignments for ***3*** in chloroform-d_3 at 25 °C.

isomer	H^6/H^{10}	H^8	H^7/H^9	H^2	H^1	H^3	H^4	H^5
Z,Z + *E,Z* (65%)	8.250	7.509	7.408	3.885	3.284	1.674	1.384	0.943
E,E + *E,Z* (35%)	8.269	7.509	7.408	3.744	3.348	1.733	1.384	0.969

Table 2.4b ^{1}H chemical shift data and assignments for ***4*** in chloroform-d_3 at 25 °C.

isomer	H^{12}	H^6	H^8	H^9	H^7	H^{10}
Z,Z + *E,Z* (60%)	8.897	8.132	7.895	7.787	7.413	7.354
E,E + *E,Z* (40%)	8.908	8.169	7.895	7.787	7.413	7.354
isomer	H^{11}	H^2	H^1	H^3	H^4	H^5
Z,Z + *E,Z* (60%)	7.114	3.824	3.315	1.645	1.32	0.888
E,E + *E,Z* (40%)	7.114	3.781	3.297	1.770	1.437	0.994

IR study

As a result of comparing the IR spectra of complex ***3*** and ***4*** with those of the corresponding uncomplexed ligand, the broad absorption assigned to the N-H amide stretching vibration at 3233 cm^{-1} is clearly invisible (Nujol mull), and the sharp stretch at 1660 cm^{-1} assigned to the carbonyl stretch of the -CO-NH- moiety virtually disappears, in the complex ***3*** and ***4***. These observations are consistent with the postulated structure as illustrated in Figure 2.3.

2.3 Conclusion

We have successfully prepared and characterised some unsymmetrical substituted *N,N*-dialkyl-*N'*-acylthiourea ligands and corresponding platinum(II) complexes. These complexes are *cis*- complexes. Each of the ligands and complexes has a configurational *E/Z* isomerism because of the restricted rotation about the thioamide C-N bond. The ^{1}H NMR spectra give a strong evidence to the formation of the configuration isomers.

2.4 Experimental

The following experimental procedures and instrumentation were used throughout this thesis for the preparation and characterisation of the *N,N*-dialkyl- and *N*-alkyl-*N'*-acylthioureas and their platinum complexes.

2.4.1 Starting materials and apparatus

The platinum salt K_2PtCl_4 was on loan from Johnson Matthey and commercially available chemical agents were used.

All ^{1}H NMR spectra were recorded in 5 mm tubes using a 400 MHz Varian spectrometer operating at 399.951 MHz and were obtained by quoting relative to the residual chloroform-d_3 solvent resonance at 7.25 ppm at 25 °C.

Infrared spectra were obtained as Nujol mull using Perkin Elmer model 983 Infrared Spectrophotometer. The melting points were measured on a Reichert-Jung Hermovar attached to a DP-4 digital thermometer. Elemental analysis was performed by the Microanalytical Laboratory of the Chemistry Department, University of Cape Town.

2.4.2 Preparation of ligand

N-(n-butyl)-N-methyl-N'-benzoylthiourea (1)

Ligand *1* was prepared by using 0.04 mol of each of the following reagents, potassium thiocyanate, benzoyl chloride and *N-(n*-butyl)-*N*-methyl-amine. The required amount of potassium thiocyanate (0.04 mol, 3.8876 g) was dissolved in dry acetone (50 ml). The acetone was dried by distillation in the presence of $CaCl_2$ and 4Å molecular sieves prior to use. The required amount of benzoyl chloride (5.6228 g) was added to this solution dropwise under nitrogen. The above mixture was heated under reflux for 40 minutes and then cooled down to room temperature. The *N-(n*-butyl)-*N*-methyl-amine (3.4868 g) was added dropwise and the solution was heated under reflux for a further 1 hr. The final reaction mixture was cooled and poured into ice water (200 ml). The precipitate formed was filtered, dried under vacuum and recrystallised from ethanol/water mixture to give white crystals as final product. The yield, m.p., C, H, and N elemental analysis and ^{1}H NMR assignments of the ligand can be found in Table 2.1 and 2.2a.

N-(n-butyl)-N-methyl-N'-naphthoylthiourea (2)

Ligand **2** was prepared by using 5.8 mmol of each of the following, potassium thiocyanate, naphthoyl chloride and *N*-methyl-*N*-butyl amine according to the above procedure. The required amount of potassium thiocyanate (5.8 mmol, 0.5637 g) was dissolved in dry acetone (50 ml). The required amount naphthoyl chloride (1.1105 g) was added to this solution dropwise under nitrogen. The above mixture was heated under reflux for 40 minutes and then cooled down to room temperature. The *N-(n*-butyl)-*N*-methyl-amine (0.5056 g) was added dropwise and the solution was heated under reflux for a further 1 hr. The final reaction mixture was cooled and poured into ice water (200 ml). The precipitate formed was filtered out and dried under vacuum. The product was recrystallised from an ethanol/water mixture to give white crystals as final product. The yield, m.p., C, H, and N elemental analysis and ^{1}H NMR assignments of the ligand can be found in Table 2.1 and 2.2b.

2.4.3 Synthesis of complexes

cis-bis(N-(n-butyl)- N-methyl- N'-benzoylthioureato)platinum(II) (3)

To 10 ml of a heated (*ca.* 60°C) solution of water containing K_2PtCl_4 (0.5 mmol, 0.2075 g), 10 ml of dioxane (or acetonitrile) was added. This solution was then added dropwise to a solution containing 1.0 mmol (0.2504 g) of ligand in 40 ml (1+1) dioxane (or acetonitrile) /water at *ca.* 60°C. After all the platinum containing solution was added, 2 mmol sodium acetate was added. The mixture was stirred for a further 30 minutes at 60 °C, and then the dioxane (or acetonitrile) was allowed to evaporate. The metal complex was then extracted into 20 ml of chloroform using a separation funnel. The chloroform solution was then passed through a general funnel containing "extrelut " (Merck TM) to remove the small amount of water from the chloroform solution. After the chloroform had been removed using a rotary evaporator, a yellow residue was obtained. A small amount of chloroform was added to dissolve the residue, and then ethanol (equal to the volume of chloroform) was added. Recrystallisation occurred which gave yellow crystals as final products. The yield, m.p., C, H, and N elemental analysis and ^1H NMR assignments of the complex can be found in Table 2.3 and 2.4a.

cis-bis(N-(n-butyl)-N-methyl-N'-naphthoylthioureato)platinum(II) (4)

The complex *4* was synthesised as described above. 1.0 mmol of ligand and 0.5 mmol of K_2PtCl_4 were used in the reaction. To 10 ml of a heated (*ca.* 60°C) solution of water containing K_2PtCl_4 (0.5 mmol, 0.2075 g), 10 ml of dioxane (or acetonitrile) was added. This solution was then added dropwise to a solution containing 1.0 mmol (0.3004 g) of ligand in 40 ml (1+1) dioxane (or acetonitrile) /water at *ca.* 60°C. After all the platinum containing solution was added, 2 mmol sodium acetate was added. The mixture was stirred for a further 30 minutes at 60 °C, then the oil-shaped metal complex was obtained. The product was dried under vacuum and recrystallised from chloroform/ethanol mixture to give yellow crystals as final product. The yield, m.p.,

C, H, and N elemental analysis and ^{1}H NMR assignments of the complex can be found in Table 2.3 and 2.4b.

References

1. K-H. Konig, M. Schuster, G.Schneeweis and B. Steinbrech, *Fresenius'z. Anal. Chem.*, 1984, **325**, 621.
2. P. Vest, M. Schuster and K-H. König, *Fresenius'z. Anal. Chem.*, 1989, **335**, 759.
3. M. Schuster, *Fresenius'z. Anal.Chem.*, 1992, **342**, 791.
4. A. Irving, K.R. Koch and M. Matoetoe, *Inorg. Chim. Acta*, 1993, **206,** 193.
5. L. Beyer, S. Behrendt, E. Kleinpeter, R. Borsdorf and E. Hoyer, *Z. Anorg. Allg. Chem.*, 1977, **437**, 282.
6. I.B. Douglass and F.B. Dains, *J. Am. Chem. Soc.*, 1934, **56**, 719.
7. H. Günther, *NMR spectroscopy: an Introduction*, John Wiley, Chichester, 1987.
8. K.R. Koch and J.D. Toit, *J. Chem. Soc. Dalton Trans.* 1994, 785-786.
9. K.R. Koch, C. Sacht, T. Grimmbacher and S. Bourne, *S. Afr. J. Chem.*, 1995, **48**(1/2), 71.

CHAPTER 3

Synthesis And Characterisation Of $[M(H_2L)_2X_2]$ (H_2L=*N*-alkyl-*N*'-acylthiourea), Kinetics And Mechanism Of *Cis-Trans* Isomerisation Of $[Pt(H_2L^1)_2Cl_2]$, (H_2L^1=*N*-(*n*-propyl)-*N*'-benzoylthiourea)

3.1. Introduction

3.1.1 General

N,N-dialkyl- and *N*-alkyl- substituted acylthioureas have been shown to have substantially different coordination chemistry[1-4]. *N,N*-dialkyl-*N'*-acylthioureas (HL) coordinate to a variety of transition metals through the sulphur and oxygen atoms and form mainly *cis*- $[M(L\text{-}S,O)_2]$ complexes; on the other hand, *N*-alkyl-*N'*-acylthioureas (H_2L) usually coordinate to 'soft' metals (Pt or Pd) through the sulphur atom only and form $[M(H_2L\text{-}S)_2X_2]$ complexes which are mixtures of *cis*- and *trans*- isomers. For example, Bourne and Koch[4] have reported that bis(*N*-(*n*-propyl)-*N'*-benzoylthiourea)dichloro-platinum(II) is a 2.3:1 mixture of *cis*- and *trans*- isomers. Subsequent to this study, we were interested to investigate whether changes of the synthesis conditions could induce changes in the *cis-trans* isomer ratio of the products of the type $[Pt(H_2L^1)_2X_2]$ (H_2L^1 = *N*-(*n*-propyl)-*N'*-benzoylthiourea; X = Cl, Br, I). Furthermore, it is of interest to see whether the isomerisation of the products could be observed in different solvents by means of ^1H NMR spectroscopy. If so, the kinetics and mechanism of the isomerisation could be investigated. Also, the synthesis of $[Pt(H_2L^2)Cl_2]$ (H_2L^2 = *N*-(*n*-propyl)-*N'*-naphthoylthiourea) and $[Pd(H_2L^1)_2X_2]$ (X = Cl, Br) complexes are investigated.

3.1.2 *Cis-trans* isomerisation

Cis-trans isomerisation of platinum(II) and palladium(II) complexes have received much attention in recent years. Although many square-planar platinum(II) and palladium(II) complexes have been isolated in their *cis*- and *trans*- forms, only a few of them exhibit observable rates of isomerisation in solution. Earlier reports on the thermal interconversions of the *cis-trans* isomers of $[Pt(L)_2X_2]$, where L = various phosphorus, nitrogen, and sulphur donor ligands and X = halogen[6-8], have been succeeded by more recent studies[9-14] which focus on the kinetics and mechanism of

isomerisation since this phenomenon is pertinent to the broader topic of square-planar substitution reactions.

Although square-planar complexes of the d^8 ions Rh^I, Ir^I, Pd^{II}, Pt^{II} and Au^{III} are legion, detection and characterisation of the geometric isomers, as well as subsequent isomerisation studies are, so far, limited almost exclusively to derivatives of platinum and palladium[15]. This is almost certainly due to the ease of preparation (and identification) of the electroneutral complexes $[MX_2L_2]$, $[MXYL_2]$ and $[MX_2LL']$ of these elements, where X or Y are anionic ligands and L and L' are uncharged ligands. These complexes may exist as *cis-* or *trans-* isomers. Dealing with the platinum and palladium complexes $[MX_2L_2]$ only, the general rule that has been found to hold is that the *cis-* isomers are enthalpy-favoured, while the *trans*-form is entropy-favoured, and is solvent dependent[15].

A further classification of the observed isomerisations is that the isomerisations can be either catalysed or spontaneous. In the literature, the majority of studies have been concerned with ligand catalysed isomerisations[6,9,12,14], while truely spontaneous isomerisations have only received much attention recently[10-11,13]. To our knowledge, the study of the isomerisation of the $[Pt(H_2L)_2Cl_2]$ (where H_2L = *N*-alkyl-*N'*-acylthiourea) complexes has, however, not been reported so far.

3.1.3 Mechanisms of isomerisation

There are two postulated and generally accepted mechanisms in catalysed *cis-trans* isomerisations. These are the consecutive displacement and pseudorotation mechanisms. The consecutive displacement isomerisation mechanism has been suggested by Basolo and Pearson[16]. It is depicted in Figure 3.1, from which it can be seen that two steps are needed to achieve the isomerisation. If the reaction goes through intermediate A, the original isomer may be reformed, but if intermediate B is produced the geometric isomer is generated. If A could be converted into B directly and this conversion is faster than either or both of the steps linking A and B with the ionic intermediate, the pseudorotation mechanism could be possible.

Figure 3.1 A consecutive displacement mechanism quoted from reference 16.

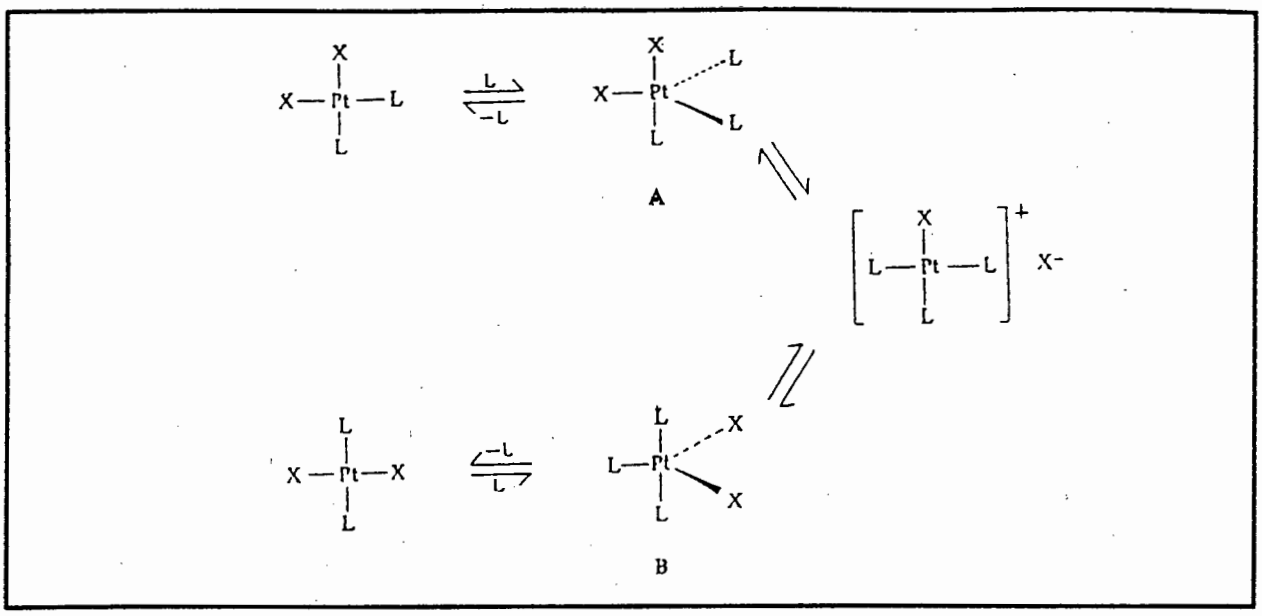

The relationship between these two mechanisms has been established by Cooper and Powell[17] who indicated the reaction profile (Figure 3.2). The reaction path to be followed, A, B or C, will depend on the nature of M, X and L (M-metal; X-halogen; L-ligand), as well as on the temperature and solvent[15].

Figure 3.2 The relationship between consecutive displacement and pseudorotation mechanisms quoted from reference 17.

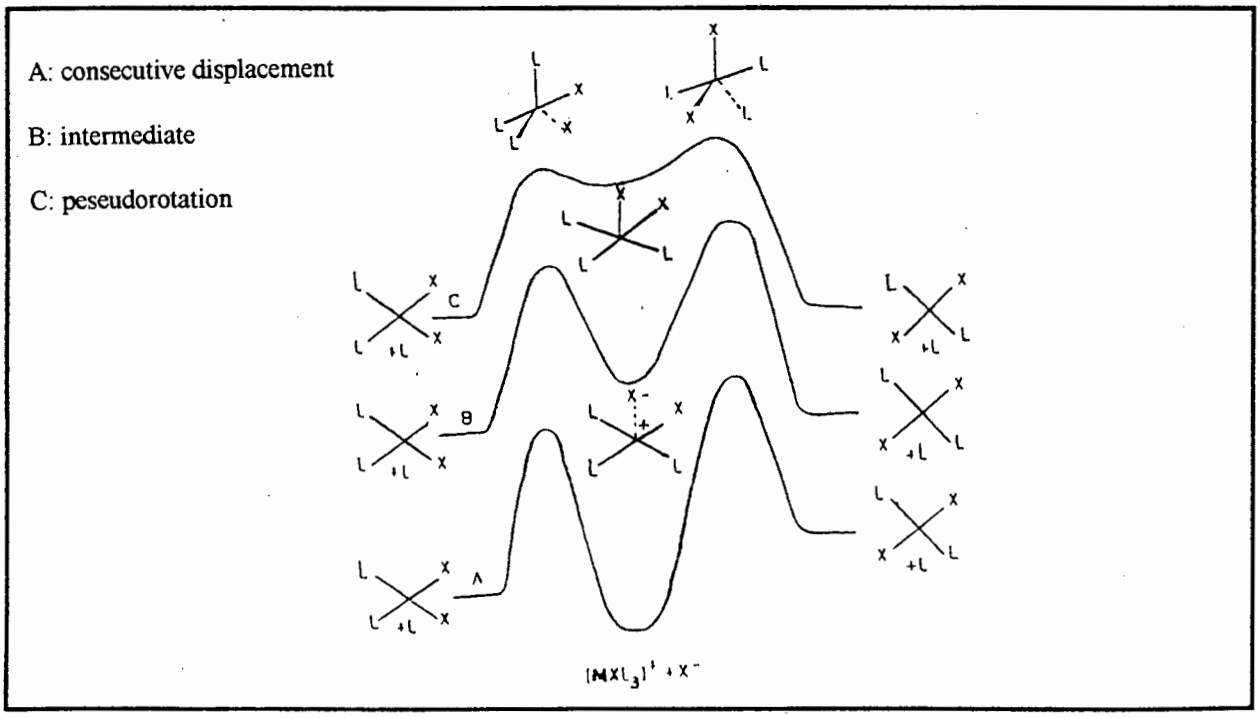

It is suggested that polar solvents favour an ionic intermediate (hence the consecutive displacement mechanism) whereas non-polar media lead to 5-coordinate intermediates (hence the pseudorotation mechanism). Although these general conclusions are well known, much still remains to be explained concerning the relationship of consecutive displacement and pseudorotation.

Truly spontaneous *cis-trans* isomerisations could be divided into three groups: reactions which are catalysed, by an unidentified catalyst (solvent catalysed or autocatalysed); reactions involving a straightforward change of geometry; and reactions involving ligand loss and rearrangement via a 3-coordinate intermediate. The border-line between these categories is somewhat blurred, and not surprisingly it is impossible to classify accurately some of the reactions encountered.

In most cases, *cis-trans* isomerisation takes place with solvent association or via a dissociated ligand as catalyst[10-11,15]. Price, Birk and Wayland[11] have postulated that the isomerisation of *trans*-$[Pt(L)_2Cl_2]$ (L = Et_2SO, n-Pr_2SO) takes place via three or four steps in chloroform-d_3. This is a good example of the solvent associated isomerisation mechanism. Al-najjar, Al-lohedan and Issa[13] have investigated the *cis*- to *trans*- isomerisation of $[PtCl_2(PBu_3)(PhCN)]$, and found evidence for an autocatalytic mechanism. This is supported by the observation of the formation of a dimer intermediate by means of ^{31}P and ^{195}Pt NMR spectroscopy.

3.2. Results and discussion

3.2.1 Synthesis and characterisation of $[M(H_2L)_2X_2]$

3.2.1.1 Synthesis of $[M(H_2L)_2X_2]$

N-(*n*-propyl)-*N'*-benzoylthiourea (H_2L^1) and *N*-(*n*-propyl)-*N'*-naphthoylthiourea (H_2L^2) (Figure 3.3) were prepared according to the procedure described in Chapter 2

and characterised by C, H and N elemental analysis and ^{1}H NMR spectroscopy. Detailed data can be found in the experimental section (3.4.1).

Figure 3.3 Schematic representation of the ligand H_2L^1 and H_2L^2.

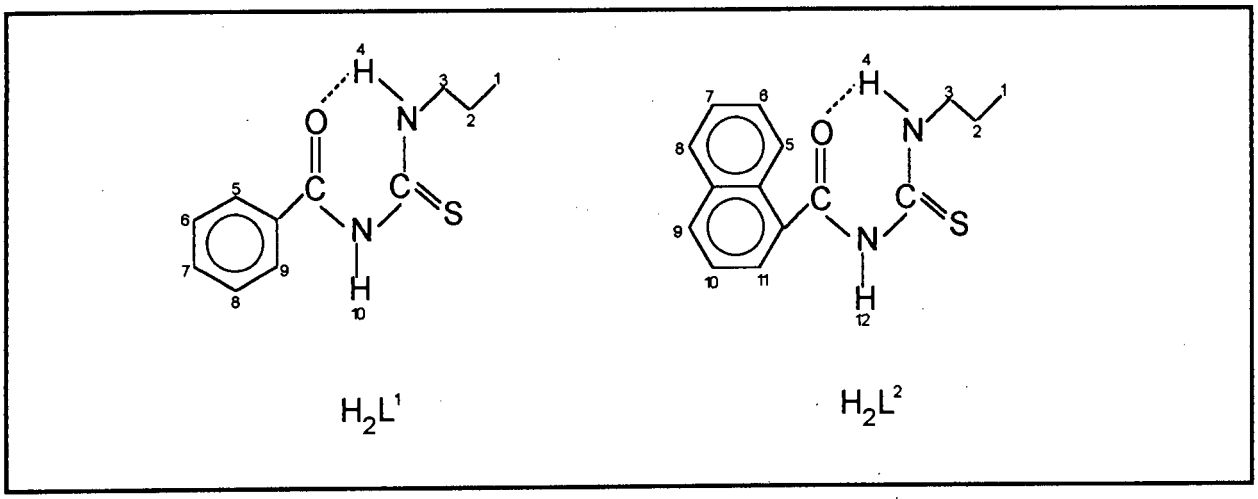

A special apparatus was used to ensure that the complex reaction conditions were as constant as possible from experiment to experiment, as shown by Figure 3.18 (page 65) in the experimental section 3.4.1.

Ligand H_2L^1 and H_2L^2 reacted with K_2MCl_4 (M = Pt, Pd) forming complexes $[M(H_2L)_2Cl_2]$ (Figure 3.4 and 3.5) in a solvent consisting of a mixture of 1,4-dioxane or acetonitrile and approximately 10% aqueous acid (to prevent deprotonation of the ligand).

The complexes $[M(H_2L)_2Br_2]$ and $[M(H_2L)_2I_2]$ were synthesised by first adding a 25 fold molar excess of NaBr or NaI respectively to the K_2MCl_4 solution to convert the $[MCl_4]^{2-}$ ion to the corresponding $[MBr_4]^{2-}$ or $[MI_4]^{2-}$ ion; these solutions were then added slowly to the ligand solution, at a fixed temperature.

Figure 3.4 Schematic representation of $[M(H_2L^1)_2X_2]$ complexes.

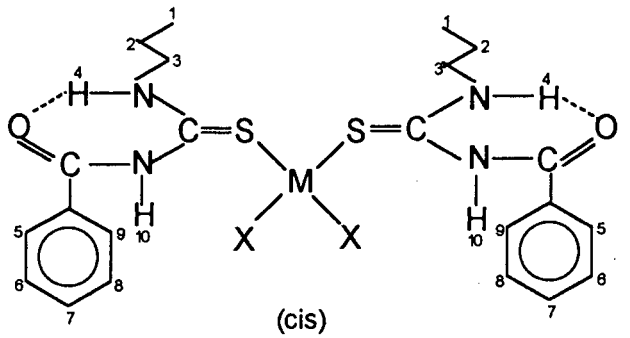

(cis)

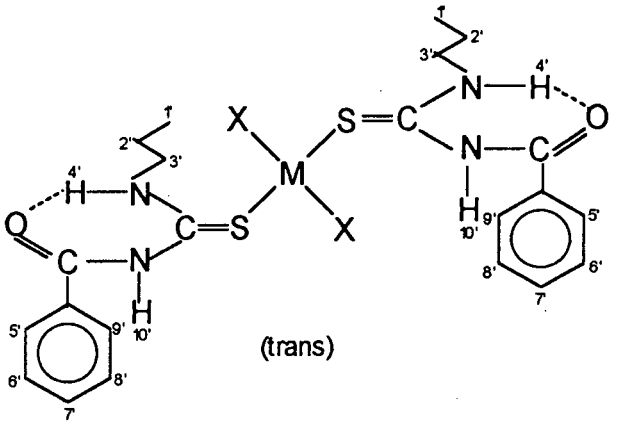

(trans)

1. M=Pt, X=Cl; *2*. M=Pt, X=Br;

3. M=Pt, X=I; *4*. M=Pd, X=Cl;

5. M=Pd, X=Br.

Figure 3.5 Schematic representation of $[Pt(H_2L^2)_2Cl_2]$ complex .

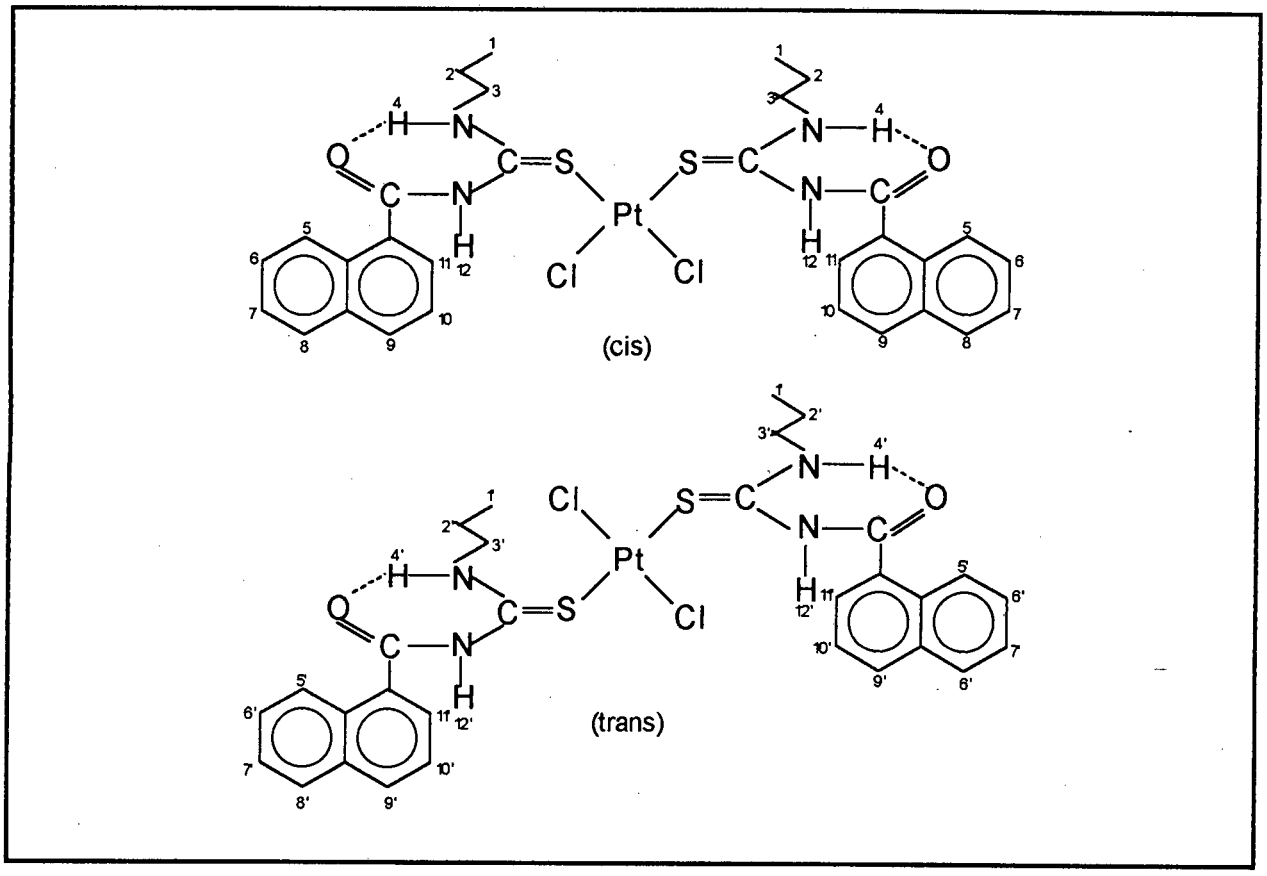

In general, the overall reaction may be postulated to take place as follows:

$$MX_4^{2-} + H_2L \xrightarrow{HX} \underset{\text{(cis)}}{\begin{matrix} H_2L & & H_2L \\ & M & \\ X & & X \end{matrix}} + \underset{\text{(trans)}}{\begin{matrix} X & & H_2L \\ & M & \\ H_2L & & X \end{matrix}} \qquad (1)$$

In general the complexes were obtained in 70-94% yields (after recrystallisation) and were characterised by C, H and N elemental analysis, and ^1H NMR as well as ^{195}Pt NMR spectroscopy. Detailed assignments of ^1H NMR spectra are found in the experimental section (3.4.1).

3.2.1.2 Characterisation of recrystallised products

Melting point

The recrystallised complexes show sharp melting points, but interestingly two melting points are observed in this transition process. This suggests that these recrystallised complexes may either be impure or exist in two isomeric forms. Considering the results of elemental analysis and ^{1}H NMR, it is concluded that these compounds are pure, and therefore must be mixtures of *cis-* and *trans-* isomers. This observation suggests that the isomerisation may have taken place during the recrystallisation process. This question is further discussed below. The physical properties of these complexes are given in Table 3.1a and the elemental analysis data are given in Table 3.1b.

Table 3.1a The physical properties of recrystallised $[Pt(H_2L^1)_2X_2]$ complexes.

X	t (hr)	T (°C)	media (HX+)	yield (%)	colour	m.p. (°C)[a]
Cl	1	25	1,4-dioxane	76.6	yellow	154-158, 162-165
Cl	6	25	1,4-dioxane	87.2	yellow	142-143, 158-160
Cl	17	25	1,4-dioxane	94.4	yellow	153-155, 160-163
Cl	1	60	1,4-dioxane	84.2	yellow	154-155, 165-168
Cl	1	85	acetonitrile	81.8	yellow	154-155, 165-169
Br	1	25	1,4-dioxane	68.4	orange	162-164, 174-178
Br	6	25	1,4-dioxane	84.4	orange	161-164, 176-179
Br	1	60	1,4-dioxane	61.6	orange	161-164, 175-178
Br	1	85	acetonitrile	70.9	orange	163-166, 175-178
I	1	25	1,4-dioxane	82.9	orange	172-173, 196-199
I	6	25	1,4-dioxane	75.0	orange	172-173, 196-198
I	1	60	1,4-dioxane	84.2	orange	172-173, 195-197
I	1	85	acetonitrile	81.1	orange	171-173, 196-197

a. Two isomers.

Table 3.1b The elemental analysis data of recrystallised $[Pt(H_2L^1)_2X_2]$ complexes.

X	t (hr)	T (°C)	medium (HX+)	C. H. N. analysis (%)
Cl	1	25	1,4-dioxane	*calc.* 37.18, 3.87, 7.89
				obs. 37.16, 4.00, 7.90
Cl	6	25	1,4-dioxane	*calc.* 37.18, 3.87, 7.89
				obs. 37.06, 4.02, 7.53
Cl	17	25	1,4-dioxane	*calc.* 37.18, 3.87, 7.89
				obs. 37.06, 4.06, 7.60
Cl	1	60	1,4-dioxane	*calc.* 37.18, 3.87, 7.89
				obs. 37.56, 3.98, 7.60
Cl	1	85	acetonitrile	*calc.* 37.18, 3.87, 7.89
				obs. 37.38, 3.98, 7.94
Br	1	25	1,4-dioxane	*calc.* 33.05, 3.53, 7.01
				obs. 33.25, 3.43, 6.90
Br	6	25	1,4-dioxane	*calc.* 33.05, 3.53, 7.01
				obs. 33.39, 3.48, 6.93
Br	1	60	1,4-dioxane	*calc.* 33.05, 3.53, 7.01
				obs. 33.37, 3.57, 7.02
Br	1	85	acetonitrile	*calc.* 33.05, 3.53, 7.01
				obs. 33.20, 3.52, 7.04
I	1	25	1,4-dioxane	*calc.* 29.57, 3.16, 6.27
				obs. 29.75, 3.14, 6.28
I	6	25	1,4-dioxane	*calc.* 29.57, 3.16, 6.27
				obs. 29.82, 3.08, 6.21
I	1	60	1,4-dioxane	*calc.* 29.57, 3.16, 6.27
				obs. 29.80, 3.18, 6.24
I	1	85	acetonitrile	*calc.* 29.57, 3.16, 6.27
				obs. 29.64, 3.12, 6.30

^{1}H NMR study

The Pt(II) complexes formed by reacting $[PtX_4]^{2-}$ (X = Cl, Br, I) with ligand H_2L^1 were all found to be a mixture of *cis-* and *trans-* isomers *after* recrystallisation in chloroform/ethanol solution. Significantly, for each complex the same *cis:trans* ratio was found under all reaction conditions studied (reaction time, temperature, reaction medium). The observed *cis:trans* ratios for all Pt(II) complexes are tabulated in Table 3.2.

Table 3.2 Observed *cis:trans* ratio of recrystallised $[Pt(H_2L^1)_2X_2]$ complexes as determined from ^{1}H NMR spectra in chloroform-d_3 at 25 °C.

X	t (hr)	T (°C)	medium HX+	^{1}HNMR δ(ppm) (H^{10}, $H^{10'}$)[a]	cis:trans (as%)
Cl	1	25	1,4-dioxane	11.80, 11.55	74:26
Cl	1	60	1,4-dioxane	11.80, 11.55	75:25
Cl	6	25	1,4-dioxane	11.80, 11.56	75:25
Cl	17	25	1,4-dioxane	11.80, 11.55	75:25
Cl	1	85	acetonitrile	11.80, 11.56	75:25
Br	1	25	1,4-dioxane	11.49, 11.31	40:60
Br	6	25	1,4-dioxane	11.49, 11.31	42:58
Br	1	60	1,4-dioxane	11.50, 11.32	42:58
Br	1	85	acetonitrile	11.50, 11.32	42:58
I	1	25	1,4-dioxane	11.36, 10.99	8:92
I	6	25	1,4-dioxane	11.36, 10.99	6:94
I	1	60	1,4-dioxane	11.36, 10.99	5:95
I	1	85	acetonitrile	11.36, 10.99	8:92

a. H^{10} - amide N-H of cis- isomer; $H^{10'}$ - amide N-H of trans- isomer.

Cis- and *trans-* isomers of $[Pt(H_2L^1)_2Cl_2]$ and $[Pt(H_2L^1)_2I_2]$ were identified as reported in the literature[4-5] . The ^{1}H NMR spectra of these complexes show that the characteristic N-H amide proton resonance of the *cis-* isomer generally appears at a lower field in comparison to the *trans-* isomer. The *cis-* isomer of the chloride

complex is at $\delta(^1H^{10})$ = 11.80 ppm; *trans-* isomer is at $\delta(^1H^{10'})$ = 11.55 ppm. For the iodide complex, the *cis-* isomer is at $\delta(^1H^{10})$ = 11.36 ppm and that for the *trans-* complex is at $\delta(^1H^{10'})$ = 10.99 ppm. According to this trend, the N-H amide proton resonances of *cis-* and *trans-* isomers of $[Pt(H_2L^1)_2Br_2]$ are assigned respectively to the peaks at 11.50 and 11.31 ppm.

From Table 3.2, it is evident that the tendency of formation of *trans-* isomers increases along the series $Cl^- < Br^- < I^-$. This is in general agreement with the *trans* effect which is observed in the order $I^- > Br^- > Cl^-$ [18]. This effect predicts that the amount of *trans-* complex should be the largest for the iodo-platinum complex, and the smallest for the chloro- complex. It can also be seen that the variation of the reaction time, temperature and reaction medium results in the same ratio of *cis:trans* isomers in solution for each compound *after* recrystallisation. This suggests that the *cis:trans* ratio may result from isomerisation in solution during the recrystallisation process, as well as perhaps in the chloroform-d_3 solution during the ^1H NMR experiment.

^{195}Pt NMR study

Confirmation that only two isomers of $[Pt(H_2L^1)_2X_2]$ complexes are formed is also obtained by means of ^{195}Pt NMR. The ^{195}Pt NMR spectra of recrystallised samples are recorded, relative to external H_2PtCl_6 ($\delta^{195}Pt = 0$) in chloroform-d_3 at 30 °C[19]. The ^{195}Pt NMR spectrum of $[Pt(H_2L^1)_2Cl_2]$ shows two resonances in the same ratio (*cis:trans*) as found from the ^1H NMR spectrum. The *cis-* isomer is at -3231 ppm, while the *trans-* isomer is assigned to the -3052 ppm peak, in agreement with published data[4]. The *cis-* or *trans-* isomers of $[Pt(H_2L^1)_2Br_2]$ and $[Pt(H_2L^1)_2I_2]$ are identified by comparing the $\delta^{195}Pt$ shift trends known for similar *cis-* or *trans-* compounds $[PtX_2L_2]$[19] (X = Cl, Br, I; L = PMe_3, SMe_2). For Cl^- and Br^- substituted complexes, the *cis-* isomer generally appears at higher field relative to the *trans-* isomer; for I^- substituted complexes however, the *cis-* isomer is at lower field. Thus, the two resonances at -3697 and -3678 ppm of ^{195}Pt NMR spectrum of $[Pt(H_2L^1)_2Br_2]$ (in a similar *cis:trans* ratio as observed in the ^1H NMR spectrum), are assigned to the

cis- and *trans*- isomers respectively. The ^{195}Pt NMR spectrum of $[Pt(H_2L^1)_2I_2]$ also shows two resonances at -4693 and -4870 ppm which are assigned to the *cis*- and *trans*- isomers respectively. However, the ^{195}Pt NMR spectrum of $[Pt(H_2L^1)_2I_2]$ gives a different *cis*:*trans* ratio to that of the ^{1}H NMR spectrum. This suggests that some isomerisation of $[Pt(H_2L^1)_2I_2]$ had taken place at 30 °C (the temperature at which the ^{195}Pt NMR spectrum is recorded) over the several hour period required to record the spectrum. Detailed data is listed in Table 3.3.

Table 3.3 ^{195}Pt NMR results for recrystallised $[Pt(H_2L^1)_2X_2]$ complexes.

X	^{195}Pt NMR δ (ppm) (*cis*-, *trans*-)	*cis*:*trans* ratio
Cl	-3231, -3052	74:26
Br	-3697, -3678	36:64
I	-4693, -4870	20:80

From the results described above, we decided to study whether recrystallisation could have induced the isomerisation of these complexes. Accordingly, crude unrecrystallised products were investigated; these products were however analytically pure.

3.2.1.3 Characterisation of unrecrystallised platinum complexes

When 1,4-dioxane is used in the mixed solvent used in the preparation of $[Pt(H_2L^1)_2Cl_2]$, this complex precipitates out from the solution with a fixed amount of 1,4-dioxane associated with the complex (observed and calculated from ^{1}H NMR spectra and confirmed by elemental analysis). Therefore, this complex should be represented as $[Pt(H_2L^1)_2Cl_2]\cdot 1/2C_4H_8O_2$ in the solid state. Interestingly, the complex $[Pt(H_2L^2)_2Cl_2]$ does not share this property (the reason is not clear). It is found that the crude unrecrystallised products $[Pt(H_2L^1)_2Cl_2]$ and $[Pt(H_2L^2)_2Cl_2]$ have sharp melting points, and give satisfactory elemental analysis results (Table 3.4), confirming the purity. Thus, the complex $[Pt(H_2L^1)_2Cl_2]$ was chosen for further investigation of the isomerisation.

Table 3.4 The characterisation data for crude unrecrystallised $[Pt(H_2L)_2Cl_2]$.

H_2L	t (hr)	T (°C)	yield (%)	colour	m.p. (°C)	C. H. N. analysis (%)
[a]H_2L^1	1	25	97.1	yellow	155-158	*calc.* 38.20, 4.27, 7.43
						obs. 38.06, 4.46, 7.40
[a]H_2L^1	17	25	94.5	yellow	154-157	*calc.* 38.20, 4.27, 7.43
						obs. 38.62, 4.39, 7.26
H_2L^2	1	25	92.7	yellow	168-170	*calc.* 44.45, 3.98, 6.91
						obs. 44.88, 4.11, 6.78

a. 1mol of crude $[Pt(H_2L^1)_2Cl_2]$ combined with 0.5mol 1,4-dioxane.

IR spectroscopy study

In order to further confirm whether the crude unrecrystallised complex $[Pt(H_2L^1)_2Cl_2]$ initially is *cis-* or *trans-*, infrared spectroscopy was used to investigate the crude complex. We found that the crude $[Pt(H_2L^1)_2Cl_2]$ complex shows only two strong peaks at 304.0 cm^{-1} and 321.0 cm^{-1} assigned to the Pt-Cl stretching frequency, which confirms that this complex is a *cis-* isomer, in agreement with the literature[20]. If the complex is only *trans-* isomer, a single IR peak should be expected, in the *ca.* 325.0 cm^{-1} region as reported[20] for *trans*-$[PtCl_2tu_2]$ complexes (where tu = thiourea).

^{1}H NMR study

The ^{1}H NMR of the crude product $[Pt(H_2L^1)_2Cl_2]$ shows that it is mainly the *cis-* isomer (as shown in Figure 3.6) for a fresh solution, but that once it is dissolved in chloroform-d_3 solution, the complex isomerises to the *trans-* isomer, eventually reaching an equilibrium distribution of *cis-* and *trans-* complexes as observed for the recrystallised sample. The *cis*:*trans* ratio measured from a freshly prepared solution of crude complex $[Pt(H_2L^1)_2Cl_2]$ and $[Pt(H_2L^2)_2Cl_2]$ are given in Table 3.5. It is then concluded that the isomerisation did take place during the recrystallisation for $[Pt(H_2L^1)_2Cl_2]$ reported in Table 3.2. By contrast, the ^{1}H NMR spectra of crude $[Pt(H_2L^1)_2Br_2]$ and $[Pt(H_2L^1)_2I_2]$ show that a ratio of cis:*trans* isomer in chloroform-

Figure 3.6 A representative ^1H NMR spectrum[a] of crude $[Pt(H_2L^1)_2Cl_2]$ (initial concentration 0.0163M) in chloroform-d_3 at 25 °C.

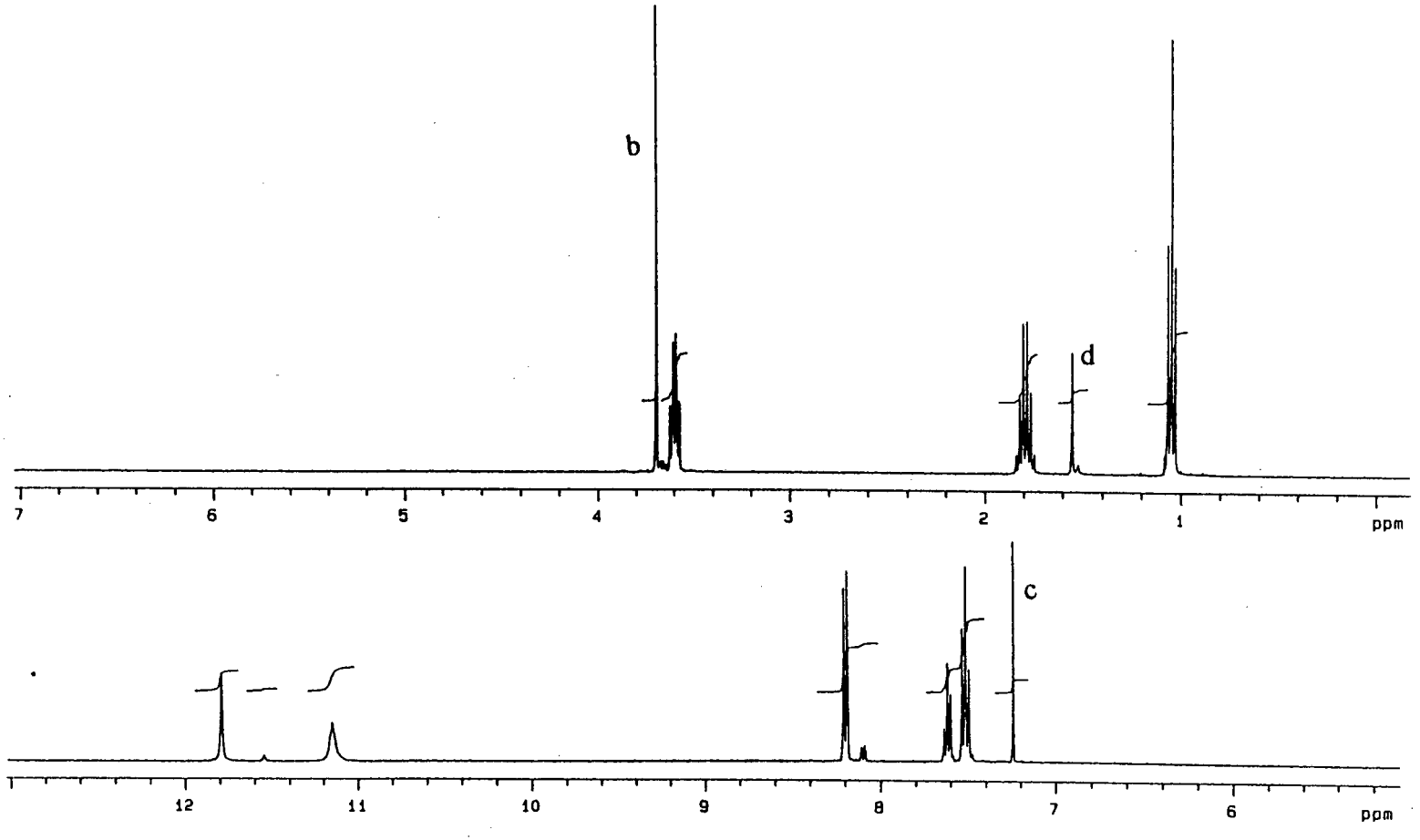

a. detailed ^1H assignments in the experimental section.
b. 1,4-dioxane associated with the complex.
c. chloroform-d_3.
d. water from chloroform-d_3.

d_3 is always similar to that found for the recrystallised products, and remains constant from the time of mixing up to 3 days in solution.

Table 3.5 *cis:trans* ratio of the crude unrecrystallised complexes $[Pt(H_2L)_2Cl_2]$ as determined from ^1H NMR spectra in chloroform-d_3 solution at 25 °C. The spectra were recorded within 3 minutes of dissolution.

H_2L	t (hr)	T (°C)	^1H NMR δ(ppm) (H^{10},$H^{10'}$)[a]	*cis:trans*
H_2L^1	1	25	11.80, 11.55	mainly cis
H_2L^1	17	25	11.80, 11.55	mainly cis
H_2L^2	1	25	11.79[b], 11.56[c]	mainly cis

a. H^{10} -.amide N-H of cis- isomer; $H^{10'}$-.amide N-H of trans- isomer.

b. H^{12} -.amide N-H of cis- isomer; $H^{12'}$-.amide N-H of trans- isomer.

3.2.1.4 Characterisation of unrecrystallised palladium complexes

Crude unrecrystallised products of $[Pd(H_2L^1)_2X_2]$ (X = Cl, Br) were also synthesised from K_2PdX_4 (X = Cl, Br) or $PdCl_2$ and H_2L^1 in HX / acetonitrile solution at 60 °C, for 30 minutes, for comparison with the platinum complexes. These complexes have been fully characterised. The Pd(II) complexes have sharp melting points and give satisfactory C, H and N analysis. Detailed data is given in Table 3.6.

Table 3.6 The characterisation data for crude unrecrystallised $[Pd(H_2L^1)_2X_2]$.

X	yield (%)	colour	m.p. (°C)	C. H. N. analysis (%)
Cl	91.4	orange	149-152	*calc.* 42.49, 4.54, 9.01
				obs. 42.89, 4.61, 9.16
Cl[a]	82.6	orange	150-152	*calc.* 42.49, 4.54, 9.01
				obs. 42.66, 4.67, 8.98
Br	81.1	orange	176-178	*calc.* 37.17, 3.97, 7.88
				obs. 37.51, 4.00, 7.85

a. $PdCl_2$ was used for the synthesis instead of K_2PdCl_4.

^{1}H NMR study

^{1}H NMR spectrum of the product formed by reacting ligand (H_2L^1) with K_2PdCl_4 (or $PdCl_2$) shows two peaks due to N-H amide proton resonances at 12.18 and 11.62 ppm in chloroform-d_3 (as shown in Figure 3.7a and 3.7b). According to the trend of corresponding platinum complexes, i.e. *cis-* isomer generally appears in the lower field, it is proposed that the chemical shift at 12.18 ppm is due to the N-H resonance of *cis-* $[Pd(H_2L^1)_2Cl_2]$; the chemical shift at 11.62 ppm is due to the N-H resonance of *trans-*$[Pd(H_2L^1)_2Cl_2]$. Interestingly, the *cis:trans* ratio of the product formed by reacting ligand with $PdCl_2$ is different from that of the product formed by reacting ligand with K_2PdCl_4.

The ^{1}H NMR spectrum of $[Pd(H_2L^1)_2Br_2]$ (Figure 3.7c) shows overlapping resonances at 11.17 ppm. From the integration of this spectrum and the crystal structure (see Chapter 5), it is clear that the chemical shift at 11.17 ppm represents two N-H resonances, namely the amide and thioamide of the *trans-* complex. The *cis:trans* ratio of $[Pd(H_2L^1)_2Cl_2]$ and $[Pd(H_2L^1)_2Br_2]$ are given in Table 3.7.

Table 3.7 *cis:trans* ratio of crude unrecrystallised complexes $[Pd(H_2L^1)_2X_2]$ as determined from ^{1}H NMR spectra in chloroform-d_3 at 25 °C.

X	^{1}H NMR δ(ppm) (H^{10}, $H^{10'}$)[a]	cis:trans (as%)
Cl	12.18, 11.62	30:70
Cl[b]	12.18, 11.62	mainly trans
Br	- , 11.17	only trans

a. H^{10} -amide N-H of cis- isomer; $H^{10'}$-amide N-H of trans- isomer.

b. $PdCl_2$ was used for synthesis instead of K_2PdCl_4.

From the Table 3.7, it is evident that the *cis:trans* ratio of $[Pd(H_2L^1)_2X_2]$ (prepared from K_2PdX_4 exactly as the platinum complexes) varies from 30:70 to only *trans-* as the halogen changes from chloride to bromide. It is also found that mainly *trans-* $[Pd(H_2L^1)_2Cl_2]$ is obtained when $PdCl_2$ is used as starting material.

Figure 3.7 A representative ^1H NMR spectrum of crude $[Pd(H_2L^1)_2X_2]$ in chloroform-d_3 at 25 °C.

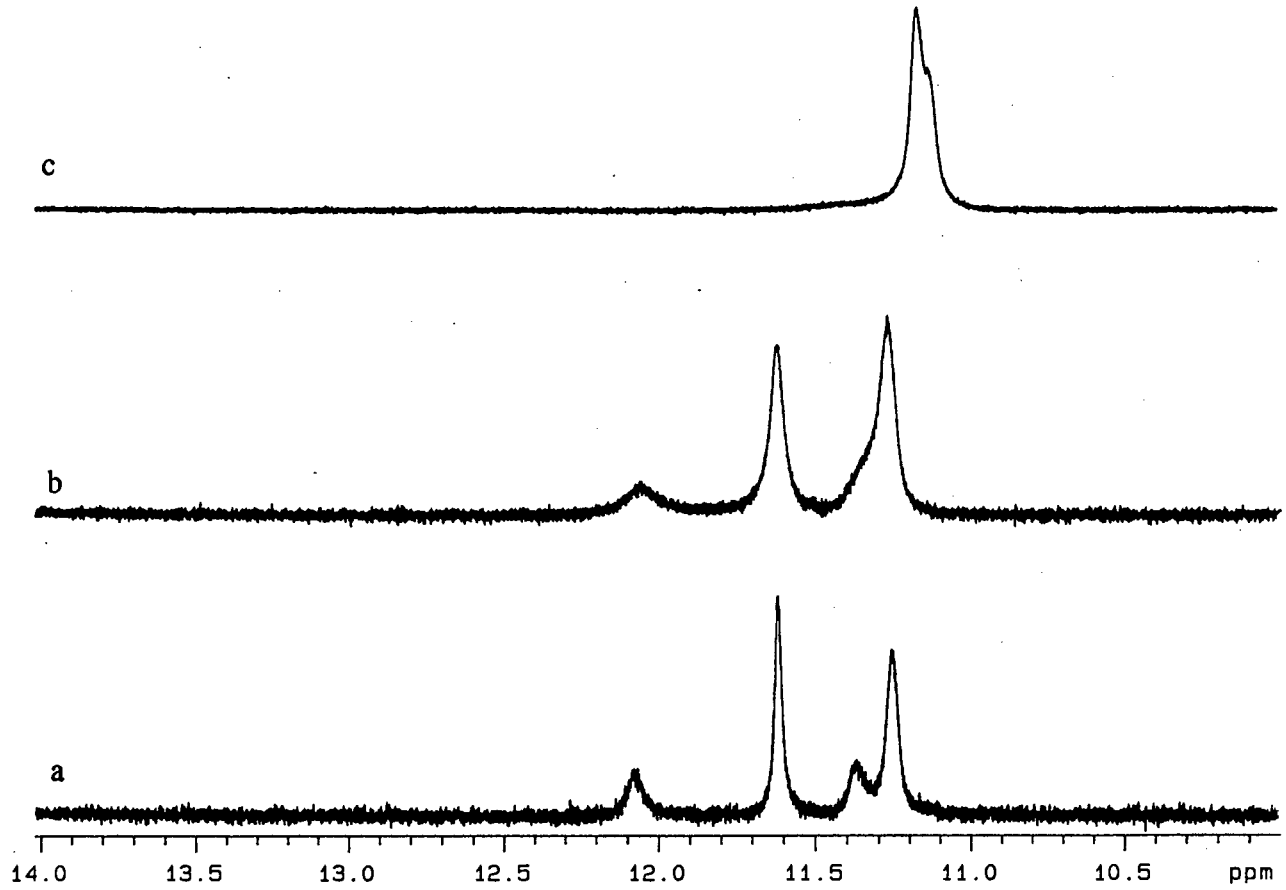

a. X=Cl *b. X=Cl* *c. X=Br.*

3.2.2 Kinetics for *cis-trans* isomerisation of $[Pt(H_2L^1)_2Cl_2]$

We have discovered that the *cis-trans* isomerisation for $[Pt(H_2L^1)_2Cl_2]$ can be conveniently investigated by following the time dependence of the ^1H NMR spectra in chloroform-d_3. The N-H amide proton resonances of this complex are selected for observation because of the simplicity of the spectrum in the region from 11.50 to 11.80 ppm. Solutions of known concentration of unrecrystallised complex in chloroform-d_3 were freshly prepared, and the ^1H NMR spectra are recorded as a function of time at a fixed temperature of 25 °C. Typically it is possible to start an experiment in less than 3 minutes after dissolving the complex in the chloroform-d_3, during which time negligible isomerisation takes place. Representative ^1H NMR spectra used for the kinetics study are shown in Figure 3.8. The *cis:trans* ratios for the isomers in solution are determined by integration of the respective resonance intensities of the N-H peaks. The *cis-trans* isomerisation was studied in a chloroform-d_3 solution of the crude product at various initial concentrations. A large number of experiments with different initial concentrations of the complex were examined to check for reproducibility of results, and test whether the system has reached equilibrium (The detailed results are presented in Appendix 1).

T_1 measurement by ^1H NMR

In order to ensure that the signal intensity of N-H resonance is proportional to the concentration of complex, the T_1 spin-lattice or longitudinal relaxation time for the N-H resonances has been measured for both diluted and concentrated solutions. It is necessary in F.T. NMR experiments to ensure that the delay between pulses is sufficiently long, otherwise the intensity of the peaks would be distorted due to relaxation effects. If too short a delay was allowed for T_1 values which are relatively long, the intensity of the resonances may not be proportional to the concentration of complex.

Figure 3.8 A representative ^1H NMR spectrum of kinetics for *cis-trans* isomerisation of crude $[Pt(H_2L^1)_2Cl_2]$ (initial concentration 0.00382M) in chloroform-d_3 at 25 °C.

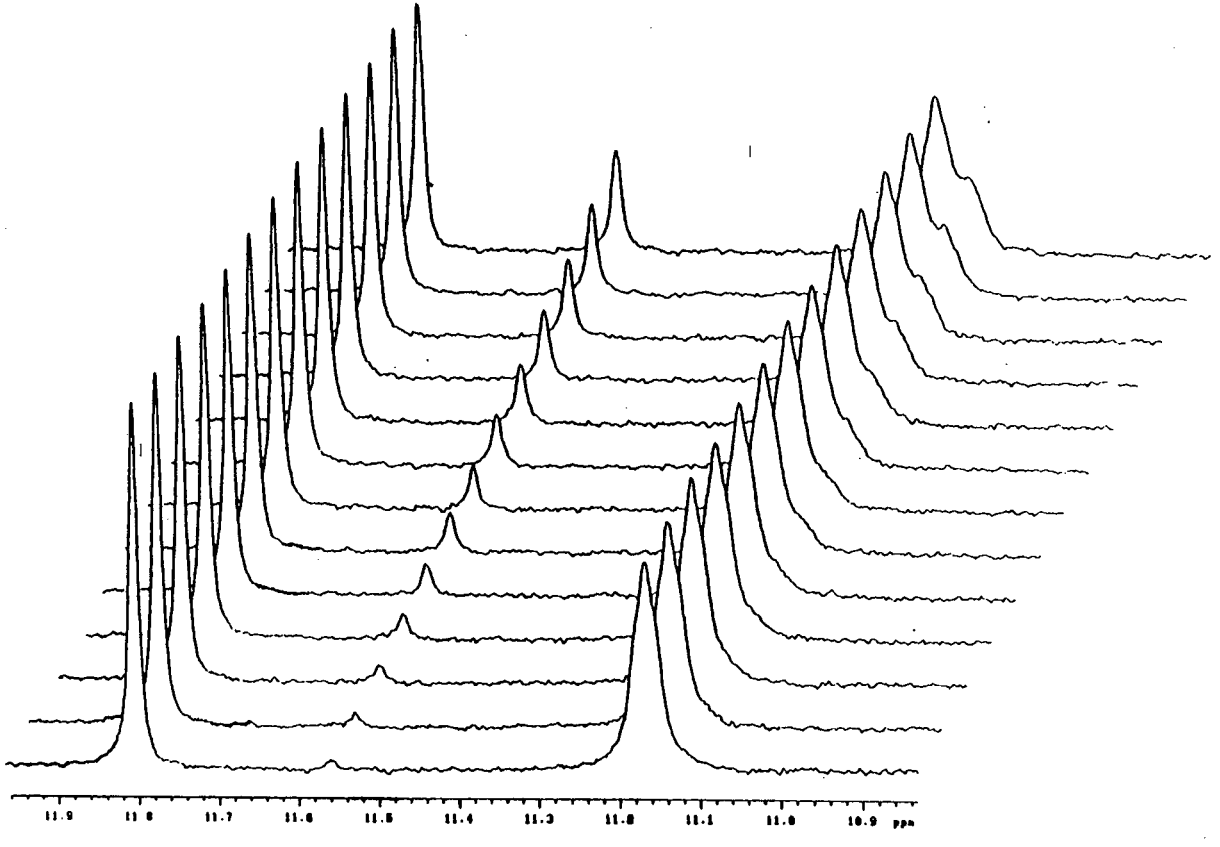

The T_1 values for solutions of $[Pt(H_2L^1)_2Cl_2]$ complex in chloroform-d_3 were thus measured by the standard inversion recovery method[21] and found to be *ca.* 0.82 - 0.85 seconds. Using these values, the minimum pulse repetition time t_r can be calculated from the Ernst equation[21]:

$$\cos \alpha = e^{-t_r / T_1} \qquad (2)$$

Where

α flip angle (Ernst angle[22])

t_r repetition time

T_1 longitudinal relaxation time

which gives a maximum value of S/N (signal-to-noise ratio). T_1 and t_r data are listed in Table 3.8.

Table 3.8 T_1 and t_r data for *cis-trans* isomerisation of $[Pt(H_2L^1)_2Cl_2]$ complex.

complex conc. ($\times 10^2$/M)	**T_1 (s)**		**t_r (s)**
	11.80ppm	11.55ppm	
0.42	0.82	0.82	0.12
2.94	0.86	0.84	0.12

For all kinetic experiments, therefore, a pulse delay of 1 or 2 seconds was introduced to ensure that complete relaxation of the ^1H resonances had occurred after each pulse. In this way it could be safely assumed that the resonance intensity of the N-H peak is proportional to the concentration of the platinum complex. The major parameters used in ^1H NMR spectra with different concentrations are summarised in Table 3.9.

Table 3.9 The major parameters used for measuring the ^1H NMR spectra at different complex concentrations in chloroform-d_3 at 25 °C.

conc. ($\times 10^2$/M)	pw	nt	at (s)	dl (s)	t_r*[a] (s)
0.381	6.8	32	2.503	1	3.503
0.420	6.8	32	2.503	2	4.503
0.660	6.8	32	2.503	2	4.503
1.065	6.8	16	2.503	2	4.503
1.628	6.8	16	2.503	2	4.503
2.774	6.8	32	3.744	1	4.744
3.116	6.8	16	2.503	2	4.503
4.080	6.8	16	2.503	2	4.503
5.350	6.8	16	2.503	2	4.503
6.230	6.8	16	2.700	1	3.700

a. t_r = at + dl, at-acquisition time; dl-delay time.*

Comparing Table 3.8 and 3.9, it is clear that the actual pulse repetition time t_r* is much longer than that predicted by the Ernst equation. In general a pulse repetition time of 5 times of the longest T_1 is necessary to ensure complete relaxation. Clearly, the signal intensity is proportional to the concentration of complex, under these conditions. Thus the following equations are reasonable.

$$I_e / I_t = x_e / x, \qquad (3)$$

$$I_o / I_c = c_o / c. \qquad (4)$$

Where,

I_e intensity of *trans-* isomer at equilibrium

I_t intensity of *trans-* isomer at various time

x_e concentration of *trans-* isomer at equilibrium

x concentration of *trans-* isomer at various time

I_o intensity of *cis-* isomer at very beginning of reaction

I_c intensity of *cis-* isomer at various time

c_o initial concentration of *cis-* isomer

c concentration of *cis-* isomer at various time.

Kinetic data analysis

The method of integration

For any general opposing reaction, the method of integration[23] is firstly used for the interpretation of kinetic data. The simplest opposing reaction, with both forward and reverse reactions of the first order, may be represented as

$$A \underset{k_r}{\overset{k_f}{\rightleftharpoons}} B. \qquad (5)$$

If the reaction is started using pure A, of concentration c_o, and if after t the concentration of B is x, and at equilibrium if the concentration of B is x_e, the reaction rate can be represented[23] as

$$\frac{dx}{dt} = \frac{k_f c_o}{x_e}(x_e - x), \qquad (6)$$

and its solution is

$$\frac{x_e}{c_o} \ln\frac{x_e}{x_e - x} = k_f t. \qquad (7)$$

Accordingly, *cis-trans* isomerisation of $[Pt(H_2L^1)_2Cl_2]$ is proposed to have the same situation. Thus $F(c) = x_e/c_o \cdot \ln[x_e/(x_e-x)]$, is plotted against time at different initial

concentrations of the complex. The slope of this plot represents the rate constant (forward). Where

$$x_e = \frac{K_e c_o}{1 + K_e}, \tag{8}$$

which comes from equilibrium constant

$$K_e = \frac{x_e}{c_o - x_e}. \tag{9}$$

K_e is obtained directly from *trans:cis* ratio of intensity of the ^{1}H NMR spectrum. The x is calculated by means of the resonance intensity according to equation (3). The representative plot is given in Figure 3.9.

Figure 3.9 A representative least-squares plot of F(c) *versus* time t, for the isomerisation of $[Pt(H_2L^1)_2Cl_2]$ complex at an initial concentration of 0.00381M.

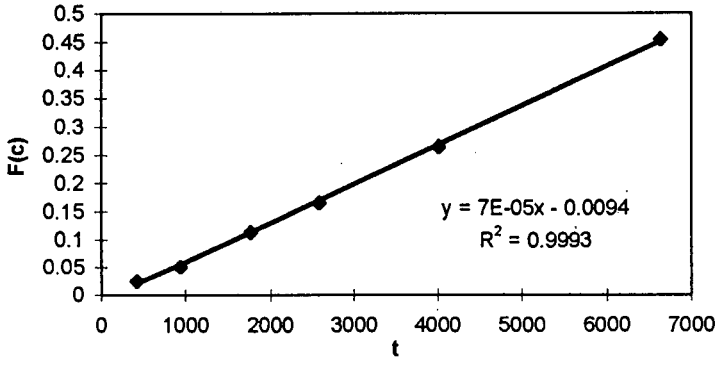

$F(c) = x_e / c_o \cdot ln[x_e/(x_e - x)]$

x_e *trans-*$[Pt(H_2L^1)_2Cl_2]$ *concentration at equilibrium;*

c_o *initial concentration of cis-*$[Pt(H_2L^1)_2Cl_2]$*;*

x *trans-*$[Pt(H_2L^1)_2Cl_2]$ *concentration corresponding time*

It is found that the F(c)-t curve is very good straight line, which means that a good fit of the mathematical model to the observed data is obtained, so this gives the rate constant (forward) for a fixed complex concentration. Interestingly, the observed rate constant (calculated from the slope of this curve) is different at various initial

concentrations of the complex (as shown in Table 3.10). If the reaction rate is first order, we would not expect that varying the concentration of the complex would change k_f. So that it is apparent that the method of integration cannot give us any idea of the order of the reaction. Thus, the differential method[23] is used to find the actual rate for this isomerisation.

Table 3.10 Apparent rate constants for *cis-trans* isomerisation of $[Pt(H_2L^1)_2Cl_2]$ complex, using the method of integration.

conc. ($\times 10^2$/M)	k_f ($\times 10^4/s^{-1}$)	conc. ($\times 10^2$/M)	k_f ($\times 10^4/s^{-1}$)
0.381	0.7	2.774	3.0
0.420	0.8	4.202	3.0
0.660	1.0	5.350	6.0
1.065	2.0	6.230	15.0
1.628	2.0		

Differential method

The differential method is concerned with the actual rates of reactions as determined by measuring the slope of concentration-time curves. The determination of accurate slopes is a matter of some practical difficulty before, but we are able to obtain the rate of reaction directly from the least-squares curve fitting of the experimental concentration-time data by using "MS-office Excel" program. If a reaction has an order of n, the rate, or velocity, v, of the reaction, may be related to the concentration of a reactant by the equation

$$v = k \cdot c^n. \qquad (10)$$

Taking logarithms,

$$\log(v) = \log(k) + n \log(c). \qquad (11)$$

If, therefore, the rate of the reaction is determined at various reactant concentrations, a plot of the logarithm(v) (initial rate) against the logarithm(c) should give a straight line, with slope n. The slope represents the order of the reaction (Letort[24] has referred to this order as the *order with respect to concentration*, or the *true order*, symbol n_c) with respect to the substance whose concentration c is being varied, and the intercept on the log(v) axis represents log(k).

In this study, the rate of the *cis-trans* isomerisation of $[Pt(H_2L^1)_2Cl_2]$ would be considered to have the same form as equation (10) and (11) at the very beginning of the reaction. The *initial rate* ($v_{initially}$) was calculated by differentiation of the least-squares equation of c-t curve (for example, Figure 3.10, all detailed curves obtained at various initial concentrations of *cis*-$[Pt(H_2L^1)_2Cl_2]$ are given in Appendix 1) according to the basic kinetic law[23]

$$v_{initially} = - (dc / dt)_{initially}. \qquad (12)$$

Where, the concentration of *cis*- isomer was calculated by using equation (4); the initial intensity of the N-H resonance of the *cis*- isomer was obtained by the least-squares equation of the intensity-time plot (see Appendix 1) at the very beginning of the reaction (t=0); the intensities of the N-H resonances at various time were directly obtained from the ^1H NMR results.

Figure 3.10 A representative concentration of *cis*-$[Pt(H_2L^1)_2Cl_2]$ plotted as a function of time (initial concentration 0.0066M).

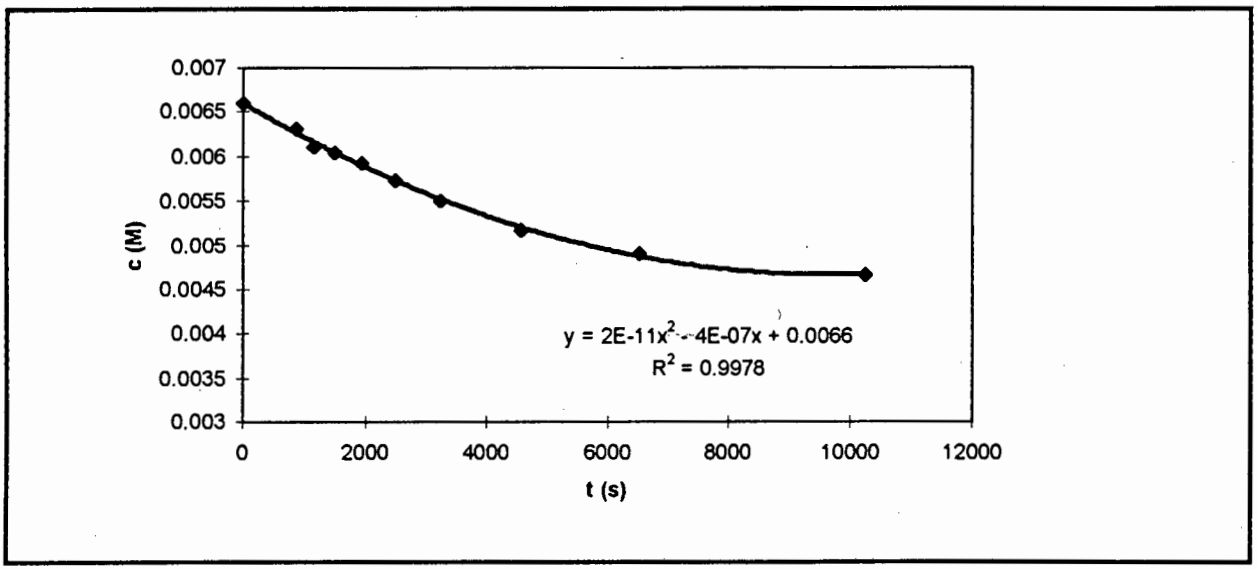

Accordingly, the rate constant and reaction order were obtained by a plot (Figure 3.11) of the logarithm($v_{initially}$) against the logarithm($c_{initially}$), where $c_{initially}$ is the initial concentration of *cis-* isomer. The slope represents the order of the reaction, and the intercept on the log($v_{initially}$) axis represents log(k_f) (equation 11).

Figure 3.11 Plot of the log($v_{initially}$) against log($c_{initially}$) using different initial concentrations for *cis-trans* isomerisation of $[Pt(H_2L^1)_2Cl_2]$ complex.

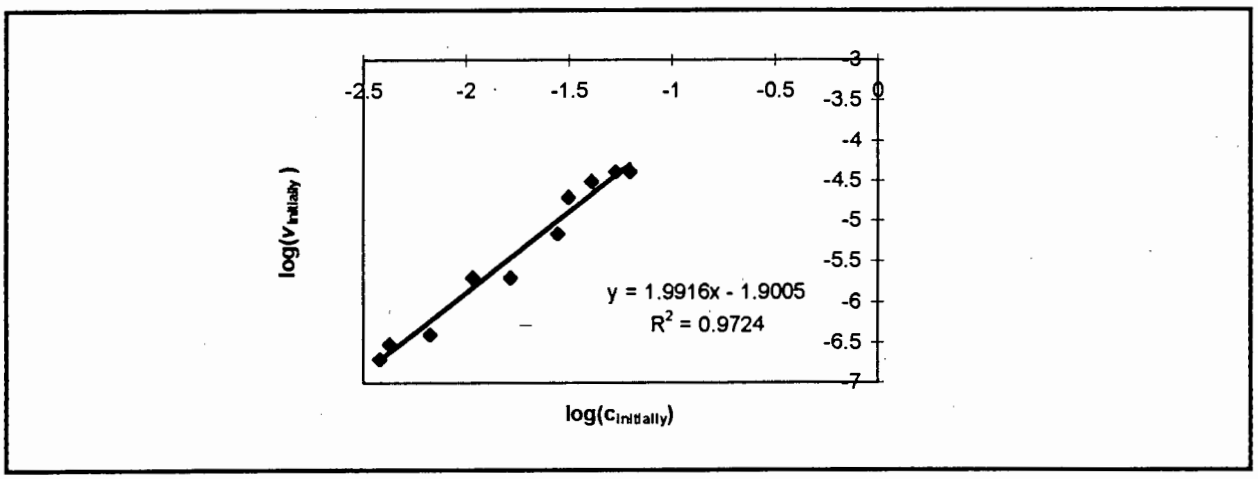

From Figure 3.11, it is clear that a plot of log($v_{initially}$) against log($c_{initially}$) gives a good straight line within experimental error. The slope of the curve is 1.9916 ≈ 2, which indicates a second order reaction (n_c = 2). The intercept on the log($v_{initially}$) axis equals to -1.9005, i.e. log(k_f) = -1.9005, so the forward rate constant k_f is calculated as 0.0126 $mol^{-1}.l.s^{-1}$. The results of kinetic studies appear in Table 3.11.

Table 3.11 Kinetic data for *cis-trans* isomerisation of $[Pt(H_2L^1)_2Cl_2]$ complex.

conc. ($\times 10^2$/M)	ini. rate ($\times 10^6$/M/s^{-1})	n_c	k_f (mol^{-1}.l.s^{-1})	k_r[a] (mol^{-1}.l.s^{-1})
0.381	0.2	2	0.0126	0.0288
0.420	0.3			
0.660	0.4			
1.065	2.0			
1.628	2.0			
2.774	7.0			
3.116	20.0			
4.080	30.0			
5.350	40.0			
6.230	40.0			

a. $k_r = k_f/K_e$, K_e directly measured (mean=0.4707) from ^{1}H NMR intensities at equilibrium.

From the results obtained, it may be concluded that the isomerisation of $[Pt(H_2L^1)_2Cl_2]$ follows second-order kinetics for opposing reactions, as these approach equilibrium

$$cis-[Pt(H_2L^1)_2Cl_2] \underset{k_r}{\overset{k_f}{\rightleftharpoons}} trans-[Pt(H_2L^1)_2Cl_2] \qquad (13)$$

To further investigate the kinetic properties and provide information on the mechanism of this isomerisation, the observed order at various times (n_t) is evaluated. The differential method can be applied by considering a single run, and measuring slopes at various times, corresponding to a number of values of the reactant concentration. Again the logarithms (v) are plotted against the logarithms(c). The slope is the order; since time is now varying Letort has referred to this order as the *order with respect to time, n_t.*

If the order with respect to time is *less* than the order with respect to concentration, the rate is falling off less rapidly with time than might have been expected. From this

it follows that there is some activation by the products of reaction; such an effect can be referred to as *auto-catalysis*. Conversely, if the order with respect to time is *more* than the order with respect to concentration, the rate is falling off more rapidly with time than might have been expected, which can only mean that some intermediate in the reaction is bringing about inhibition.

Accordingly, in this work, the logarithm of the rate against the logarithm of the concentration at various times, for example, in Figure 3.12, are plotted. n_t is obtained as less than (n_t = 1.8039) the true order (n_c = 2) at the beginning of the reaction (t = 0~43 min); and more than (n_t = 5.9345) the true order at the end of the reaction (t = 67~111 min). This suggests that the isomerisation of *cis*-$[Pt(H_2L^1)_2Cl_2]$ is auto-catalysed by intermediates formed at the beginning of the reaction, and is inhibited by the product at the end of the reaction. These results provide useful information for the investigation of the mechanism.

Figure 3.12 A representative plot of the log(v) against log(c) at initial concentration of 0.00381M.

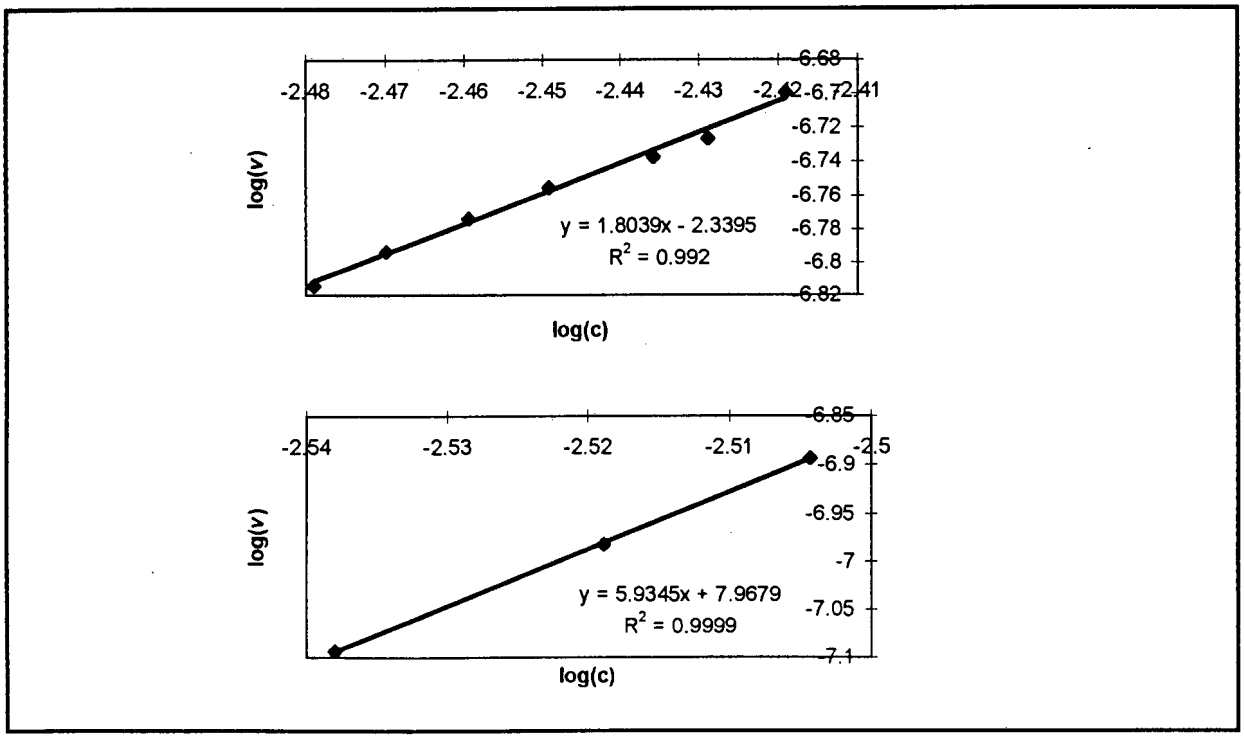

So far, the differential method has been successfully used to obtain the reaction order and rate constant. This method is less used even though Laidler[23] has concluded in his book, that if slopes (for getting the order of reaction) can be determined with high precision, then the differential method is a very powerful one and provides accurate kinetic parameters.

3.2.3 Mechanism for *cis-trans* isomerisation of $[Pt(H_2L^1)_2Cl_2]$

In general it is thought that intramolecular isomerisation for square-planar d^8 complexes is very unlikely, due to the high energy expected for the transition state. Dissociative or medium-assisted interchange mechanisms are more likely[11]. The kinetic results obtained in section 3.2.2 for the *cis-trans* isomerisation of $[Pt(H_2L^1)_2Cl_2]$, show clearly that the isomerisation is a second order reaction. A second order reaction for which rate = $k_f [Pt]^2$, implies that two complex molecules may collide to form an "activated complex" prior to dissociation into the products. It is thus reasonable to suggest, that the initial step in the isomerisation reaction involves the formation of an "activated complex" involving a dimeric species as shown in the scheme 3.1 below. From this dimeric species, there are two pathways to reach the final product.

Scheme 3.1 Postulated mechanisms for the *cis-trans* isomerisation of $[Pt(H_2L^1)_2Cl_2]$.

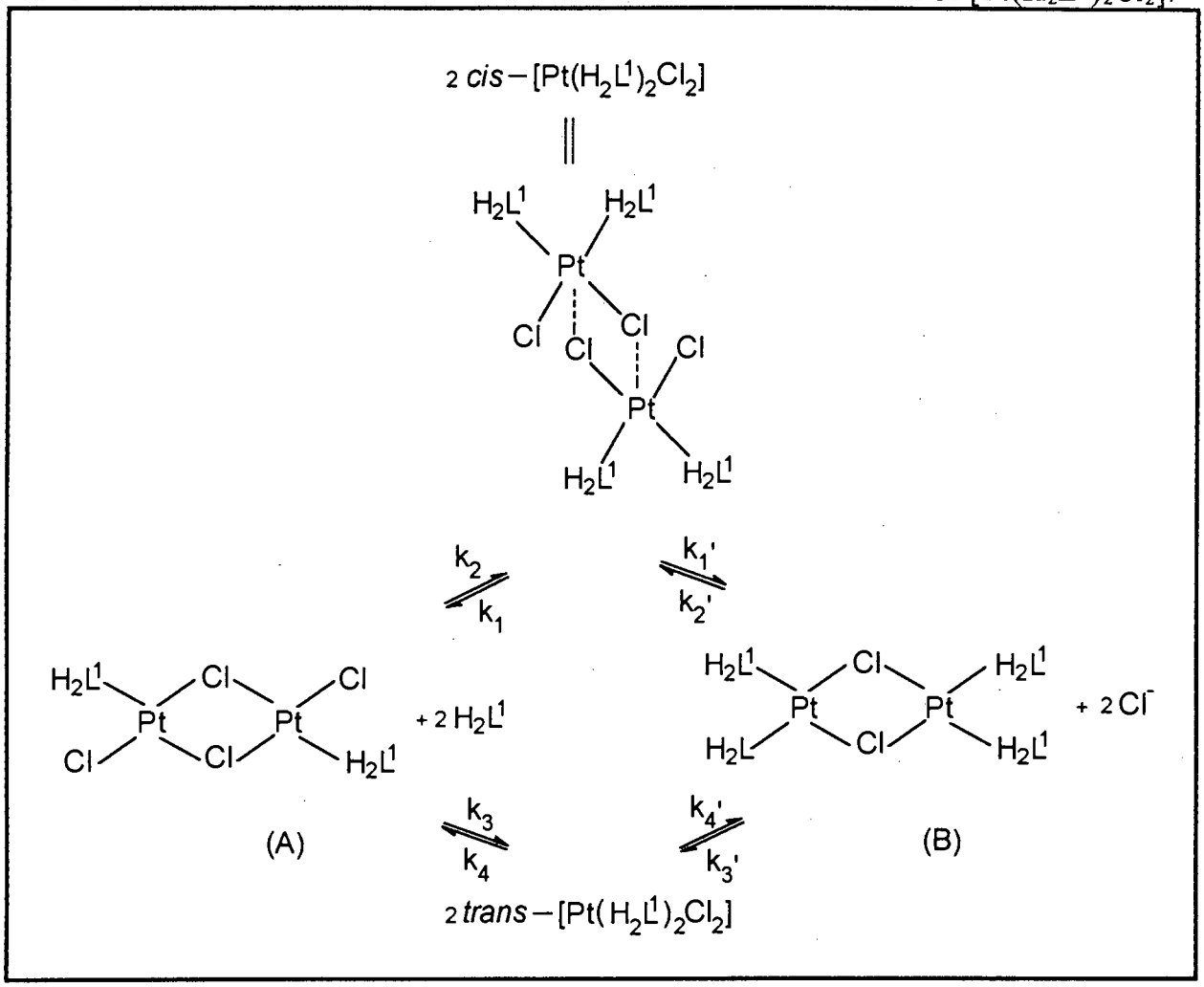

This idea is supported by the findings of Kitching, Moore and Doddrell[25], who have suggested that the *trans*-$[Pd(sulfoxide)_2Cl_2]$ isomerises via a chloro-bridged dimer in chloroform solution.

We thus suggest that our intermediate could also be a chloro-bridged dimer as shown in the Scheme 3.1. Thus, two kinds of chloro-bridged dimers can be postulated. One (A) is uncharged as the two sulphur donor ligands are lost; another (B) is charged as the two chloride ions may be lost. Furthermore, we also postulate that the unbound ligand or chloride ion may then act as a catalyst for the isomerisation.

In general it is possible to write rate expressions for the postulated mechanism in Scheme 3.1. The rate expressions for both these pathways are then in the same form:

$$-\frac{d\{cis-[Pt(H_2L^1)_2Cl_2]\}}{dt} = k_f\{cis-[Pt(H_2L^1)_2Cl_2]\}^2 - k_r\{trans-[Pt(H_2L^1)_2Cl_2]\}^2 \qquad (17)$$

where

$$k_f = \frac{k_1k_3}{k_2 + k_3} \qquad \text{or} \qquad k_f = \frac{k_1'k_3'}{k_2' + k_3'}$$

$$k_r = \frac{k_2k_4}{k_2 + k_3} \qquad \text{or} \qquad k_r = \frac{k_2'k_4'}{k_2' + k_3'}$$

These rate constants are obtained by means of the steady-state treatment[23] of intermediates (detailed calculation steps are given in Appendix 2).

In order to confirm the postulated mechanisms for the *cis-trans* isomerisation of $[Pt(H_2L^1)_2Cl_2]$, some more analysis of the experimental data and more experiments were carried out.

Comparison of k_f calculated using equation (17) to k_f obtained by the differential method

According to the postulated mechanism, the rate constants can be calculated at various times using equation (17) using ten different initial concentrations (results are presented in Table 3.12). The equation (17) can be rearranged as:

$$k_f = (dx/dt) / (c^2 - x^2/K_c) \; . \qquad (18)$$

where

x concentration of *trans*- isomer

c concentration of *cis*- isomer

K_e equilibrium constant $K_e = k_f / k_r$

The calculated values of k_f are tested by "Dixon's Q test"[26]. In this test, the difference between the outlier and the measurement nearest to it is compared with the range of the set of measurements. The ratio of these two differences without regard to sign, given the symbol Q, i.e.

$$Q = |(k_{f,m} - k_{f,m-1}) / (k_{f,max} - k_{f,min})|, \qquad (19)$$

is then compared with a critical value found from tables for the size of the sample at the required significance level ($p = 0.05$). As usual the null hypothesis is adopted if the outlier occurs because of chance and therefore should not be discarded. If the probability that such a value can occur is large then the null hypothesis is retained, if the probability is small the null hypothesis is rejected and the value is discarded.

Accordingly, the smallest value 0.0062 of all k_f calculated is chosen to do "Q" test. The Q calculated is 0.036 which is less than Q critical value ($Q_{critical} = 0.464$, from tables for sample size 10), so this smallest value of k_f should not be discarded. The largest value 0.0200 is also tested. The Q calculated is 0.275 which is also less than Q critical value. So that this largest value should be retained.

The calculated values of k_f can then be compared with those obtained by using the differential method (section 3.2.2). The good agreement between the calculated values deduced from the rate equation (17) and those obtained by the differential method of analysis data shown in Table 3.12, supports that the postulated mechanism, since consistent results are obtained.

Table 3.12 A series of rate constants calculated from experimental data as determined in chloroform-d_3 at 25 °C.

initial conc. ($\times 10^2$/M)	k_f^a ($mol^{-1}.l.s^{-1}$)	k_f^b ($mol^{-1}.l.s^{-1}$)	k_f^c ($mol^{-1}.l.s^{-1}$)
0.381	0.0144	0.0128 ± 0.00564	0.0126
0.420	0.0162		
0.660	0.0115		
1.065	0.0200		
1.628	0.0062		
2.774	0.0069		
3.116	0.0146		
4.080	0.0155		
5.350	0.0156		
6.230	0.0067		

a. calculated from equation (17), *b. average of ten values calculated,*

c. from the intercept of plot in Figure 3.11.

Effect of trace unbound ligand added on the rate of cis-trans isomerisation of $[Pt(H_2L^1)_2Cl_2]$

We found experimentally that the unbound ligand catalyses the isomerisation. Addition of a trace of free (unbound) ligand to a $[Pt(H_2L^1)_2Cl_2]$ solution in chloroform-d_3 catalyses the isomerisation to the equilibrium mixture. The time to equilibrium (t_e) in the solvent is largely decreased from 2 hours (absence of free ligand) to less than mixing time (*ca.* 3 min), whereas, the equilibrium constant is not significantly changed within experimental error. The compared data are given in Table 3.13.

Table 3.13 Effect of free ligand added for *cis-trans* isomerisation of $[Pt(H_2L^1)_2Cl_2]$ in chloroform-d_3 at 25 °C.

complex conc. ($\times 10^2$/M)	**free ligand conc. ($\times 10^2$ /M)**	**K_e**	**t_e (s)**
1.628	-	0.4721	5000
1.759	0.1016	0.5079	< 180

Effect of Cl^- added on the rate of cis-trans isomerisation of $[Pt(H_2L^1)_2Cl_2]$

We also found that the chloride ion added also catalyses the *cis-trans* isomerisation of $[Pt(H_2L^1)_2Cl_2$. The addition of a saturated solution (< 0.04 M) of $N(C_2H_5)_4^+Cl^-$ to *cis*-$[Pt(H_2L^1)_2Cl_2]$ in chloroform-d_3 increases the rate of isomerisation to equilibrium. Whereas, the equilibrium constant is slightly decreased compared to that in the absence of Cl^-. This could be expected as the effective polarity of the solution is expected to be much higher than for pure chloroform. The compared data are found in Table 3.14.

Table 3.14 Effect of Cl^- added for *cis-trans* isomerisation of $[Pt(H_2L^1)_2Cl_2]$ in chloroform-d_3 at 25 °C.

complex conc. ($\times 10^2$/M)	**$N(C_2H_5)_4^+Cl^-$ conc. ($\times 10^2$/M)**	**K_e**	**t_e (s)**
4.020	-	0.4921	1334
4.020	< 4.020	0.4084	< 180

From the Table 3.13 and 3.14, it is clear that adding a free ligand to a solution gives a similar result with adding Cl^- to a solution, i.e. leading to an increase in the rate of isomerisation, and the rapid establishment of equilibrium of the *cis-trans* mixture (generally within the time taken to dissolve the complex in the solvent used for ^1H

NMR). It is apparent that the chloride has the same function to *cis-trans* isomerisation as the ligand.

Effect of ligand exchange on the rate of cis-trans isomerisation of $[Pt(H_2L^1)_2Cl_2]$

In order to ascertain whether the Pt complex dissociates into an intermediate state as postulated in Scheme 3.1 can be demonstrated, i.e. a loss of ligand from Pt complex to form dimer, we expect rapid ligand exchange to form scrambled mixed-ligand complexes since the ligand *catalyses* the reaction. The effect of ligand exchange was thus further investigated.

Firstly, similar but different ligand (H_2L^3 = *N*-isopropyl-*N'*-benzoyl-thiourea) was added into a solution of the complex $[Pt(H_2L^1)_2Cl_2]$ in chloroform-d_3 in a 1:1 mole ratio. From the ^1H NMR spectrum (Figure 3.13), it is evident that the peak at 10.73 ppm is due to the unbound ligand (H_2L^1) N-H thioamide proton resonance. This means that the ligand can be lost from the Pt complex studied, and exchange rapidly takes place.

Secondly, another complex $[Pt(H_2L^2)_2Cl_2]$ (H_2L^2 = *N*-(*n*-propyl)-*N'*-naphthoyl-thiourea) was added into a solution of the complex $[Pt(H_2L^1)_2Cl_2]$ in a 0.9:1 mole ratio. The ^1H NMR spectrum (Figure 3.14) of this mixture in chloroform-d_3 shows the formation of the mixed-ligand complexes within the mixing time. The overall process can be represented in the following way[15]:

$$[Pt(H_2L^1)_2Cl_2] + [Pt(H_2L^2)_2Cl_2] \rightleftharpoons 2\,[Pt(H_2L^1)(H_2L^2)Cl_2] \qquad (19)$$

The ^1H NMR spectrum of this mixed solution at equilibrium is given in Figure 3.15. Considering both spectra (Figure 3.14 and 3.15), the ligand exchange process occurs

Figure 3.13 A representative ^{1}H NMR spectrum for effect of ligand added (H_2L^3) to [$Pt(H_2L^1)_2Cl_2$] in chloroform-d_3 at 25 °C.

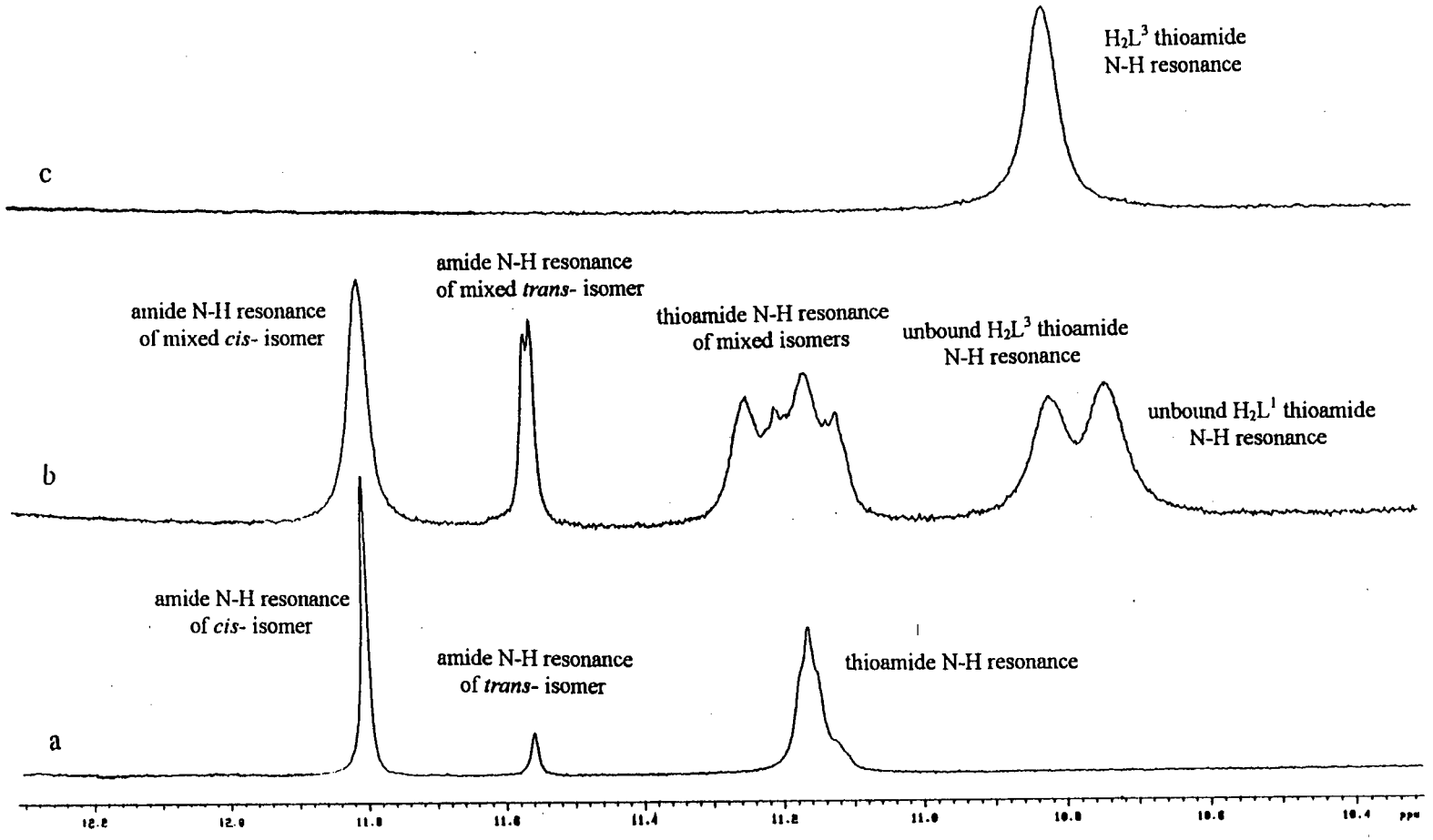

a. [$Pt(H_2L^1)_2Cl_2$] *b. [$Pt(H_2L)_2Cl_2$]+H_2L^3* *c. H_2L^3*

Figure 3.14 A representative ^{1}H NMR spectrum for effect of $[Pt(H_2L^2)_2Cl_2]$ added to $[Pt(H_2L^1)_2Cl_2]$ in chloroform-d_3 at 25 °C.

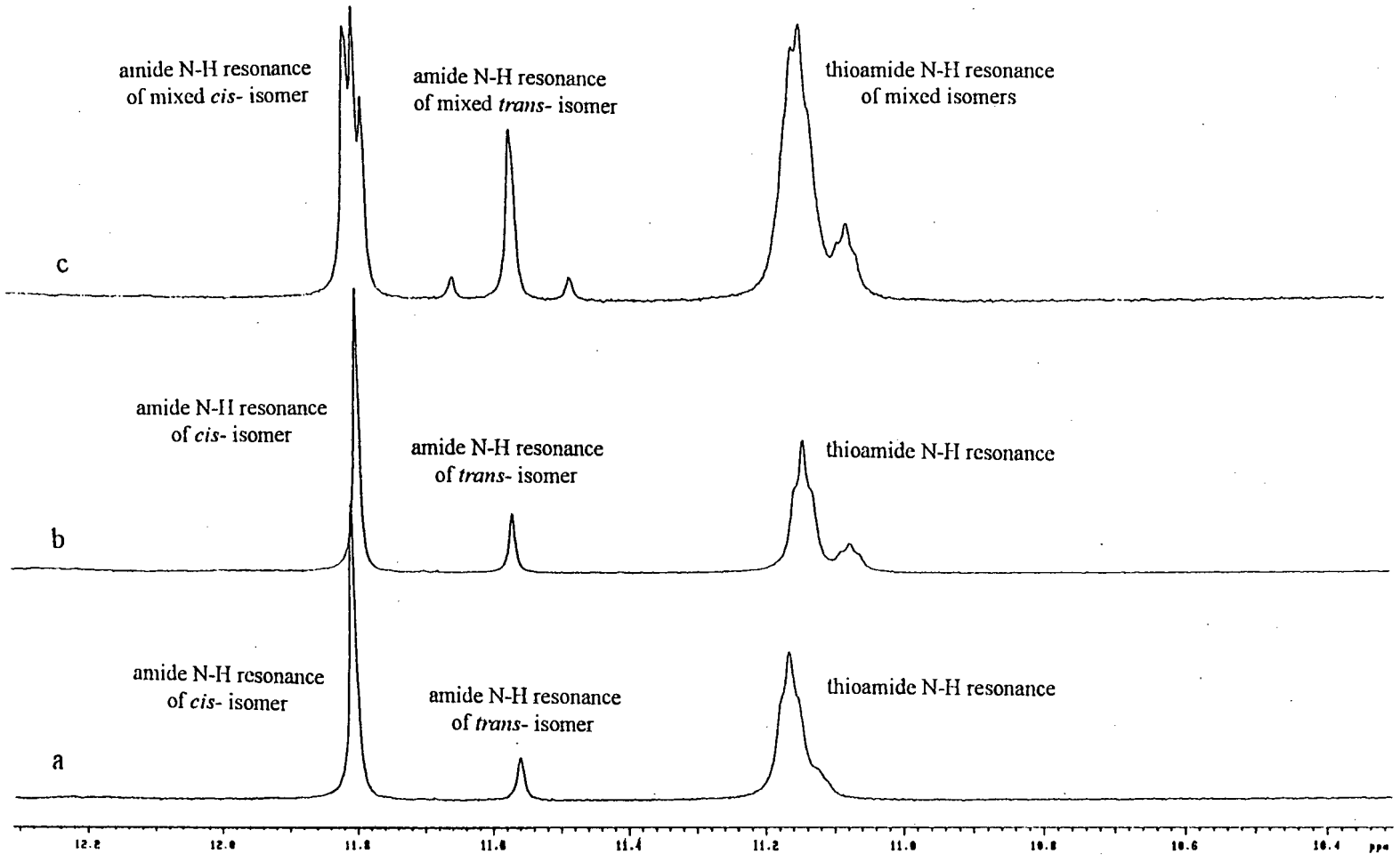

a. $[Pt(H_2L^1)_2Cl_2]$ *b. $[Pt(H_2L^2)_2Cl_2]$* *c. $[Pt(H_2L^1)_2Cl_2]$ and $[Pt(H_2L^2)_2Cl_2]$*

Figure 3.15 A representative ^{1}H NMR spectrum of mixture of $[Pt(H_2L^1)_2Cl_2]$ and $[Pt(H_2L^2)_2Cl_2]$ at equilibrium in chloroform-d_3 at 25 °C.

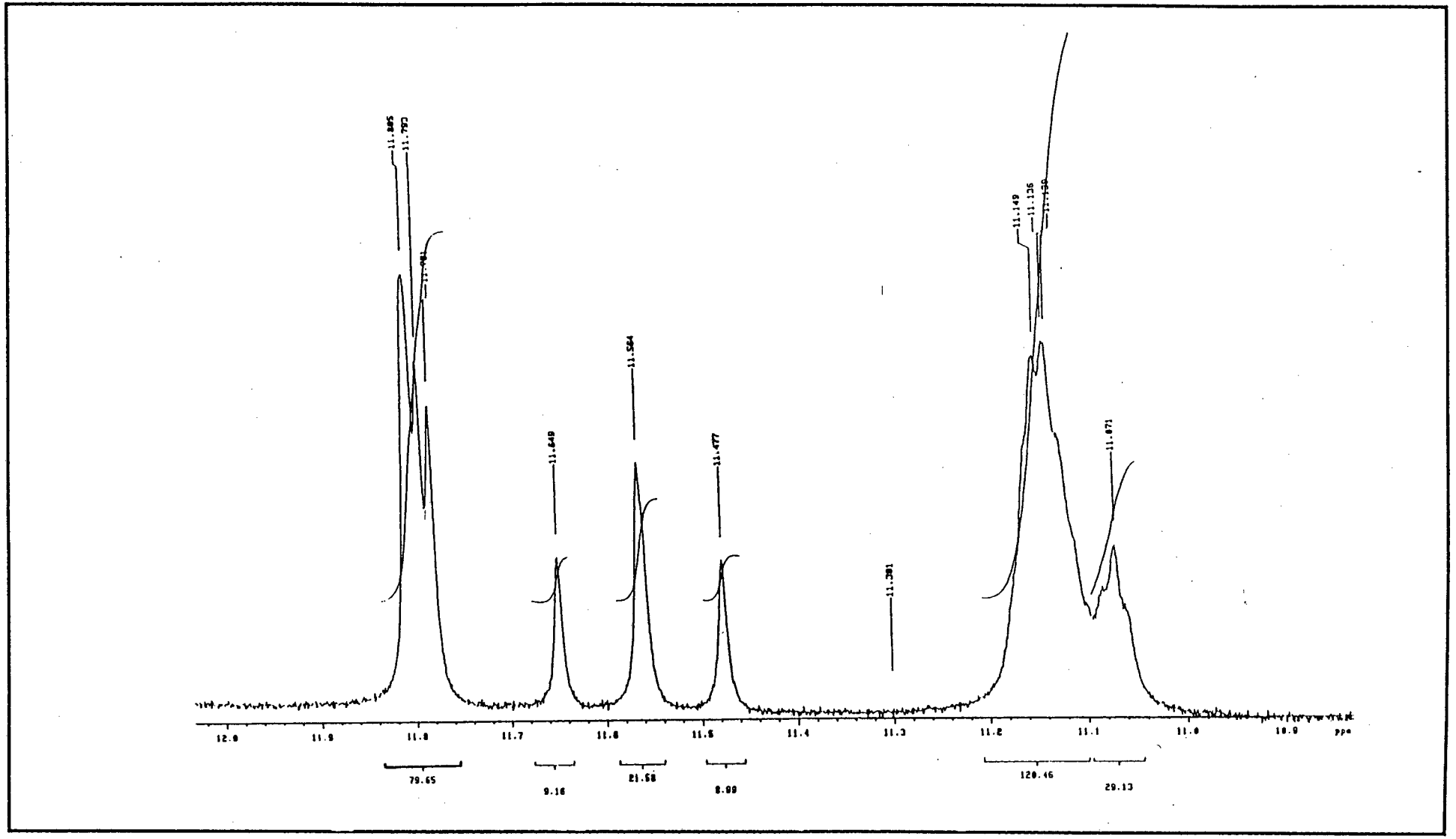

very rapidly on mixing the $[Pt(H_2L^2)_2Cl_2]$ to the fresh solution of *cis*-$[Pt(H_2L^1)_2Cl_2]$. This process is followed by a slower isomerisation from the *cis*- to *trans*- complexes as is seen from Figure 3.15, which shows the increase of the *trans*- mixed-ligand complex N-H resonances (at 11.65 ppm and 11.48 ppm) with time.

Unfortunately, we have not been able to obtain direct evidence for presence of the dimer in the ^1H NMR spectrum. Moreover, we have not been able to make pure $[Pt_2(H_2L^1)_2Cl_4]$ in order to determine the effect of dimer on the isomerisation of $[Pt(H_2L^1)_2Cl_2]$. Al-najjar and Al-lohedan[13] have nevertheless provided strong evidence by ^{31}P and ^{195}Pt NMR spectroscopy for an initial dimer formation which is intermediate in spontaneous *cis-trans* isomerisation of $[PtCl_2(PBu_3)(PhCN)]$. This finding supports our postulated mechanism.

3.2.4 Effect of solvent on the equilibrium constant, K_e, for the *cis-trans* isomerisation of $[Pt(H_2L^1)_2Cl_2]$

In general, K_e represents a equilibrium constant for the *cis-trans* isomerisation of $[Pt(H_2L^1)_2Cl_2]$, i.e.

$$K_e = [trans\text{-}] / [cis\text{-}]. \qquad (16)$$

The effect of the solvents on the equilibrium constant, K_e, for the *cis-trans* isomerisation of $[Pt(H_2L^1)_2Cl_2]$ was investigated in six solvents. Sufficient time was allowed for the isomerisation to reach equilibrium. In the case of benzene, isomerisation was very rapid, but for the more polar solvents, the solutions were kept at room temperature for several days in order to ensure that equilibrium had been reached. This could conveniently be monitored using ^1H NMR spectra of these solutions. The dielectric parameters of the non-deuterated solvents[26] and the equilibrium constants corresponding to that found in each solvent are shown in Table 3.15. A plot of effect of solvent is given in Figure 3.16.

Table 3.15 The equilibrium constants for *cis-trans* isomerisation of $[Pt(H_2L^1)_2Cl_2]$ in six solvents at 25°C.

solvent	dielectric parameter D	equilibrium constant K_e
nitromethane-d_3	38.6	0.16
N,N-dimethylformamide-d_7	36.7	0.23
acetone-d_6	20.5	0.28
tetrahydrofuran-d_8	7.39	0.39
chloroform-d_3	4.7	0.47
benzene-d_6	2.27	0.88

Figure 3.16 A plot of K_e for different solvents at 25 °C.

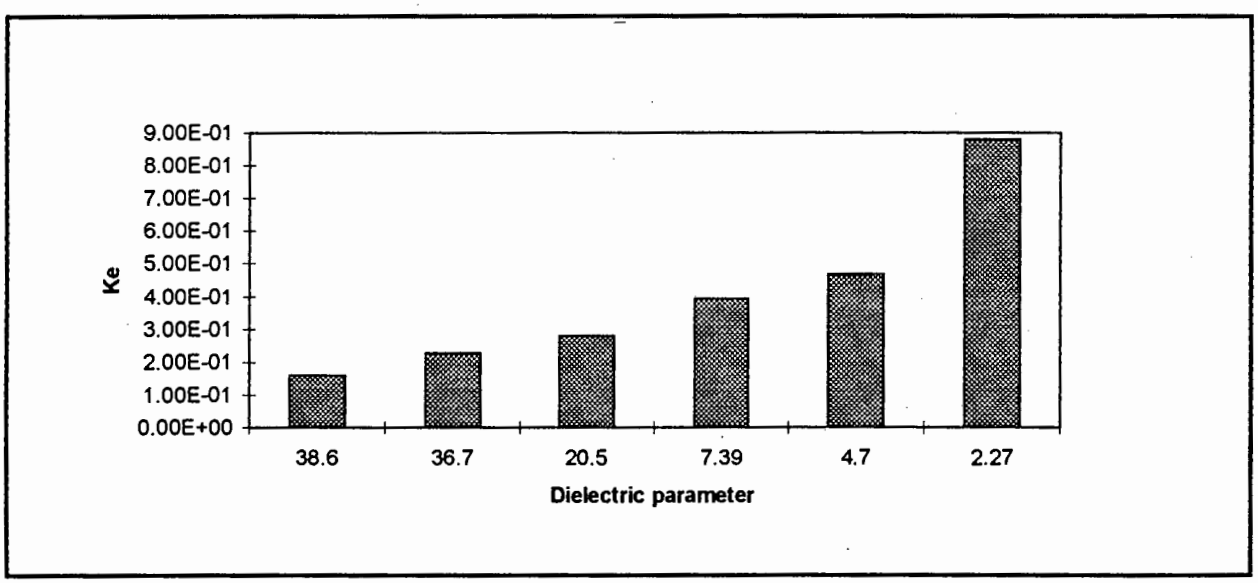

It is evident from Figure 3.16 that the equilibrium constant increases as the dielectric parameter of the solvent decreases. The *cis-* isomers are strongly favoured by polar solvents; the *trans-* isomers are favoured by non-polar solvents. This can be understood from the fact that the *cis*-$[Pt(H_2L^1)_2Cl_2]$ complex is more polar than the *trans-* complex, so that the tendency for the more polar solvent nitromethane to stabilise the polar *cis*-$[Pt(H_2L^1)_2Cl_2]$ is thus to be expected. Similar observations have also been previously made for the isomerisation of $[Pt(PR_3)_2Cl_2]$ complexes[6].

3.2.5 Thermodynamic parameters for *cis-trans* isomerisation of $[Pt(H_2L^1)_2Cl_2]$

The temperature dependence for *cis-trans* isomerisation of $[Pt(H_2L^1)_2Cl_2]$ was studied in the three solvents, chloroform-d_3, benzene-d_6 and DMF-d_7. The solutions were investigated by means of variable-temperature measurements, and sufficient time to equilibrate was allowed before final spectra at each temperature were recorded.

The thermodynamic properties were obtained by least-squares analysis of $\log(K_e)$ *vs.* 1/T plots. A linear trend was a proof that the system was in true equilibrium. A representative plot of these data in chloroform-d_3 is given in Figure 3.17. The other plots in benzene-d_6 and DMF-d_7 are found in Appendix 3. The thermodynamic data for this isomerisation in these three solvents are listed in Table 3.16. The values of ΔH, ΔS and ΔG in these three solvents were calculated according to following equations[23]:

$$\Delta G = -RT \ln(K_e) \quad \text{and} \quad \Delta G = \Delta H - T\Delta S \tag{14}$$

$$\log(K_e) = -\Delta H / 2.303R \cdot 1/T + 1/2.303R \cdot \Delta S \tag{15}$$

where

ΔH	enthalpy	T	Kelvin temperature
ΔS	entropy	K_e	equilibrium constant
ΔG	free energy	$R = 1.986$ cal.K^{-1}.mol^{-1}	

Figure 3.17 A representative least-squares plot of $\log(K_e)$ *vs.* 1/T for the isomerisation of $[Pt(H_2L^1)_2Cl_2]$ in chloroform-d_3.

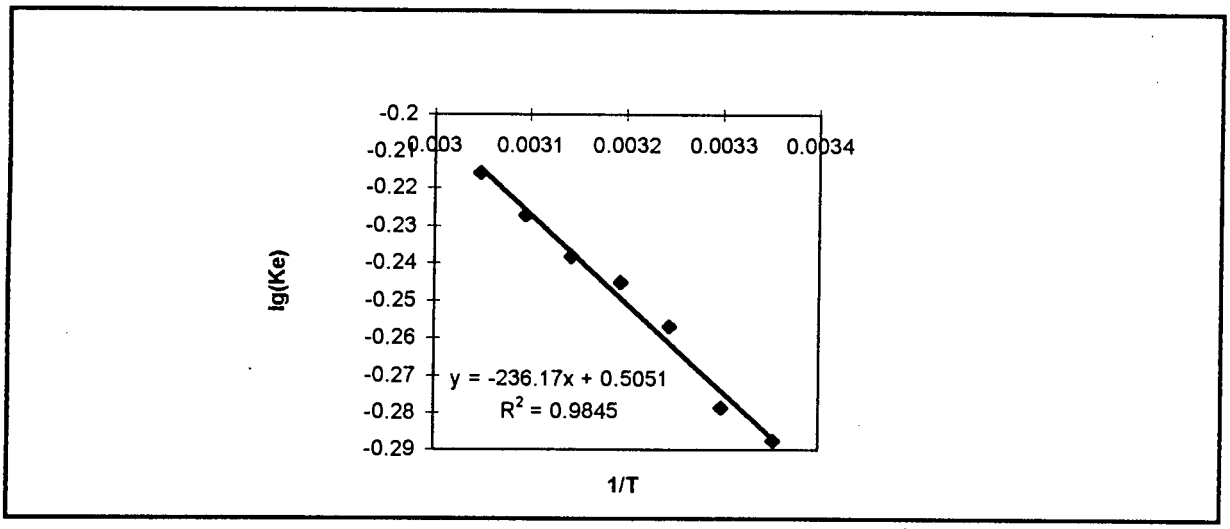

Table 3.16 Thermodynamic data for *cis-trans* isomerisation of $[Pt(H_2L^1)_2Cl_2]$.

solvent	dielectric parameter [26]	ΔH (kcal.mol^{-1})	ΔS (cal.mol^{-1}.K^{-1})	ΔG, 25°C (kcal.mol^{-1})
DMF-d_7	36.7	1.65	2.60	0.87
chloroform-d_3	4.7	1.08	2.31	0.39
benzene-d_6	2.27	2.82	9.12	0.10

It can be seen from the data in Table 3.16 that in all solvents investigated the *cis*-isomer is thermodynamically more stable than the corresponding *trans*- isomer and heat is consumed (enthalpy is always positive) in the transformation of the *cis*- into *trans*- isomer. Accordingly, the *cis*- isomer is enthalpy favoured in agreement with similar complexes reported in the literature[15]. In addition, ΔH for the isomerisation process is of similar magnetite to other square-planar platinum complexes (1.2 - 2.5 kcal.mol^{-1})[6, 9, 16];

In benzene-d_6 solution, ΔS is substantially greater than in DMF-d_7 and chloroform-d_3, but it is similar to other platinum complexes (9.4 - 14.2 cal.mol^{-1}.K^{-1})[9, 16]. These data indicate, as has previously been concluded for the isomerisation of square planar platinum complexes[9,15], that this spontaneous isomerisation process is entropy controlled. In DMF-d_7 and chloroform-d_3 solutions, the dominance of *cis*- isomers is

apparently the result of this entropy effect because of their smaller values of ΔS, compared with the less polar benzene solvent.

3.3 Conclusion

A series of complexes $[M(H_2L)_2X_2]$ have been synthesised. The tendency of formation of *trans-* isomers increases when M is substituted from Pt to Pd, and X is substituted from Cl to Br to I. The *cis*-$[Pt(H_2L^1)_2Cl_2]$ complex precipitates from the solution with a fixed amount of 1,4-dioxane associated and isomerises into a *cis-trans* mixture reaching equilibrium at very different rates in six solvents. The equilibrium constant K_e is related to the polarity of the solvent.

The *cis-trans* isomerisation of $[Pt(H_2L^1)_2Cl_2]$ has been studied kinetically in chloroform-d_3 solution. We find a second order process relative to the concentration of *cis-* isomer, i.e.

$$-\frac{d\{cis-[Pt(H_2L^1)_2Cl_2]\}}{dt} = k_f\{cis-[Pt(H_2L^1)_2Cl_2]\}^2 - k_r\{trans-[Pt(H_2L^1)_2Cl_2]\}^2$$

The results of kinetic studies suggest that this isomerisation is an auto-catalytic reaction. Many tests have been done to support the postulated mechanism. It was found that added unbound ligand and/or chloride ions catalyse the isomerisation process. Moreover ligand exchange studies suggest a rapid ligand exchange, yielding products consistent with the postulated mechanism.

3.4 Experimental

3.4.1 Synthesis and characterisation of $[M(H_2L)_2X_2]$

Commercially available chemicals were used. The general apparatus and analysis methods are the same as those described in Chapter 2.

The ligands were prepared according to the procedure of Douglass and Dains[1] as described in Chapter 2. 0.05 mol of potassium thiocyanate, benzoyl chloride (or naphthoyl chloride) and n-propylamine were used.

The complexes $[M(H_2L)_2X_2]$ were synthesised by means of the method reported by Bourne and Koch[4], and one typical procedure is given for each. A special apparatus was designed to control the reaction temperature accurately for preparing the complexes. It is shown in Figure 3.18. Where, A is a temperature regulated addition funnel; B is a thermostatic water pump; C is a stirring (micro-engine) with speed control.

Figure 3.18 The apparatus used to control the temperature in synthesis.

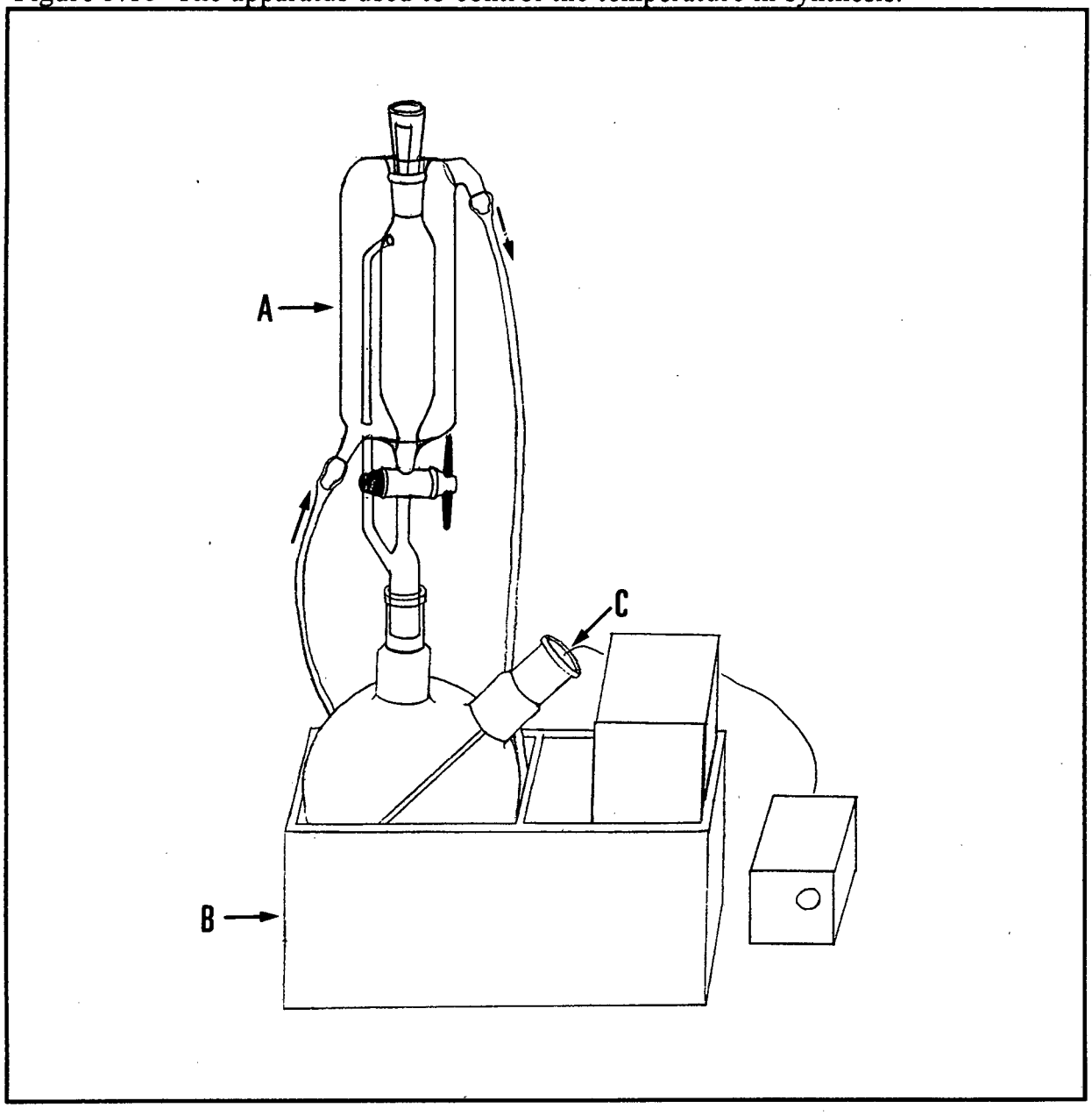

A. temperature regulated addition funnel *B. thermostatic water pump* *C. stirring with speed control.*

Synthesis of $[M(H_2L)_2Cl_2]$

30 ml of solution of 10% aqueous HCl / 1,4-dioxane (or 10% aqueous HCl / acetonitrile, 1:2) containing 0.25 mmol of K_2MCl_4 was added dropwise to a solution containing 0.50 mmol of ligand in 30 ml of the same solvent at given temperature (25,

60, or 85 °C) over a period of 15 minutes. The mixture was then stirred for a desired period of time at the same temperature. After cooling the mixture to room temperature, ice-water (200 ml) was added to the mixture. A bright yellow precipitate was obtained which was collected by filtration. The product was washed with cold water and ethanol, dried under vacuum. Recrystallisation of the crude product from chloroform-ethanol and drying under vacuum gave the product in good yield.

Synthesis of $[M(H_2L)_2Br_2]$

30 ml of solution of 10% aqueous HBr / 1,4-dioxane (or 10% aqueous HBr / acetonitrile, 1:2) containing 0.25 mmol of K_2MCl_4 and 25 fold molar[3] of NaBr was stirred for 1 hr at room temperature, which was then added dropwise to a stirred solution containing 0.50 mmol of ligand in 30 ml of the same solvent at given temperatures. The mixture was stirred for a desired period of time at the same temperature. The product was obtained as described for $[M(H_2L)_2Cl_2]$ above. Recrystallisation from chloroform-ethanol and drying under vacuum gave the product as orange crystals in good yield.

Synthesis of $[M(H_2L)_2I_2]$

30 ml of solution of 10% aqueous HI / 1,4-dioxane (or 10% aqueous HI / acetonitrile, 1:2) containing 0.25 mmol of K_2MCl_4 and 25 fold molar[3] of NaI was stirred for 1 hr at room temperature, which was then added dropwise to a solution containing 0.50 mmol of ligand in 30 ml of the same solvent at given temperature. The product was obtained as described for $[M(H_2L)_2Cl_2]$ above. Recrystallisation from chloroform-ethanol and drying under vacuum gave the product as a red crystal in good yield.

All products were characterised by means of melting points, C, H and N elemental analysis, ^{1}H NMR spectroscopy (all recorded in chloroform-d_3 otherwise specified) and infrared spectroscopy. The detailed data for all new products (except H_2L^1 and $[Pt(H_2L^1)_2Cl_2]$, which have been reported[4]) prepared are given bellow:

***N*-(*n*-propyl)-*N'*-benzoylthiourea - H_2L^1** 70.5% yield, m.p. 133-134 °C. *Calc.* for $C_{11}H_{14}N_2OS$: C,59.43; H,6.35; N,12.60%. *Obs.* C,59.64; H,6.47; N,12.64%. δ^1H: 10.73 (1H,s,H^4), 9.05 (1H,s,H^{10}), 7.81 (2H,d,H^5/H^9), 7.60 (1H,t,H^7), 7.48 (2H,d,H^6/H^8), 3.64 (2H,s,H^3), 1.74 (2H,s,H^2), 1.01 (3H,t,H^1) ppm.

***N*-(*n*-propyl)-*N'*-naphthoylthiourea - H_2L^2** 73.8% yield, m.p. 163-165 °C. *Calc.* for $C_{15}H_{16}N_2OS$: C,66.15; H,5.92; N,10.29%. *Obs.* C,66.58; H,6.16; N,10.22%. δ^1H: 10.76 (1H,s,H^4), 8.97 (1H,s,H^{12}), 8.33 (1H,d,H^5), 8.01 (1H,d,H^{11}), 7.90 (1H,d,H^9), 7.74 (1H,d,H^8), 7.63 (2H,t,H^7/H^{10}), 7.53 (1H,t,H^6), 3.71 (2H,s,H^3), 1.81 (2H,s,H^2), 1.07 (3H,t,H^1) ppm.

bis[*N*-(*n*-propyl)-*N'*-benzoylthiourea]dichloroplatinum - $[Pt(H_2L^1)_2Cl_2]$ The results of yield, m.p. and C, H and N analysis are found in Table 3.1a and 3.1b. δ^1H: 11.80 (2H,s,H^{10}), 11.56 (2H,s,$H^{10'}$), 11.14 (2H,t,H^4/), 11.10 (2H,t,$H^{4'}$), 8.20 (4H,d,H^5/H^9), 8.10 (4H,d,$H^{5'}/H^{9'}$), 7.62 (2H,t,$H^7/H^{7'}$), 7.52 (4H,t,$H^6/H^8/H^{6'}/H^{8'}$), 3.67 (4H,s,$H^{3'}$), 3.59 (4H,s,H^3), 1.78 (4H,s,$H^2/H^{2'}$), 1.04 (6H,t,$H^1/H^{1'}$) ppm.

bis[*N*-(*n*-propyl)-*N'*-benzoylthiourea]dibromoplatinum - $[Pt(H_2L^1)_2Br_2]$ The results of yield, m.p. and C, H and N analysis are found in Table 3.1a and 3.1b. δ^1H: 11.49 (2H,s,H^{10}), 11.31 (2H,s,$H^{10'}$), 11.00 (2H,t,$H^4/H^{4'}$), 8.21 (4H,d,H^5/H^9), 8.11 (4H,d,$H^{5'}/H^{9'}$), 7.62 (2H,t,$H^7/H^{7'}$), 7.52 (4H,t,$H^6/H^8/H^{6'}/H^{8'}$), 3.66 (4H,s,$H^{3'}$), 3.59 (4H,s,H^3), 1.80 (4H,s,$H^2/H^{2'}$), 1.06 (6H,t,$H^1/H^{1'}$) ppm.

bis[*N*-(*n*-propyl)-*N'*-benzoylthiourea]diiodoplatinum - $[Pt(H_2L^1)_2I_2]$ The results of yield, m.p. and C, H and N analysis are found in Table 3.1a and 3.1b. δ^1H: 11.52 (2H,t,H^4), 10.89 (2H,t,$H^{4'}$), 11.34 (2H,s,H^{10}), 10.99 (2H,s,$H^{10'}$), 8.14 (4H,d,$H^5/H^9/H^{5'}/H^{9'}$), 7.62 (2H,t,$H^7/H^{7'}$), 7.50 (4H,t,$H^6/H^8/H^{6'}/H^{8'}$), 3.69 (4H,s, H^3/H3'), 1.82 (4H,s,$H^2/H^{2'}$), 1.06 (6H,t,$H^1/H^{1'}$) ppm.

bis[*N*-(*n*-propyl)-*N'*-benzoylthiourea]dichloropalladium - $[Pd(H_2L^1)_2Cl_2]$ The results of yield, m.p. and C, H and N analysis are found in Table 3.4. δ^1H: 12.18 (2H,s,H^{10}), 11.62 (2H,s,$H^{10'}$), 11.39 (2H,t,H^4), 11.26 (2H,t,$H^{4'}$), 8.20 (4H,d, H^5/H9), 8.09 (4H,d, $H^{5'}/H^{9'}$), 7.61 (2H,t,$H^7/H^{7'}$), 7.51 (4H,t,$H^6/H^8/H^{6'}/H^{8'}$), 3.66 (4H,s, $H^3/H^{3'}$), 1.80 (4H,s,$H^2/H^{2'}$), 1.05 (6H,t,$H^1/H^{1'}$) ppm.

bis[*N*-(*n*-propyl)-*N'*-benzoylthiourea]dibromopalladium - $[Pd(H_2L^1)_2Br_2]$ The results of yield, m.p. and C, H and N analysis are found in Table 3.4. δ^1H: 11.17 (4H,b,$H^{10'}$/ $H^{4'}$), 8.14 (4H,d,$H^{5'}/H^{9'}$), 7.63 (2H,t,$H^{7'}$), 7.51 (4H,t,$H^{6'}/H^{8'}$), 3.68 (4H,s, $H^{3'}$), 1.81 (4H,s,$H^{2'}$), 1.05 (6H,t,$H^{1'}$) ppm.

bis[*N*-(*n*-propyl)-*N'*-naphthoylthiourea]dichloroplatinum - $[Pt(H_2L^2)_2Cl_2]$
The results of yield, m.p. and C, H and N analysis are found in Table 3.4. δ^1H: 11.79 (2H,s,H^{12}), 11.56 (2H,s,$H^{12'}$), 11.13 (2H,b,H^4), 11.06 (2H,b,$H^{4'}$), 8.44 (2H,d,H^5), 8.30 (2H,d,H^{11}), 8.12 (2H,d,$H^{5'}/H^{11'}$), 7.99 (2H,d,$H^9/H^{9'}$), 7.87 (2H,d,$H^8/H^{8'}$), 7.51 (6H,t,$H^{10}/H^6/H^7/H^{7'}/H^{10'}/H^{6'}$) ppm.

3.4.2 Kinetics determination for *cis-trans* isomerisation of $[Pt(H_2L^1)_2Cl_2]$

Information regarding the kinetics of the isomerisation reaction in chloroform-d_3 was obtained from the rates of disappearance of the ^{1}H NMR resonance (H^{10}) for the *cis*-isomer and the appearance of the resonance ($H^{10'}$) for the *trans*- isomer.

All ^{1}H NMR spectra for kinetics of isomerisation were recorded in chloroform-d_3 using 5 mm tubes and a Unity-400 Fourier Transform spectrometer, operating at 399.95 MHz at 25 °C. A pulse delay of 1-2 seconds was included following an excitation pulse of *ca* 30 °, to allow sufficient time for complete relaxation of all resonances. Typically 16 transients were acquired for each spectrum. All ^{1}H NMR chemical shifts were referred to the central line of the chloroform-d_3 at 7.25 ppm relative to tetramethylsilane.

A fresh solution of a weighed complex was dissolved in a fixed volume 0.6 cm^3 of chloroform-d_3, and rapidly dissolved at room temperature. The sample was then placed into the spectrometer with the minimum time, the spectrometer set up to record the experiment all within generally less than 3 minutes. The time from mixing to the starting of the experiment was recorded.

The acquisition time for each spectrum was 0.9-1.2 minutes, so for slow rates of isomerisation the extent reaction was negligible. An automatic time-arranged experiment was set up, so acquiring a series of ^{1}H NMR spectra as a function of time under identical conditions and constant temperature. Sufficient time intervals were allowed for the system to reach equilibrium. From the intensity *v.s.* time data the rates of isomerisation were obtained as explained in section 3.2.2.

The temperature dependence experiments were examined by adding trace of the ligand (as known to save time to reach equilibrium) between 25-55 °C in three solvents respectively. The solvent dependence experiments were carried out in six organic solvents at 25 °C.

References

1. I.B. Douglass and F.B. Dains, *J. Am. Chem. Soc.*, 1934, **56**, 719.
2. L. Beyer and E. Hoyer, *Z. Chem.*, 1981, **21**, 81.
3. K.R. Koch , A. Irving and M. Matoetoe, *Inorg. Chim. Acta*, 1993, **206**, 193.
4. S. Bourne and K.R. Koch, *J. Chem. Soc., Dalton Trans.* 1993, 2071.
5. K.R. Koch, unpublished work.
6. J. Chatt and R.G. Wilkins, *J. Chem. Soc.*, 1952, **274**, 4300.
7. E.G. Cox, H. Saenger and W. Wardlaw, *J. Chem. Soc.*, 1934, 182.
8. G.B. Kauffman and D.O. Cowan, *Inorg. Synth.*, 1960, **6**, 211.
9. R. Roulet and C. Barbey, *Hel. Chim. Acta.*, 1973, **56**, 2179.
10. D.A. Redfield and J.H. Nelson, *Inorg. Chem.*, 1973, **12**, 15.
11. J.H. Price, J.P. Birk and B.B. Wayland, *Inorg. Chem.*, 1978, **17**, 2245.
12. G. Annibale, M.Bonivento, L. Canovese, L. Cattalini, G. Michelon and M.L. Tobe, *Inorg. Chem.*, 1985, **24**, 797.
13. I.M. Al-Najjar, H.A. Al-Lohedan and Z.A. Issa, *Inorg. Chimica Acta*, 1988, **143**, 119.
14. F.M. Macdonald and P.J. Sadler, *Polyhedron*, 1991, **10**, 1443.
15. Gordon K. Anderson and Ronald J. Cross, *Chem. Soc. Rev.*, 1980, **9**, 185.
16. F. Basolo and R.G. Pearson, " *Mechanisms of Inorganic Reactions* ", 2nd ed, Wiley, New York, N.Y., 1967, 424.
17. D.G. Cooper and J. Powell, *J. Amer. Chem. Soc.*, 1973, **95**, 1102.
18. J. E. Huheey, " *Inorganic Chemistry, Principles of Structure and Reactivity*", Harper & Row, New York, 1978.
19. P.S. Pregosin, *Coord. Chem. Rev.*, 1982, **44**, 247.
20. D.M. Adams and J.B. Cornell. *J. Chem. Soc. (A)*, 1967, 884.
21. L. Rabenstein, *J. Chem. Education.* 1984, **61**, 911.
22. R.R. Ernst and W.A. Anderson, *Rev. Sci. Inst.*, 1966, **37**, 93.
23. K. J. Laidler, " *Reaction Kinetics* ", Volume One, Pergamon Press, Oxford, 1963.
24. M. Letort, Thesis, University of Paris, 1937; *J. Chim. Phys.*, 1937, **34**, 206; *Bull. Soc. Chim. France*, 1942, **9**, 1.
25. W. Kitching, C.J. Moore and D. Doddrell, *Inorg. Chem.*, 1970, **9**, 541.

26. J.C. Miller and J.N. Miller, "*Statistics for Analytical Chemistry*", Ellis Horwood, Chichester, 1984.

27. J. Burgess, "*Metal Ions in Solution*", Pub. Ellis Hovwood Ltd., 1978, 32.

CHAPTER 4

Synthesis And Characterisation Of Novel Metallomesogens Based On *Trans*-Bis(*N*-alkyl-*N*'-acylthiourea)dihaloplatinum(II) Complexes

4.1 Introduction

Metallomesogens, metal complexes of organic ligands which exhibit liquid crystalline (mesogenic) character, have been intensively studied during the last decade. The extraordinary physical properties of these substances: vivid colours, pronounced birefringence, dichroism and unusually strong optical nonlinear effects[1]; may result in numerous potential applications in electronic devices and elsewhere. Most work has concentrated on organic materials, but recent developments have highlighted the many new possibilities which can result from the introduction of one or more metals into a liquid crystal; there are, after all, some sixty metals which can, in principle be coordinated[2]. A major requirement for metallomesogens to find applications in new device technology is that the metal-ligand bonds are strong and inert and the complexes stable. This can be accomplished with, for example, chelating ligands and the 5d metals.

4.1.1 Classification of mesogenic substances (liquid crystals)

Liquid crystals constitute a state of matter intermediate between the solid and the liquid phase. The physical properties of liquid crystals have been related to general aspects of their molecular and supramolecular structure[3]. The terms *mesomorph* and *mesophase* are also used. A *mesogen* is the molecule which gives rise to a mesophase.

Generally, liquid crystals can be divided into two broad families, the *thermotropics* and the *lyotropics*. Thermotropic liquid crystals undergo a phase change on heating or cooling; the crystal phase melts to the mesophase, which then clears to the isotropic liquid at a higher temperature. Lyotropic phases are formed by suitable molecules in solution and the appearance of the mesophase is controlled by both concentration and temperature. Thermotropics can be sub-divided into *enantiotropic* and *monotropic* according to their behaviour on either heating or cooling. Enantiotropic liquid crystals change phase on heating as well as cooling, while monotropic liquid crystals generally change phase on cooling. In terms of the structure of molecules, thermotropics can further be sub-divided into *calamitic* (reed- or rodlike) and *discotic* (disklike).

Rodlike thermotropics form two broad classes *nematics* and *smectics*. Other mesophases are not described here because of their irrelevance to this study. A summary of the different types of mesogens is given in Figure 4.1.

Figure 4.1 Sub-classification of mesogens.

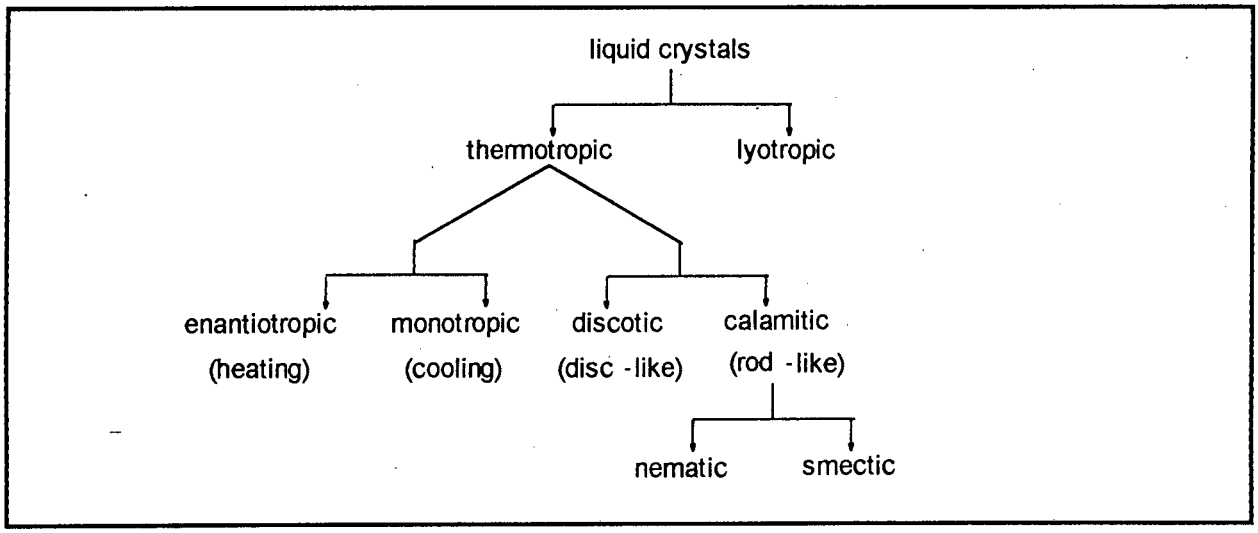

The transition from the true crystal phase to the mesophase is often termed the melting point, and the transition from highest temperature mesophase to the isotropic is the clearing point. The mesophases often appear turbid while the isotropic liquid is clear. In the case of non-mesogenic substances, the melting and clearing points coincide.

4.1.2 Identification of the mesophases

Once a complex has been synthesised, there are three different techniques which are used to identify whether the material possesses mesogenic character. The techniques include (a) polarising hot-stage optical microscopy, (b) differential scanning calorimetry (DSC) and (c) low angle X-ray scattering in the mesophase. The polarising optical microscopy is usually the first and easiest technique used to characterise thermotropic mesophases and is indispensable to the observation of liquid crystals. The DSC provides essential supplementary thermodynamic information to phase identification and a measurement of the magnitude of heat change and temperature at which physical changes occur in a substance during heating and

cooling processes. It also provides a direct measure of the enthalpy and entropy of each phase transition.

4.1.3 *trans*-bis(*N*-acylthiourea)diiodoplatinum(II) as metallomesogens

We have known that some modified *N*-alkyl-*N'*-acylthioureas display mesogenic properties[4]. From Chapter 3 we found that the iodo complexes $[Pt(H_2L)_2I_2]$ (H_2L=*N*-alkyl-*N'*-benzoylthiourea) are mainly *trans*-. To investigate the mesogenic properties of complexes, a series of new *trans*-bis(*N*-acylthiourea)diiodoplatinum(II) (*1-7*) complexes were synthesised and characterised in the hope of being able to prepare metallomesogens. The complexes that were prepared are shown in Figure 4.2. In order to compare the mesogenic properties of the corresponding palladium complexes from the same ligands with the corresponding diiodo-platinum metallomesogens (*3, 6, 7*), the complexes *trans*-bis(*N*-acylthiourea)dihalopalladium(II) (*8, 9, 10*) were synthesised and the properties investigated (Figure 4.3). Each of the complexes synthesised is considered to have a thin elongated molecular shape, a reasonably rigid core and easily polarisable groups which are a prerequisite for liquid-crystalline behaviour. A prerequisite for the desired rod-like structure is the intramolecular hydrogen bond of the *N*-alkyl-*N'*-acylthiourea locking the potential chelate moiety into a planar six-membered ring[5]. This ring would behave like a phenyl ring.

The main focus of this chapter is to discuss the synthesis of metallomesogens and to determine the influence (if any) of the nature of the substituents R and R', on the mesogenic behaviour of these complexes. R and R' (Figure 4.2 and Figure 4.3) are varied as follows:

1. R = H; R' = $C_{12}H_{25}$, $C_{14}H_{29}$, $C_{16}H_{33}$
2. R = H; R' = C_8H_{17}
3. R = $OC_{12}H_{25}$; R'= C_8H_{17}
4. R = C_7H_{15}; R'= OC_6H_{13}
5. R = OC_7H_{15}, $OC_{12}H_{25}$; R'= C_6H_{13}
6. R = OC_7H_{15}; R'= OC_5H_{17}
7. R = C_6H_{13}; R'= $C_{12}H_{25}$
8. R = $OC_{12}H_{25}$; R'= C_8H_{17}
9. R = OC_7H_{15}; R'= OC_5H_{17}
10. R = C_6H_{13}; R'= $C_{12}H_{25}$

Figure 4.2 Schematic representation of the general structure of $[Pt(H_2L)_2I_2]$.

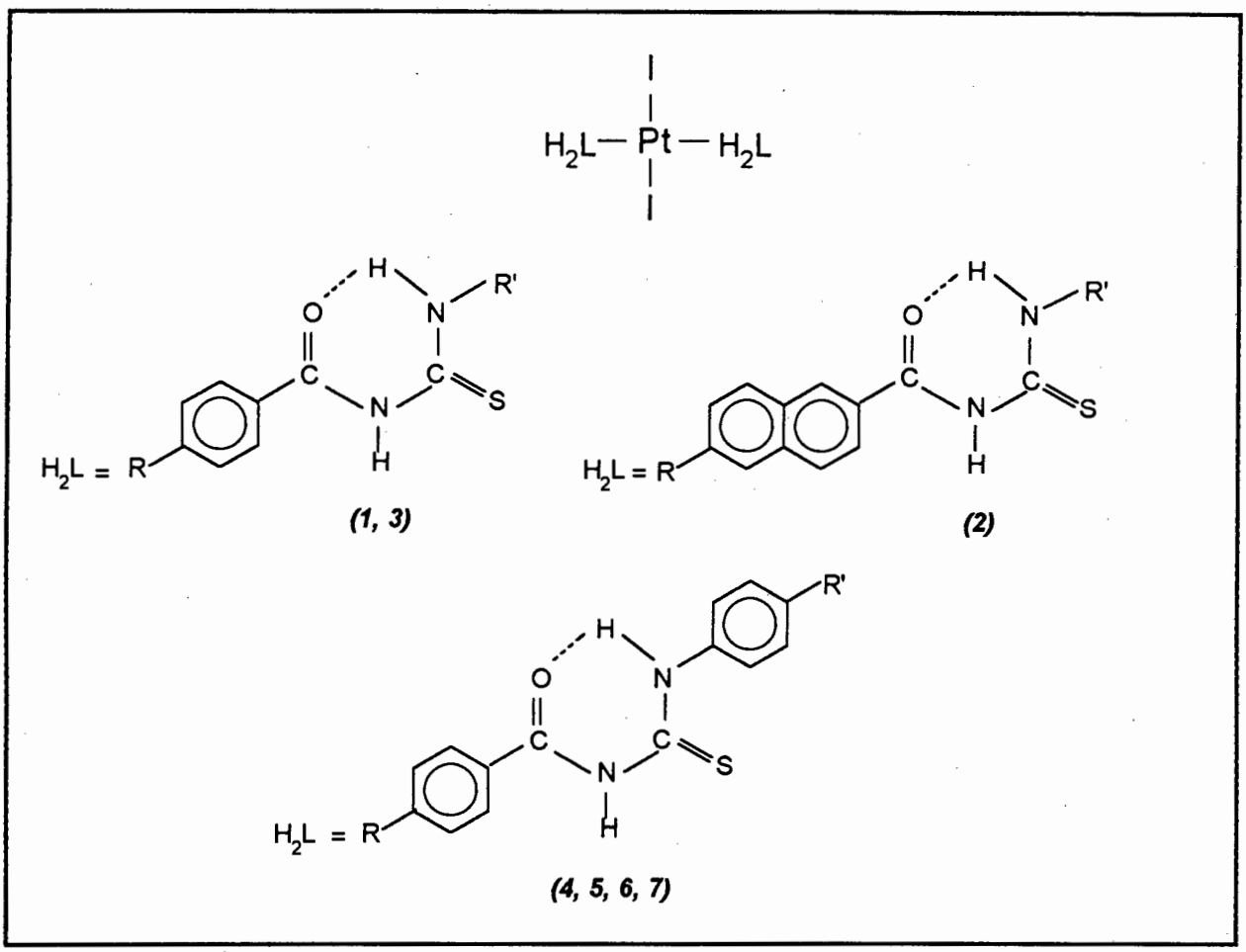

Figure 4.3 Schematic representation of the general structure of $[Pd(H_2L)_2X_2]$.

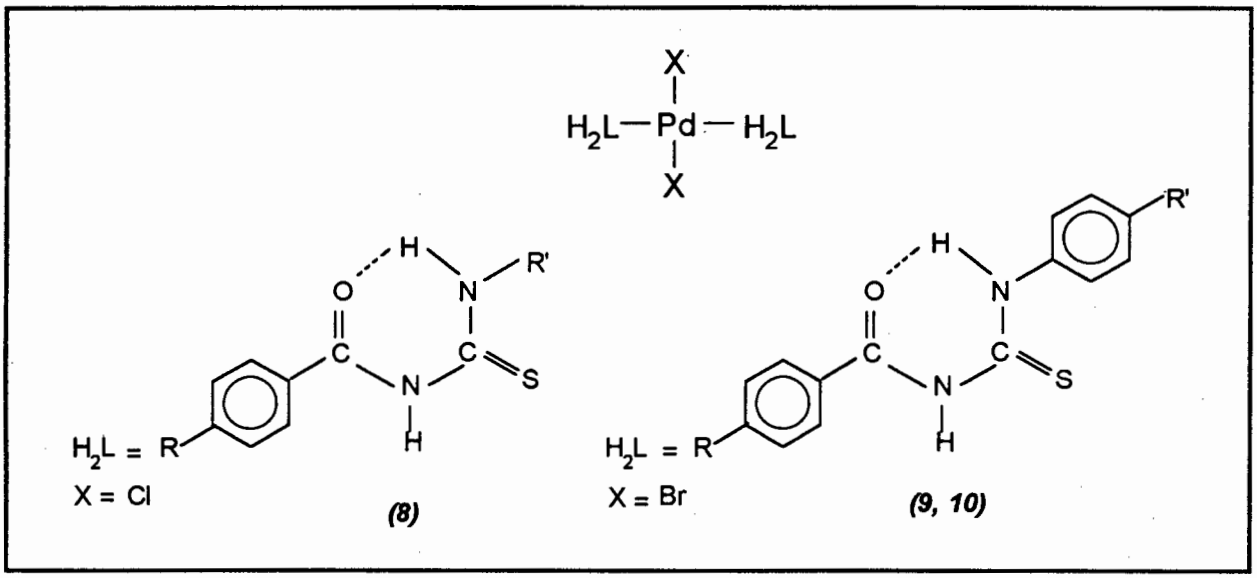

All the metal complexes have been characterised with respect to their potential mesogenic phases. Furthermore, the entropy and enthalpy involved with these phase transitions have been measured. Characterisation techniques include:

- polarising optical microscopy — to identify the mesophase
- differential scanning calorimetry — to provide information regarding phase transition temperature, entropy and enthalpy values.

4.2 Results and discussion

All the complexes under discussion are synthesised according to the similar method described in Chapter 3 and characterised by satisfactory C, H and N elemental analysis and ^{1}H NMR spectroscopy. Analytical data and detailed ^{1}H assignments of all the new complexes (***1-10***) are recorded in the experimental section 4.4. Each of the complexes has been investigated with the aid of polarising optical microscopy, and, for some of them, also differential scanning calorimetry (DSC).

Optical polarising microscopy, with a temperature-controlled hot-stage, has been used to determine whether the complex is a metallomesogen or not and to identify the type of mesophase formed, if any. DSC studies are used to further confirm that the complex is metallomesogen and to determine the temperatures at which the respective phase transitions occur. Furthermore an estimation of the enthalpy and entropy associated with each phase transition is determined from the DSC thermograms. The enthalpy and entropy values are calculated accordingly to the following equations:

$$\Delta H\ (J.mol^{-1}) = \text{heat flow} \times \text{molar mass} \qquad (1)$$

$$\Delta S\ (J.K^{-1}.mol^{-1}) = \Delta H / T \qquad (2)$$

where

ΔH enthalpy

ΔS entropy

T phase transition temperature in Kelvin

4.2.1 Characterisation of *trans*-bis(*N*-alkyl-*N'*-benzoylthiourea)diiodoplatinum (II) (*1*)

The complex involving the short alkyl chain ligand (C_3) studied in Chapter 3 does not show any unusual melting and solidifying behaviour. It is reasonable to expect that the longer alkyl chain molecules are likely to have mesogenic properties. Thus, the complexes ***1a-1c*** have been synthesised and their properties investigated. The representative structure of ***1c*** is given in Figure 4.4 , with the observed melting points recorded in Table 4.1.

Figure 4.4 Schematic representation of complex ***1c***.

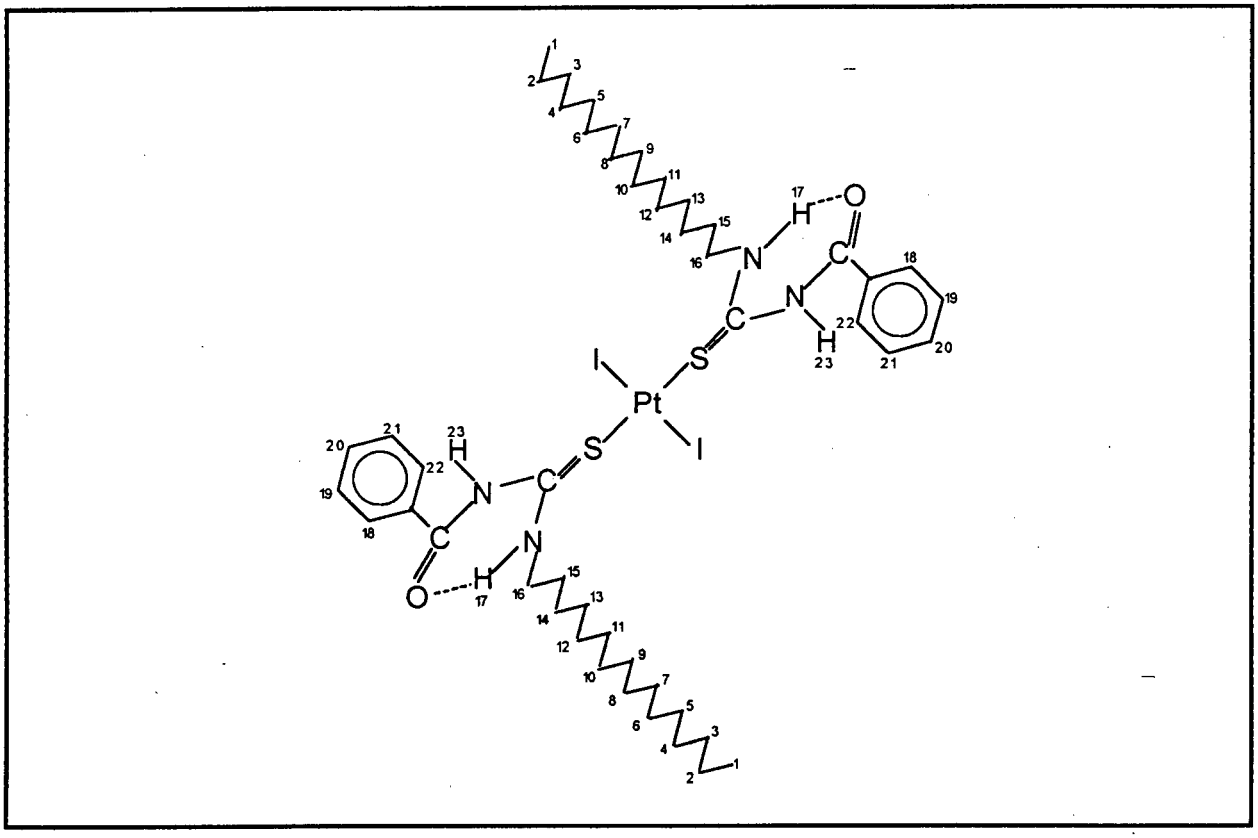

Table 4.1 The melting points for the non-mesogenic complexes ***1a*** - ***1c***.

complex	R'	m.p. (°C)
1a	$C_{12}H_{25}$	121-122
1b	$C_{14}H_{29}$	118-120
1c	$C_{16}H_{33}$	122-124

Interestingly, the melting points of ***1a-1c*** were very similar in spite of the increase of the alkyl chain from C_{12} to C_{16}. No mesogenic properties were observed with the aid of polarising microscopy for these complexes. The complexes passed directly from the solid state into an isotropic liquid at a sharp melting points; slow cooling of the isotropic liquid did not show any sign of mesogenic behaviour.

4.2.2 Characterisation of *trans*-bis(*N*-octyl-*N'*-naphthoylthiourea)di-iodoplatinum (II) (*2*)

In view of the fact that the complexes ***1a*** - ***1c*** did not possess mesogenic character, it was decided to investigate the influence of increasing steric size of the acyl group from phenyl to naphthoyl. Accordingly, the *trans*-bis(*N*-octyl-*N'*-naphthoylthiourea)-diiodoplatinum (II) (*2*) was synthesised. The proposed structure of this complex is given in Figure 4.5.

Figure 4.5 Schematic representation of complex *2*.

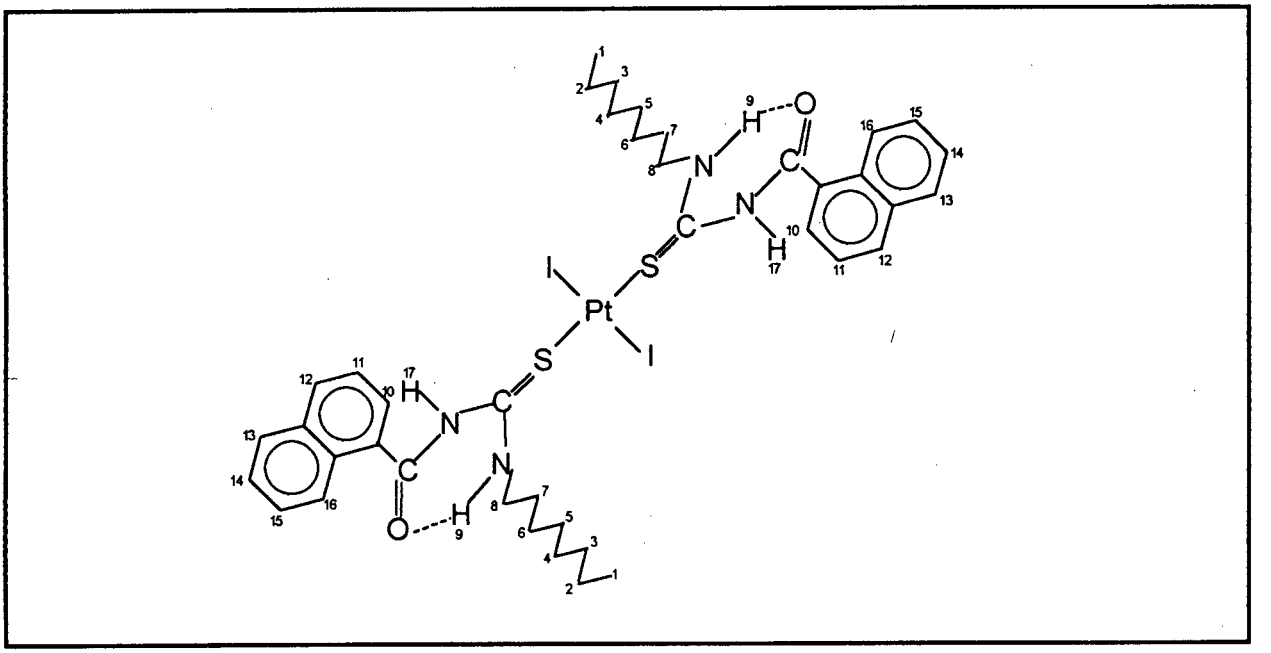

Unfortunately, the complex *2* also does not show any mesogenic properties. The substance melts directly from the solid state into an isotropic liquid on heating. Slow

cooling of the isotropic liquid does not show any liquid crystalline character. The observed melting point is 174 -177 °C.

4.2.3 Characterisation of *trans*-bis(*N*-octyl-*N'*-(*p*-dodecyloxy)benzoylthiourea)diiodoplatinum (II) (*3*)

From the result of complex *2*, increasing the steric size of the aromatic group does not induce any liquid-crystalline behaviour; but increases the melting point of the complex substantially. This is not desirable since ideally one requires lower melting points for potential applications. We thus decided to ascertain whether the effect of inclusion of a long alkoxyl chain to the acylthiourea group would induce mesogenic properties. Accordingly, the *trans*-bis(*N*-octyl-*N'*-(*p*-dodecyloxy)benzoylthiourea)-diiodoplatinum (II) (*3*) (Figure 4.6) was prepared and examined for liquid crystalline character with the aid of polarising optical microscopy and DSC. It has been found that the ligand (*N*-octyl-*N'*-(*p*-dodecyloxy)benzoylthiourea) does not show any mesogenic properties[4].

Figure 4.6 Schematic representation of complex *3*.

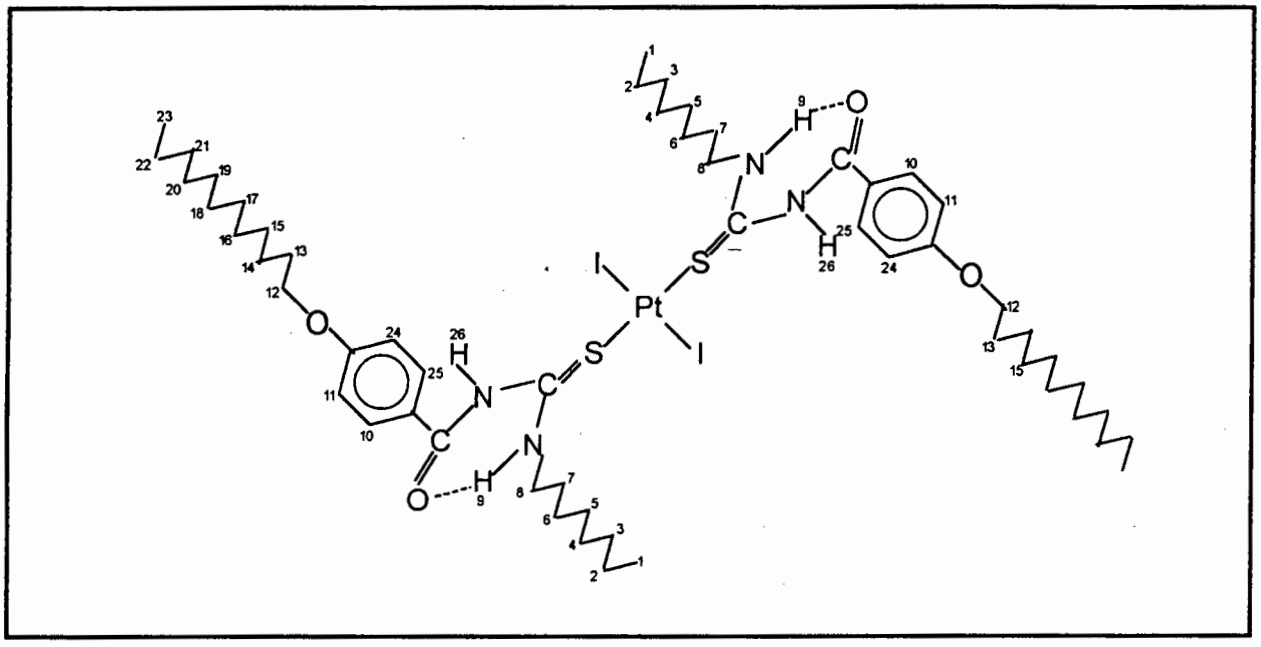

Polarising optical microscopy

When the needle-shaped crystals of complex ***3*** are heated to 65 °C, movement of the needle-shaped crystals is observed. This movement suggests a solid-solid phase transition, as has been found in a large number of metallomesogens[6-7]. Continuous slow heating of complex ***3*** to 98 °C results in a transition from the solid state to a smectic B (S_B) mesophase which is identified by direct comparison with the picture shown in the literature by Lee and Oh[8]. Further heating the mesophase to 110 °C results in the complex reaching the clearing point, and conversion to the isotropic liquid.

Cooling the isotropic liquid gives rise to the formation of a smectic A (S_A) phase (or which might be regarded as a columnar[9] mesophase (Micrograph 4.1)). On further cooling, a typical focal-conic fan texture is observed. The colour changes from brown to green (Micrograph 4.2) (right middle), and the colour of some of the columnar phase changes from red to green (Micrograph 4.3) (right top). Also, the whole mesophase becomes brighter at the same time.

Micrograph 4.1 Focal-conic fan texture of mesophase formed on cooling of ***3*** at 86.2 °C.

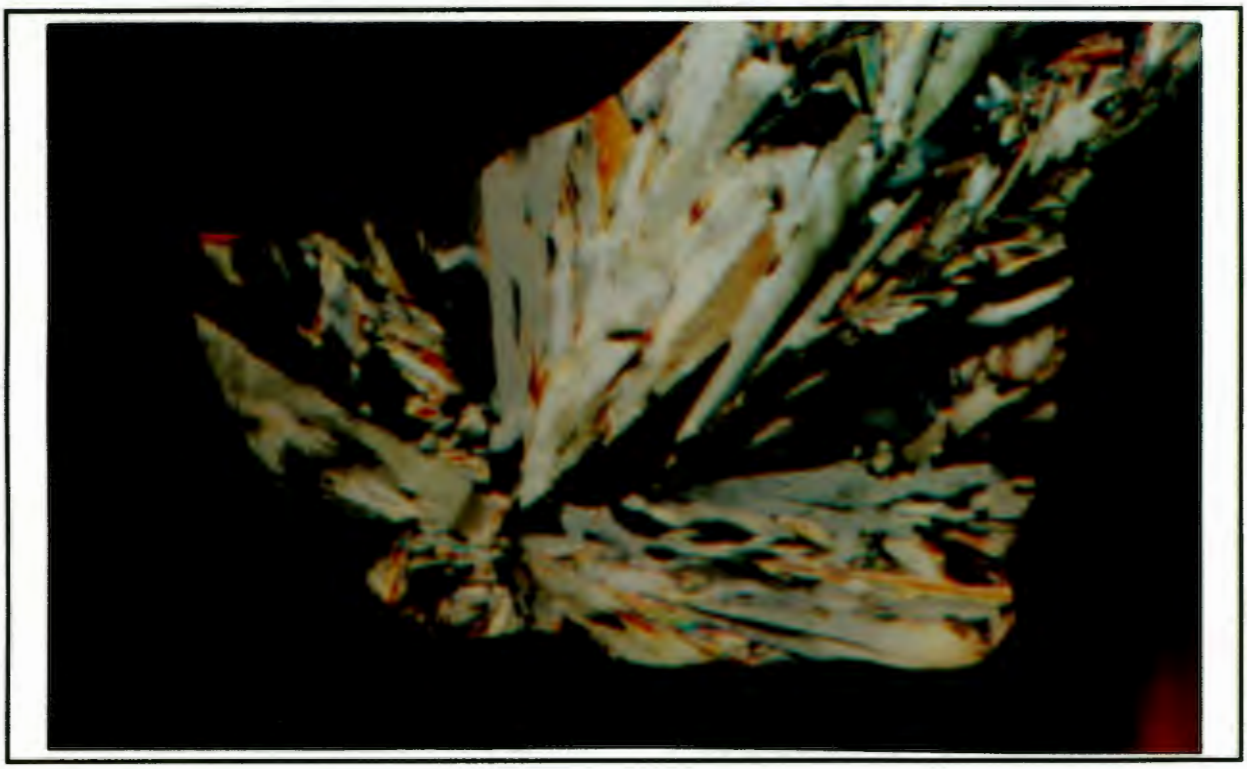

After further cooling of the mesophase, the majority of the sample is crystallised at 66 °C while the minor sample keeps in the mesophase.

After cooling to 35 °C, the sample is heated again. The major sample is changed from the solid phase to the mesophase and the colour of some of the mesophase changed from green to red at 70 °C. Continuous heating of the complex results in the clearing point being reached at 110 °C. These phase transitions are different from that observed in the first heating process, which suggests that the phase transitions are not reversible. The phase transitions are summarised in Table 4.2. The temperatures are reported directly from the DSC peaks.

Differential scanning calorimetry (DSC)

The transition temperatures and associated thermodynamic data for the *trans*-bis(*N*-octyl-*N'*-(*p*-dodecyloxy)benzoylthiourea)diiodoplatinum (II) (***3***) are summarised in Table 4.2.

Table 4.2 Transition temperatures, mesophase and thermodynamic data for ***3***.

transition	T (°C)	ΔH (kJ.mol^{-1})	ΔS (J.K^{-1}.mol^{-1})
[a] C→C	65.85	5.29	15.54
C→S	101.98	60.93	162.40
S→I	111.80	65.26	169.51
[b] C→S + S→S	77.05	23.23	66.32
S→I	112.20	65.37	169.62
[c] I→S	82.29	60.28	169.57
S→C	65.81	16.49	48.64

Transition temperatures, enthalpy and entropy values obtained from DSC traces at a heating rate of 10 °C. min^{-1} and cooling rate of 2 °C. [a]*first heating* [b]*second heating* [c]*first cooling*
C: crystal phase *S: smectic phase* *I: isotropic phase*

The first DSC heating trace (Figure 4.7) of complex ***3*** shows the evidence of three endothermic peaks at 65.85, 101.98 and 111.80 °C respectively. It is postulated that

Micrograph 4.2 The focal-conic fan texture of mesophase formed on cooling of *3* at 83.2 °C.

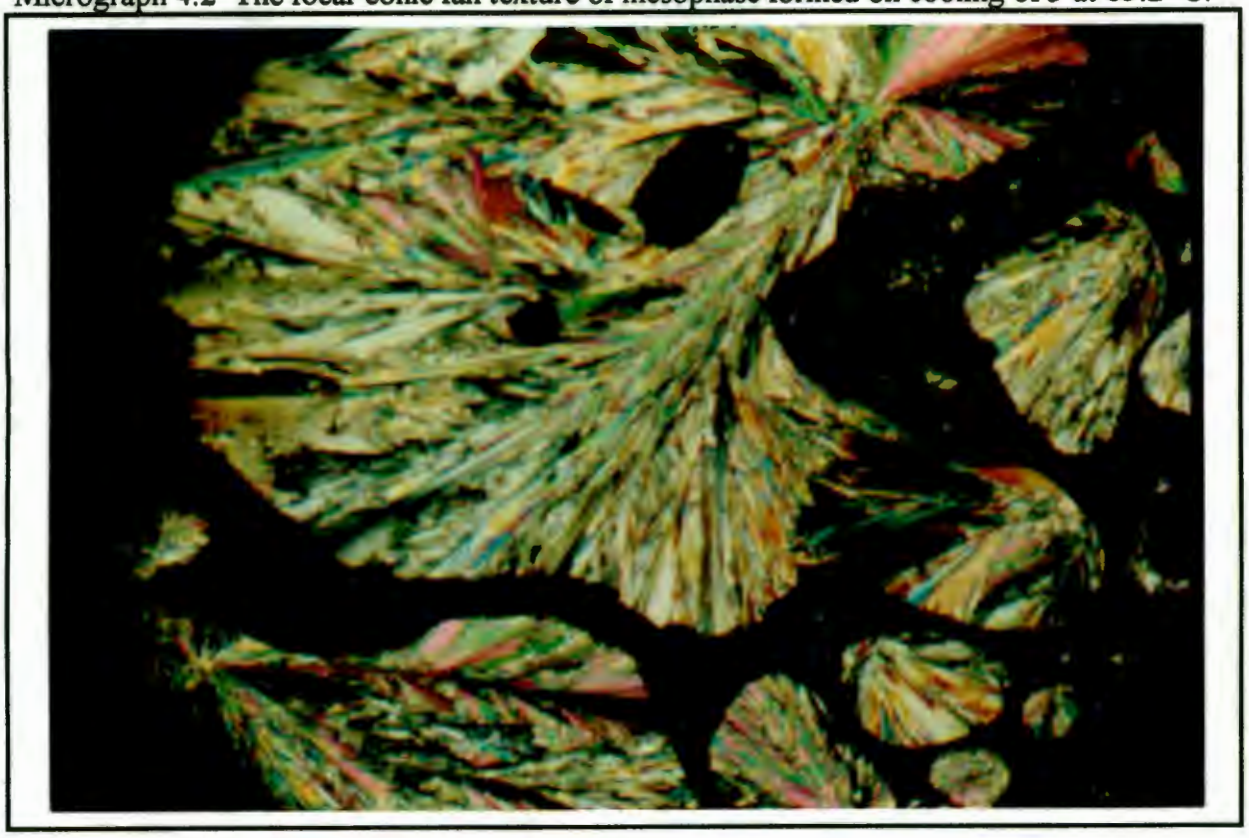

Micrograph 4.3 The color change of mesophase formed on cooling of *3* at 73.0 °C.

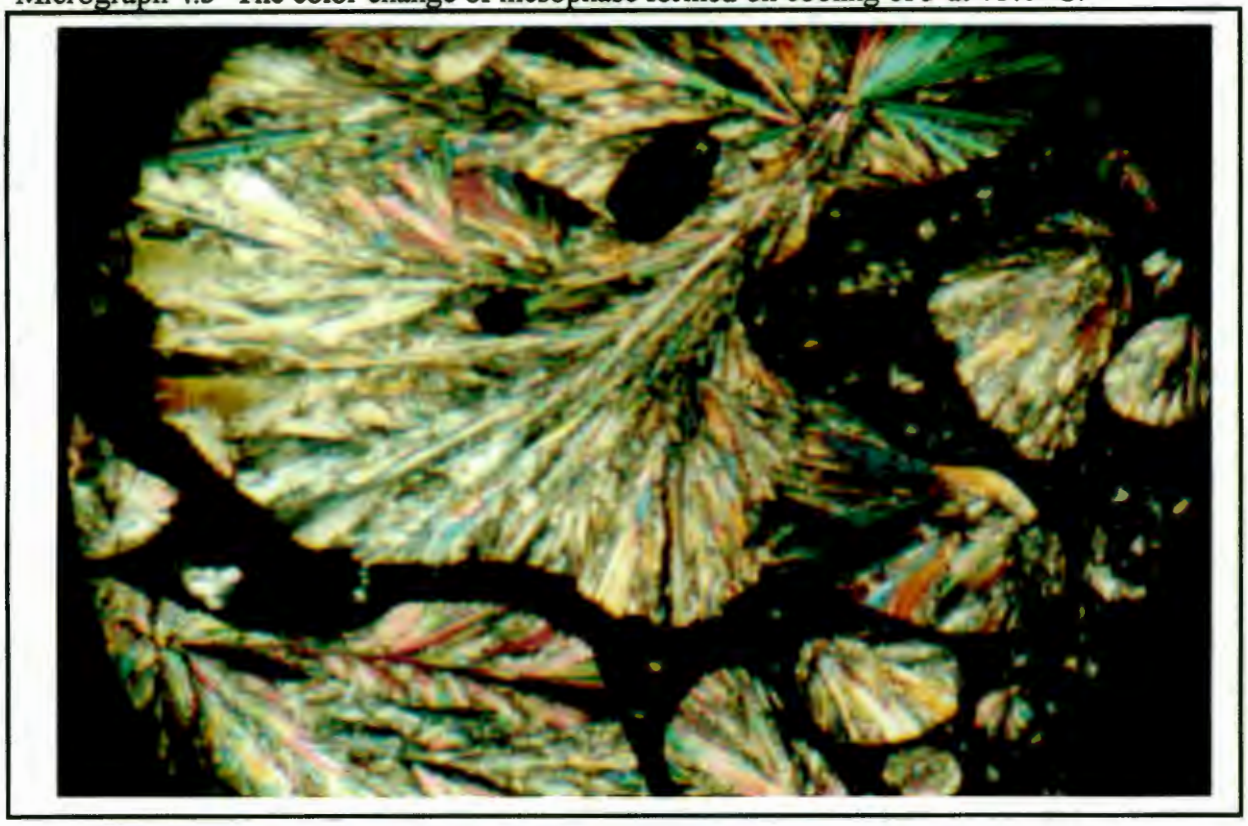

Figure 4.7 DSC heating and cooling traces of complex *3*.

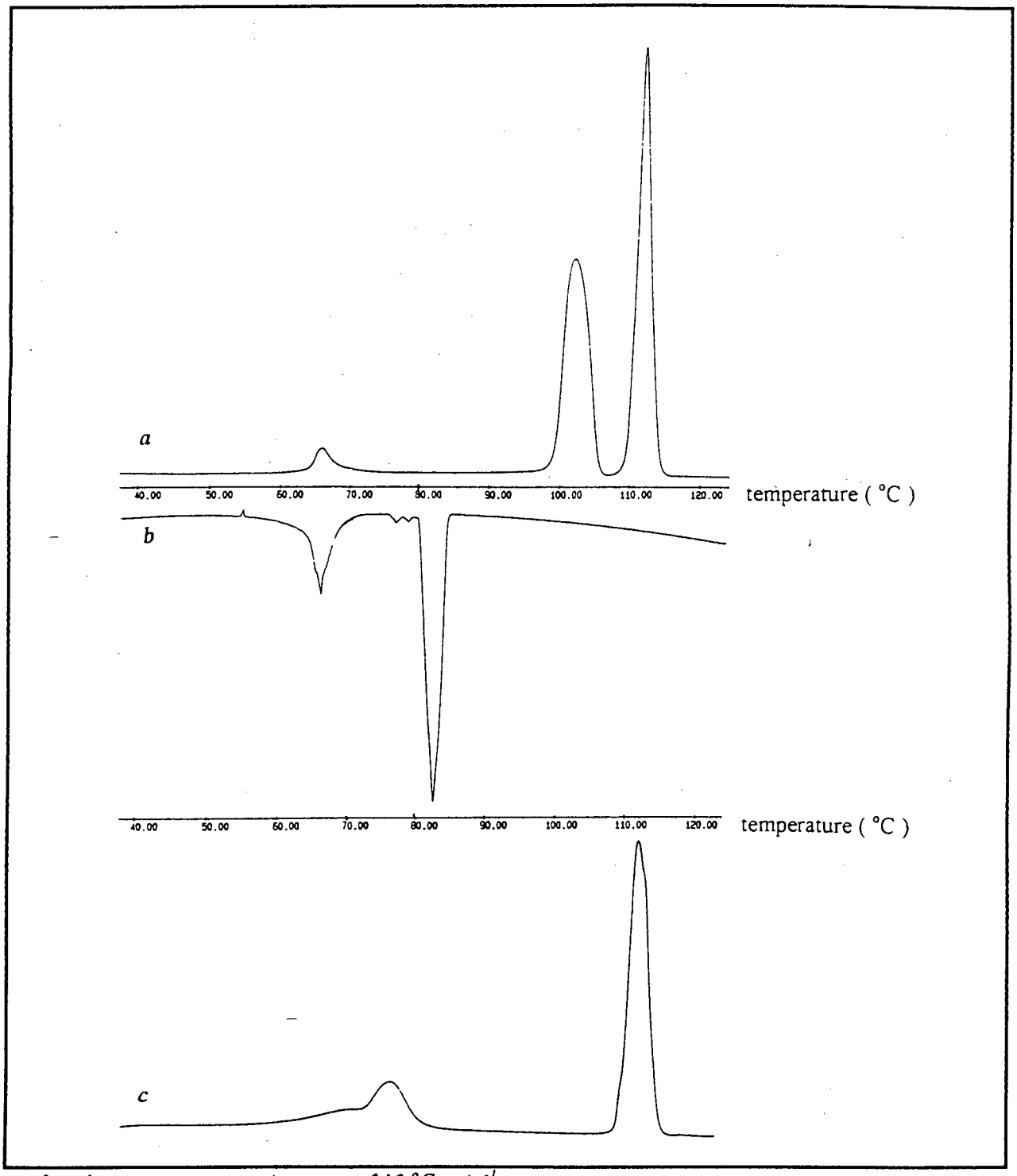

a. first heating at a scanning rate of 10 °C. min^{-1}

b. cooling at a scanning rate of 2 °C. min^{-1}.

c. second heating at a scanning rate of 10 °C.min^{-1}.

the small peak at 65.85 °C (lower than the melting point) is due to a solid-solid transition, as it occurs at a similar temperature range to the temperature at which the

phenomenon is also observed for other compounds synthesised by J. Andersch *et al*[10]. On the other hand, it is also possible that some of the complex could isomerise to the *cis*- isomer to form a mixture after the first heating process. Thus the mesogenic property exhibited in the first heating process disappears in the second heating process. We would think that such isomerisation is unlikely as confirmed by ^{1}H NMR study.

This complex is thermally *stable* after the first heating process over the temperature range of the mesophase and does not decompose at the clearing point. These results are confirmed by two identical ^{1}H NMR spectra of this complex, measured by using the samples after the first heating process and the original complex.

In summary, of all analytical results for *3* above, we can conclude that this complex has the following special metallomesogenic properties:

- lower melting point — 112.20 °C,
- wider mesophase range — 16.48 °C,
- high thermal stability,
- involving a non-mesogenic ligand.

4.2.4 Characterisation of *trans*-bis(*N*-(*p*-hexyloxy)aniline-*N*'-heptylbenzoylthiourea)diiodoplatinum(II) (*4*)

In view of the fact that the ligand *N*-(*p*-hexyloxy)aniline-*N*'-heptylbenzoylthiourea exhibits liquid crystalline behaviour[4], we decided to ascertain whether the diiodoplatinum (II) complex of this ligand could possess mesogenic properties. Accordingly, *trans*-bis(*N*-(*p*-hexyloxy)aniline-*N*'-heptylbenzoylthiourea)diiodoplatinum(II) (*4*) (Figure 4.8) was synthesised and its properties investigated.

Figure 4.8 Schematic representation of complex *4*.

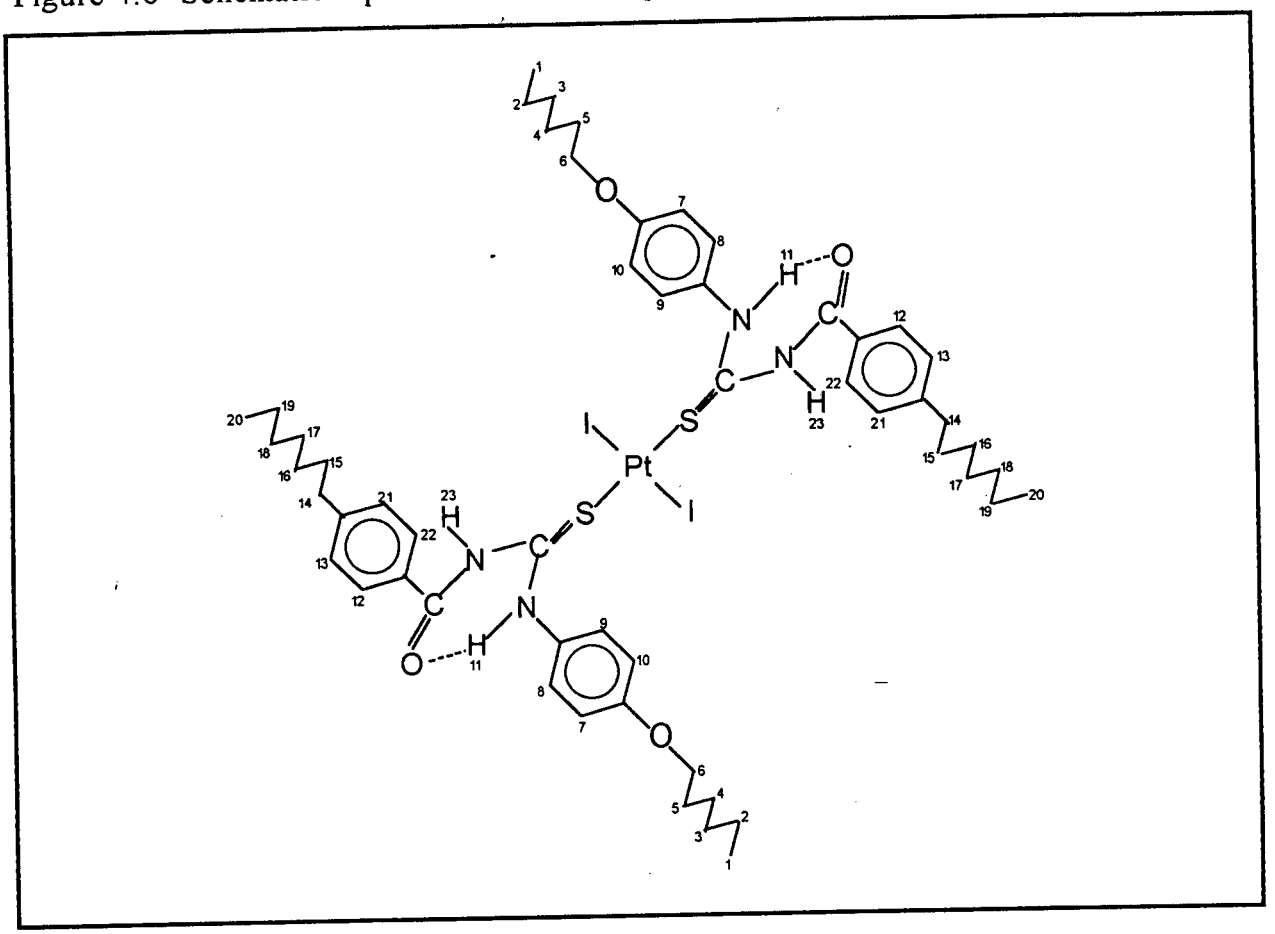

Surprisingly, no liquid-crystalline behaviour is observed with the aid of polarising optical microscopy, on either heating the solid material or slow cooling (1 °C.min^{-1}) of the isotropic liquid. This is different from the behaviour of the corresponding ligand which exhibits mesogenic property.

DSC studies (Figure 4.9) confirm the optical observations that complex *4* shows no mesogenic behaviour. On heating the solid material, only one endothermic peak corresponding to the melting point (166-168 °C); and on cooling the isotropic liquid, one large exothermic peak representing crystallisation at 147.81 °C. The small peaks might be due to solid-solid transitions or crystallisation of some *cis*- complex which is formed by thermal isomerisation of the *trans*- complex.

Figure 4.9 DSC heating and cooling traces of complex *4*.

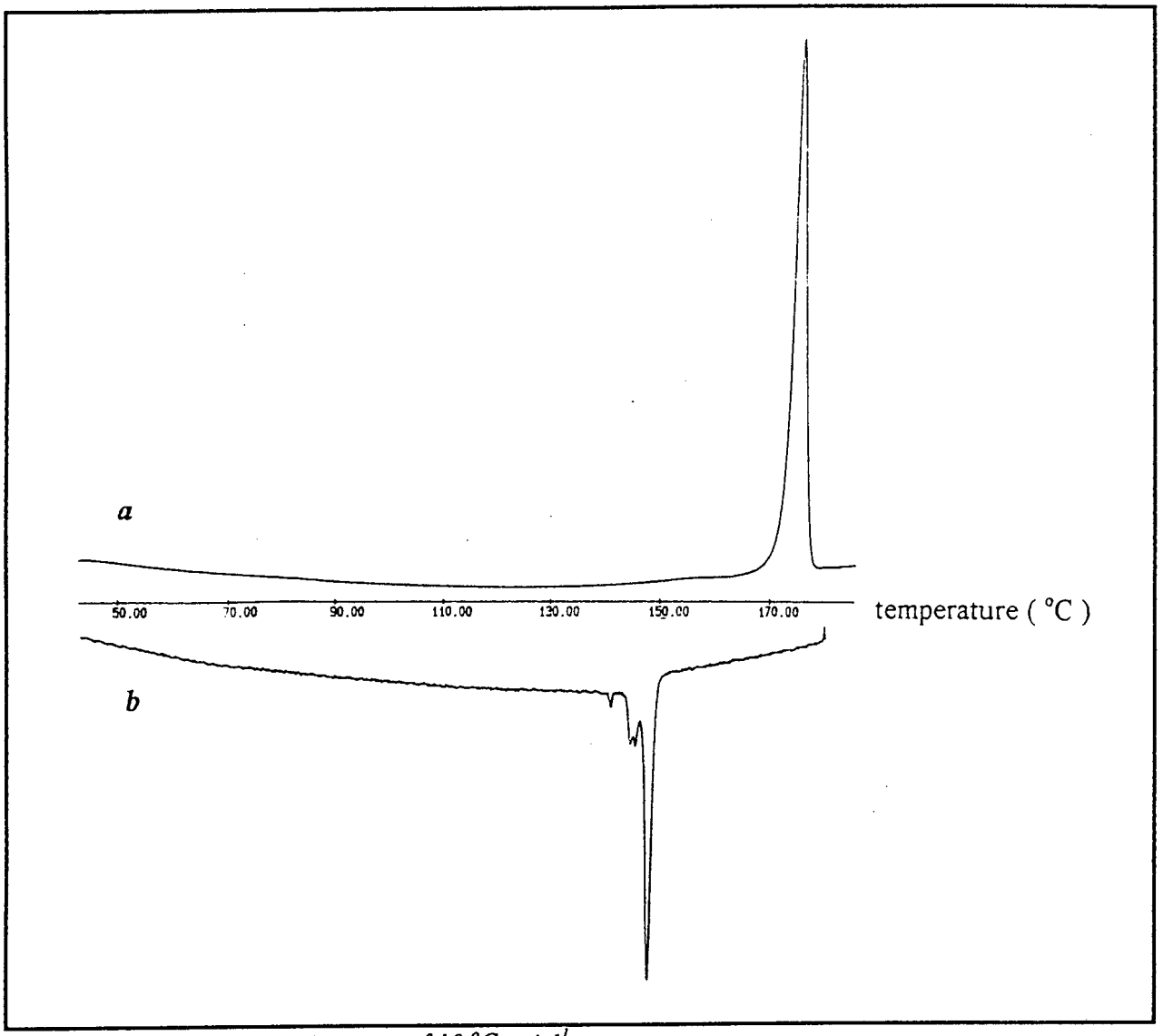

a. first heating at a scanning rate of 10 °C. min^{-1}.

b. cooling at a scanning rate of 2 °C. min^{-1}.

4.2.5 Characterisation of *trans*-bis(*N*-(*p*-alkyl)aniline-*N'*-(*p*-alkoxyl)-benzoylthiourea)diiodoplatinum(II) (*5*)

To understand the interesting results above, i.e. the ligand has a liquid-crystalline property while the Pt complex has not; we decided to verify whether a change of the position of the oxygen atom and the length of the alkoxyl chain of some mesogenic ligands could induce the mesogenic properties. Thus, *trans*-bis(*N*-(*p*-hexyl)aniline-*N'*-(*p*-heptyloxy)benzoylthiourea)diiodoplatinum(II) (*5a*) and *trans*-bis(*N*-(*p*-hexyl)-

aniline-*N'*-(*p*-dodecyloxy)benzoylthiourea)diiodoplatinum(II) (***5b***) were synthesised. The representative structures of these complexes are found in Figure 4.10.

Figure 4.10 Schematic representation of complex ***5a and 5b***.

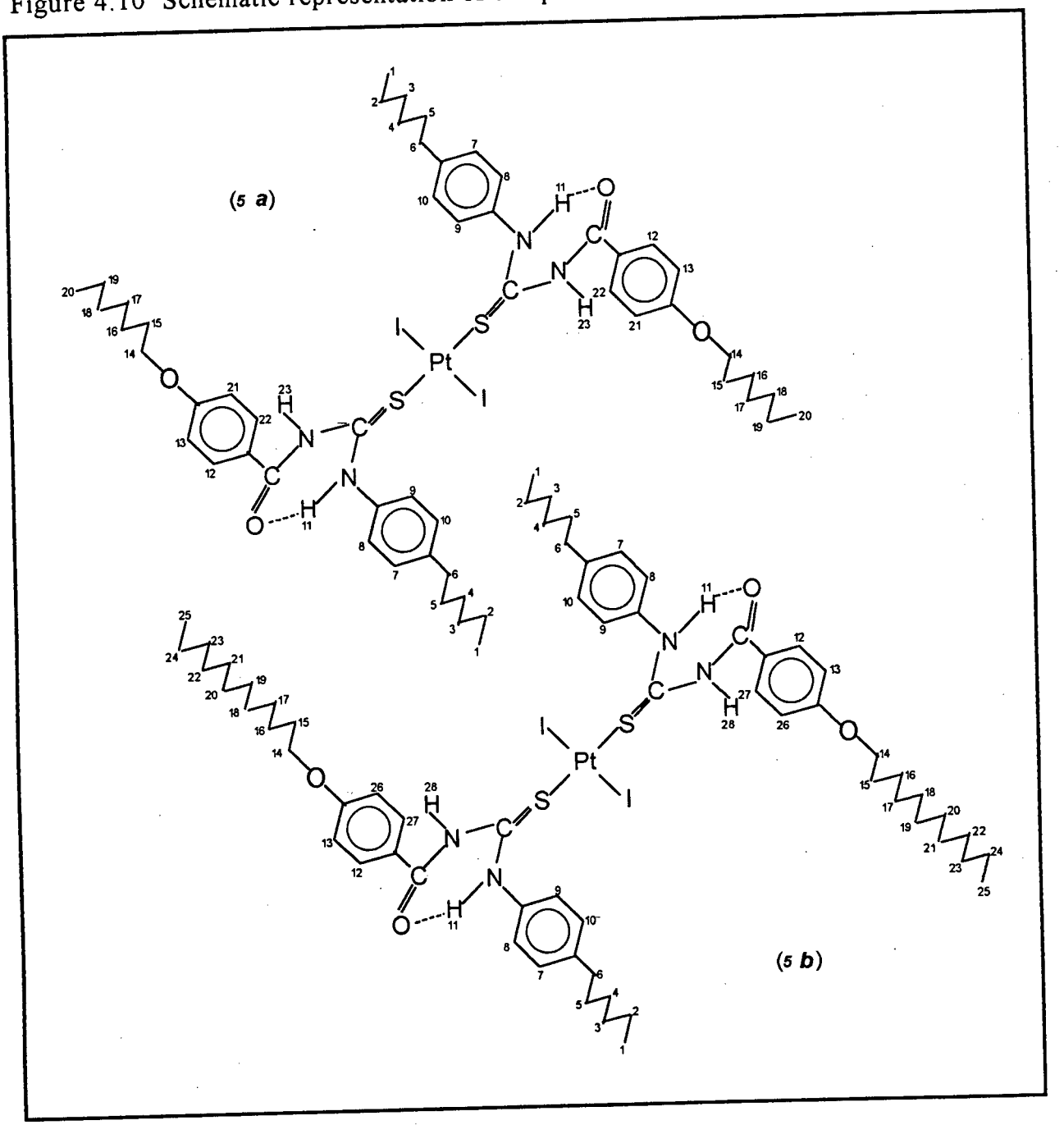

Polarising optical microscopy

Complex ***5a*** also fails to exhibit any mesogenic behaviour either on heating the solid or cooling from the isotropic liquid. This complex is transformed from the solid state

directly to the isotropic liquid on heating to 169 °C. Cooling to 147 °C results in crystallisation of the isotropic liquid. This result suggests that the change of the position of the oxygen atom does not induce the mesogenic properties. Would the increase of the length of the alkoxy chain induce liquid-crystalline behaviour? Thus, complex ***5b*** was prepared and investigated.

Complex ***5b*** does not exhibit mesogenic behaviour on heating the crystalline material. It melts directly from the solid state to the isotropic liquid at a sharp melting point (169-171 °C). However, cooling of the isotropic liquid gives rise to a distinct liquid-crystalline phase; hence ***5b*** displays a monotropic liquid-crystalline property.

The mesophase formed by ***5b*** is believed to be a smectic phase (S) as evident from the texture observed by polarising optical microscopy. On cooling the isotropic liquid of ***5b*** from 175 °C to 146 °C, the mesogenic phase separates out to form a typical focal-conic fan texture (Micrograph 4.4), usually associated with a smectic phase. Other textures characteristic of a smectic phase are also observable in thinner layers of the complex between the glass plates under the microscope (Micrograph 4.5). Such phenomena are in agreement with those observed by J. Andersch *et al*[10] who have found that the smectic phases are varied (e.g. S_c - S_x, S_x - S_E) with the thickness of the smectic layer and the temperature. Further cooling allows for the mesophase to convert to a solid phase at 77 °C. The mesophase is identified as a smectic phase on the basis of:

- the viscosity of the phase and
- the formation of a typical focal-conic fan texture, associated with this type of phase[4,8].

Differential scanning calorimetry (DSC)

The enthalpy and entropy changes estimated from the DSC thermograms (which confirm this mesogenic behaviour) are recorded in Table 4.3. DSC heating and cooling traces are given in Figure 4.11.

Micrograph 4.4 The focal-conic fan texture formed on cooling of ***5b*** at 146.2 °C.

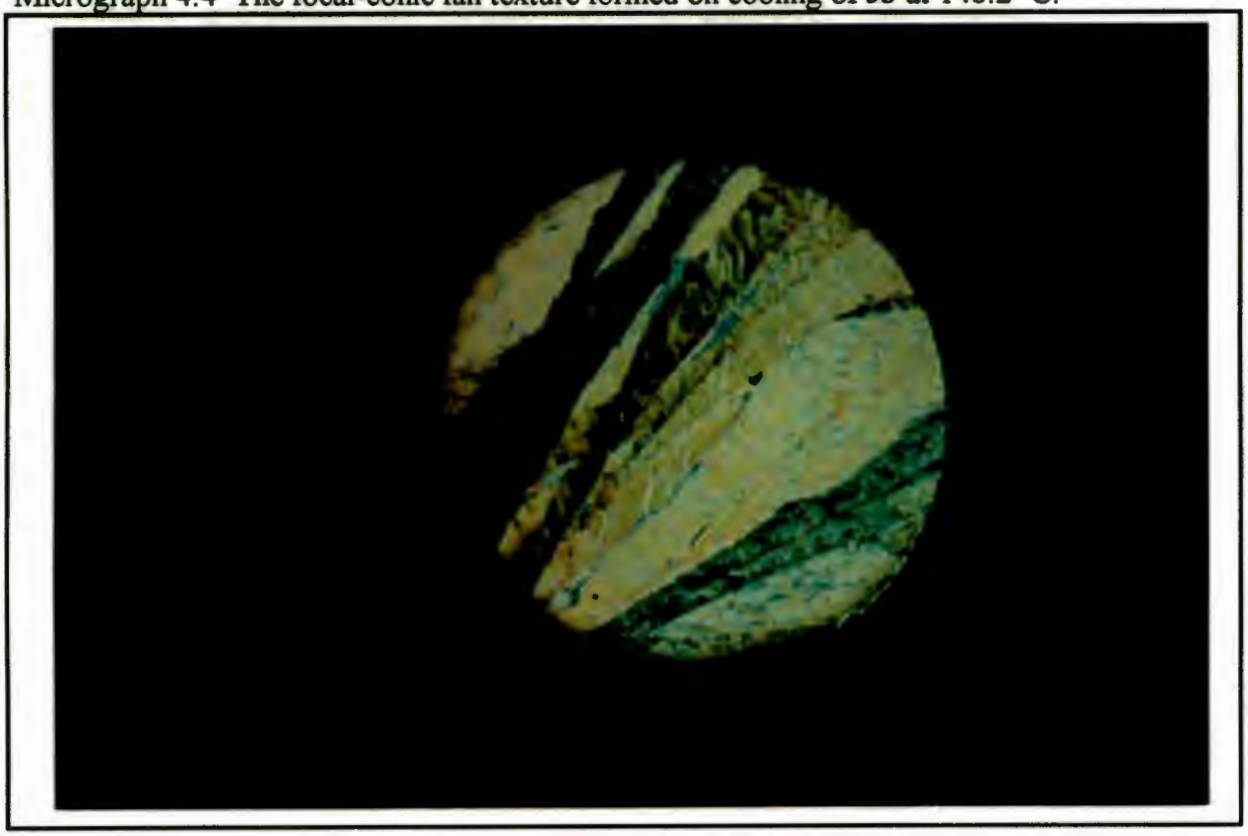

Micrograph 4.5 The other texture of mesophase formed on cooling of ***5b*** at 138.1 °C.

Table 4.3 Transition temperatures, mesophase and thermodynamic data of complex ***5b*** calculated from the DSC cooling trace.

transition	T(°C)	ΔH (kJ.mol^{-1})	ΔS (J.K^{-1}.mol^{-1})
I → S + S→S	144.10	52.52	125.86
S → C	85.72	21.29	59.32

Transition temperatures, enthalpy and entropy values obtained from DSC trace at a cooling rate of 2 °C. min^{-1}. I: isotropic phase S: smectic phase C: crystalline phase

Figure 4.11 DSC heating and cooling traces of complex ***5b***.

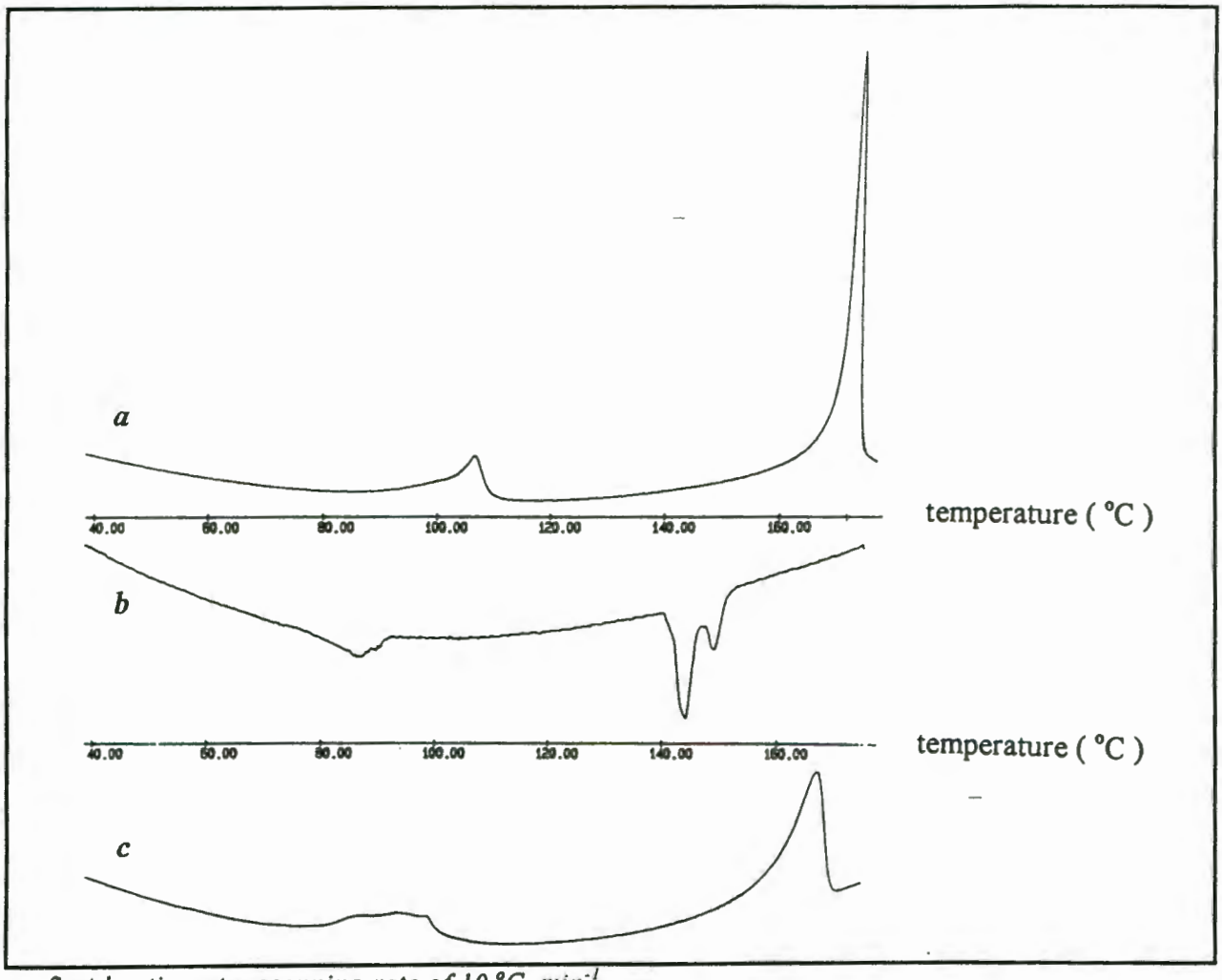

a. first heating at a scanning rate of 10 °C. min^{-1}.

b. cooling at a scanning rate of 2 °C. min^{-1}.

c. second heating at a scanning rate of 10 °C. min^{-1}.

The first heating trace of complex ***5b*** shows two peaks at 106.45 and 170.01 °C, assigned to transitions of solid to solid state and solid to isotropic phase respectively.

The cooling trace of ***5b*** shows three peaks at 149.26, 144.10 and 85.72 °C. The exothermic peaks at 149.26 and 144.10 °C are due to the transition from the isotropic to the mesophase and possibly from one mesophase to another mesophase, respectively. However, we could not observe the transition from mesophase to mesophase optically. The enthalpy associated with these two transitions is estimated to be 52.52 $kJ.mol^{-1}$. The broad exothermic peak at 85.72 °C is due to the transition from mesophase to a solid material. The enthalpy associated with this transition is 21.29 $kJ.mol^{-1}$.

The second heating trace of this complex also shows two endothermic peaks. Comparision with the first heating trace, the slightly broadened peaks may be due to the decomposition or thermal isomerisation (*trans*- to *cis*-) of part of the sample.

4.2.6 Characterisation of *trans*-bis(*N*-(*p*-pentyloxy)aniline-*N'*-(*p*-heptyloxy)benzoylthiourea)diiodoplatinum(II) (6)

In view of the fact that complex ***4*** and ***5a*** do not show any mesogenic properties, we decided to determine what effect, if any, the presence of *two* alkoxyl chains in the ligand molecule has on the potential mesogenic character of the iodo complex. Thus, the *trans*-bis(*N*-(*p*-pentyloxy)aniline-*N'*-(*p*-heptyloxy)benzoylthiourea)diiodo-platinum(II) (***6***) was synthesised (Figure 4.12).

Heating of complex ***6*** results in a direct transformation from the solid state into the isotropic liquid at 200 °C. Slow cooling of the isotropic liquid to 134 °C allows for the separation of the smectic phase from the isotropic liquid (Micrograph 4.6). The viscosity (and response to mechanical stress) (Micrograph 4.7), as well as the observed mesogenic texture suggests that the mesophase is a smectic A phase. Crystallisation of the sample occurs at 66 °C.

Figure 4.12 Schematic representation of complex ***6***.

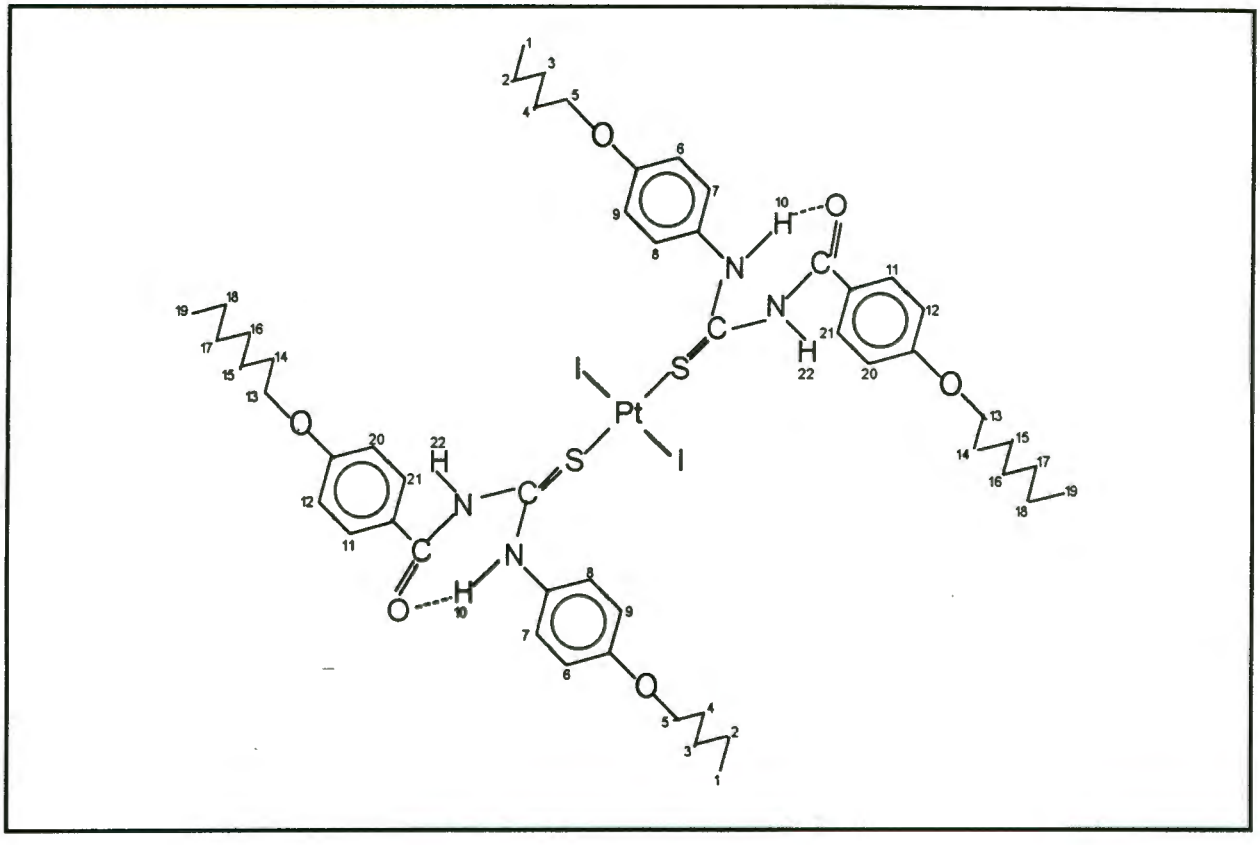

A comparison of complex ***6*** with complex ***4***, ***5a*** and ***5b*** suggests that the number of alkoxyl chain and the length of the alkoxyl chain of the ligands are important factors for mesogenic properties of the complexes to be exhibitd. If both aromatic rings of the ligands carry alkoxyl substituents, this will result in mesogenic behaviour of the corresponding Pt complexes. For one single alkoxyl substituent on either the benzoyl or the aniline moiety, the alkoxyl chain should be long enough in order that the complex display mesogenic property. The melting point of complex ***4***, ***5a*** and ***5b*** are very similar, while the melting point of complex ***6*** is much higher. The data is compared in Table 4.4.

Table 4.4 The melting points for complex ***4***, ***5a***, ***5b*** and ***6***.

complex	R	R'	alkoxy groups	m.p. (°C)	mesogenic
4	C_7H_{15}	OC_6H_{13}	2	169-170	no
5a	OC_7H_{15}	C_6H_{13}	2	166-169	no
5b	$OC_{12}H_{25}$	C_6H_{13}	2	169-171	yes
6	OC_7H_{15}	OC_5H_{11}	4	198-200	yes

Micrograph 4.6 The four-brushed texture of mesophase formed on cooling of ***6*** at 133.9 °C.

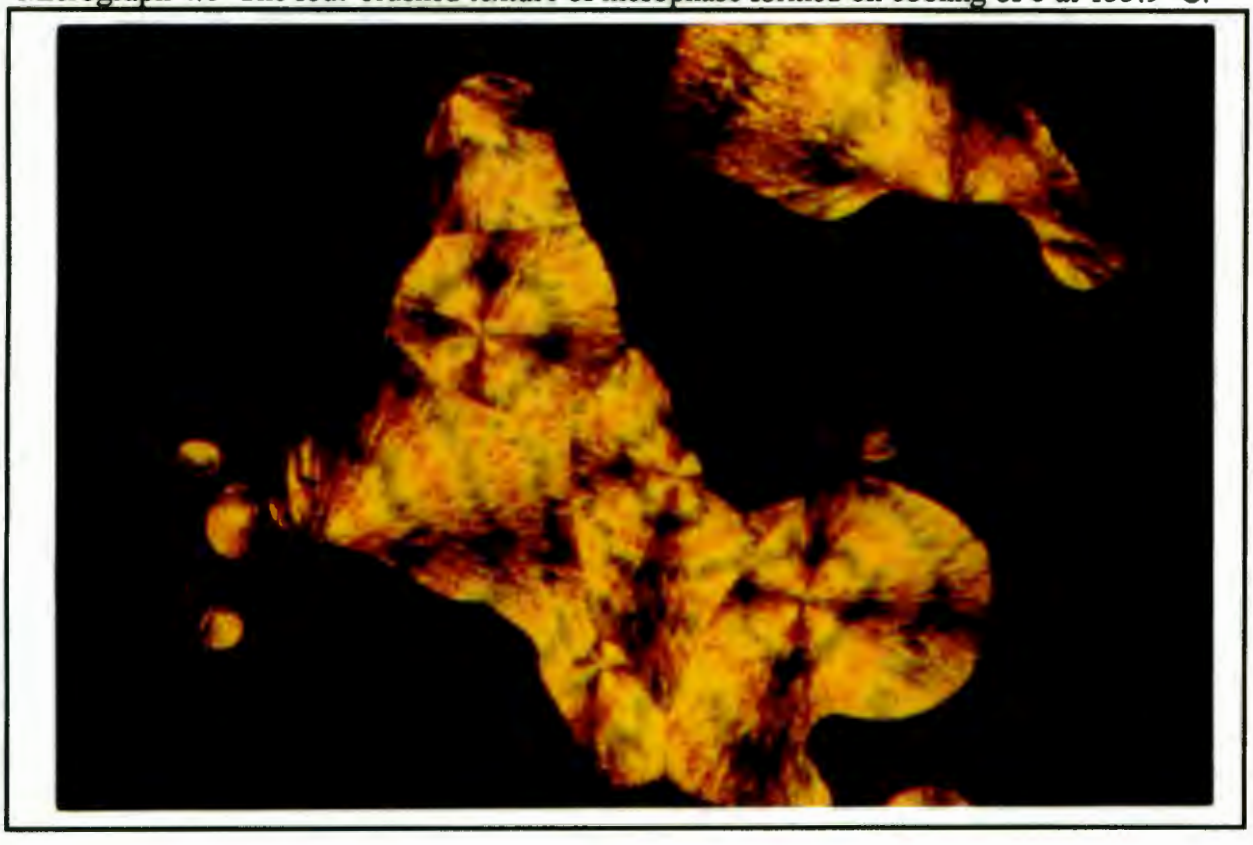

Micrograph 4.7 The natural schlieren texture of mesophase formed by pressing ***6*** at 133.9 °C.

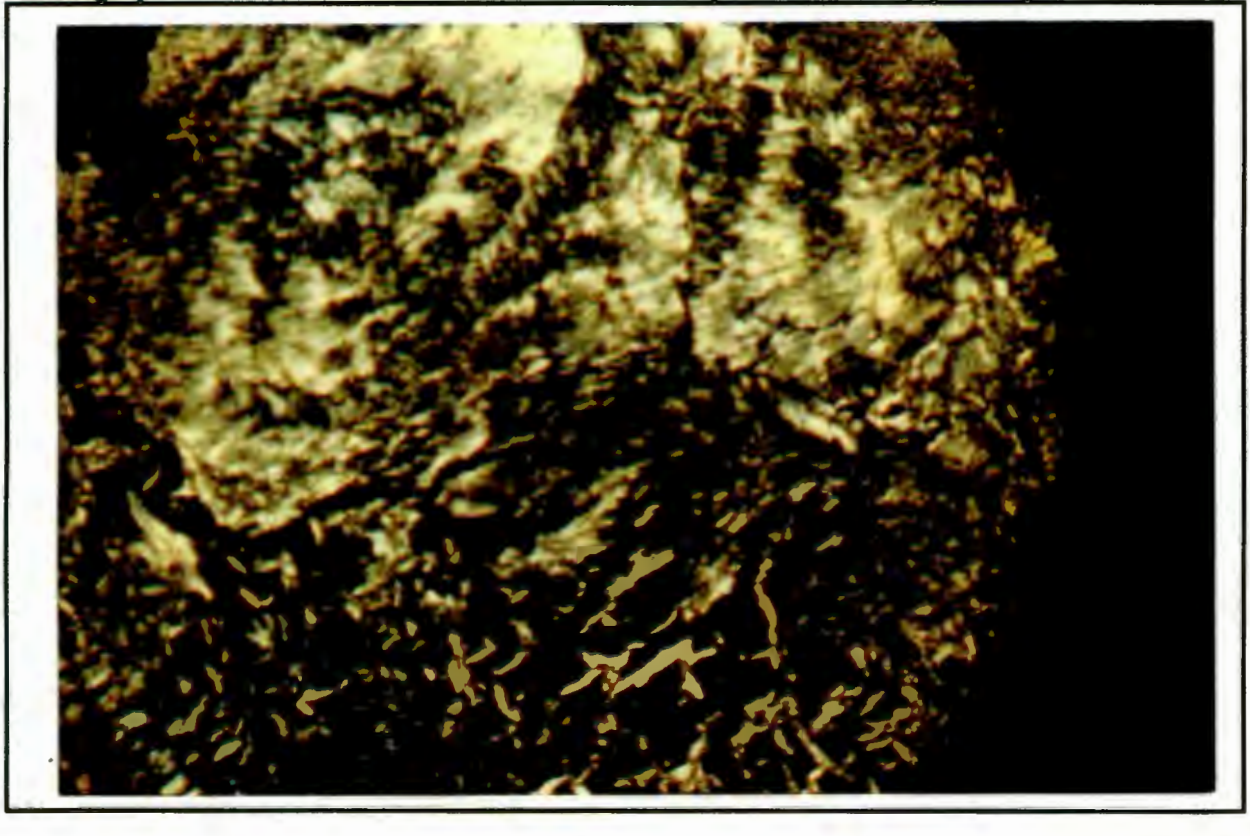

4.2.7 Characterisation of *trans*-bis(*N*-(*p*-dodecyl)aniline-*N'*-(*p*-hexyl)-benzoylthiourea)diiodoplatinum(II) (7)

From the results obtained for complexes ***5b*** and ***6***, it is clear that both inclusion of one longer alkoxyl chain (C_{12}) and two alkoxyl chain (C_5 and C_7) in the ligand are able to induce a liquid-crystalline behaviour of the complex. We decided to study whether the long chain alkyl substituents alone could induce mesogenic properties. Accordingly, *trans*-bis(*N*-(*p*-dodecyl)aniline-*N'*-(*p*-hexyl)benzoylthiourea)diiodo-platinum(II) (*7*) was synthesised and characterised (Figure 4.13).

Figure 4.13 Schematic representation of complex *7*.

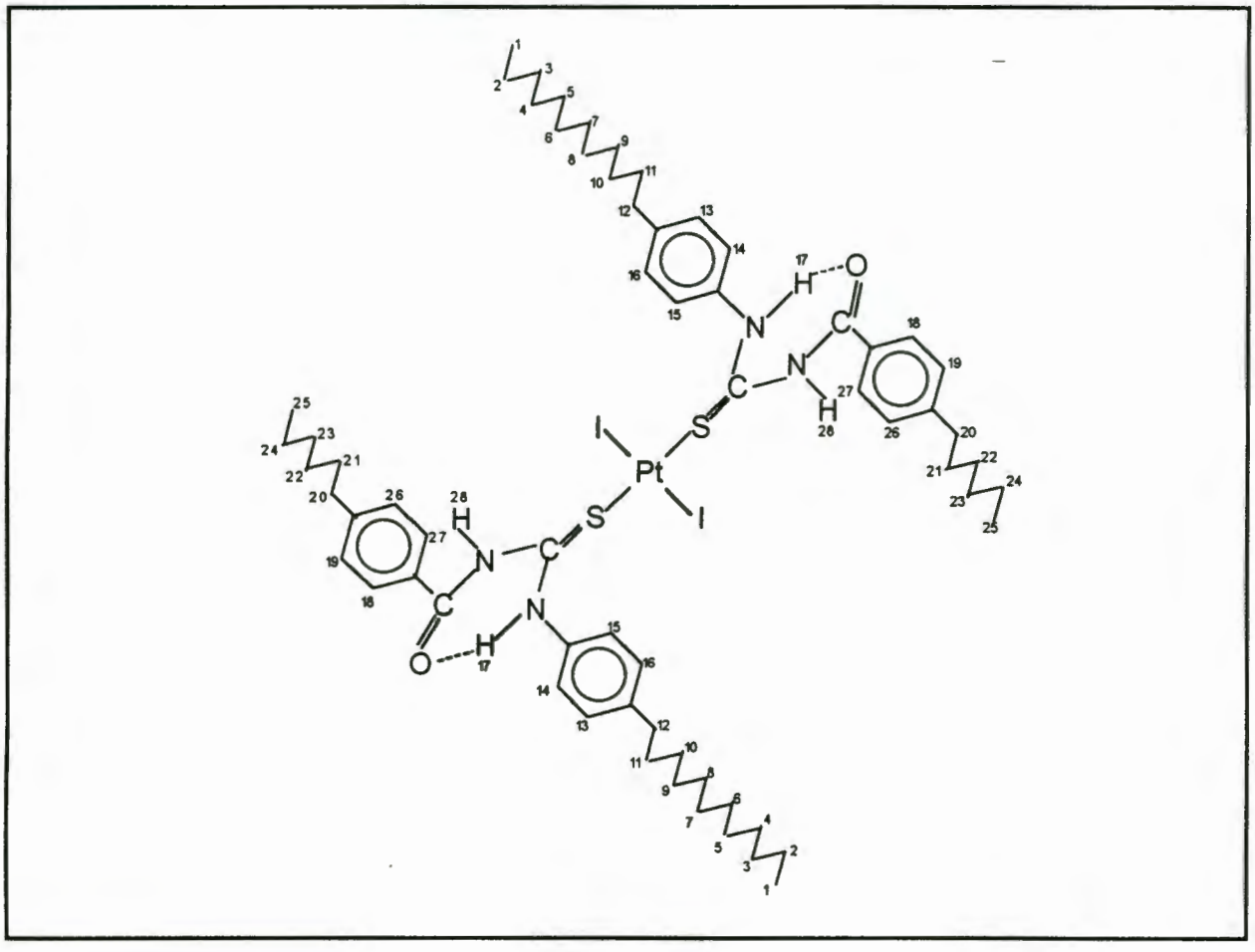

Polarising optical microscopy

Complex *7* does not exhibit liquid-crystalline properties on heating the crystalline solid. On heating to 68 °C, a distinct movement of the crystals is observed. Further heating of the complex *7* results in a direct melting at a sharp point (168-171 °C). Cooling of the isotropic liquid of the complex *7* results in the formation of a mesogenic phase (Micrograph 4.8 and 4.9). Again this shows that the complex is a monotropic metallomesogen. The viscosity and focal-conic fan texture observed suggest that the mesophase formed is also a smectic phase (S).

Interestingly, the corresponding ligand has been reported to not show any mesogenic properties on either heating or cooling by Grimmbacher[4]. But, our observation of this ligand disagree with this previous observation. We find that this ligand is indeed a liquid crystal. This different observation may be due to the use of a different polarising microscopy or disimilar cooling rates.

Differential scanning calorimetry (DSC)

The first heating trace (Figure 4.14) of complex *7* shows two peaks, assigned to a transition of solid to solid phase as well as melting. The cooling trace of *7* shows three peaks at 140.52, 133.62 and 35.00 °C. The exothermic peak at 140.52 °C is due to the transition from the isotropic to the mesogenic phase. The peak at 133.62 °C is assigned to a mesogenic transition. These transitions occur at similar temperatures as observed optically, but the mesogenic transition is not observed clearly by polarising optical microscopy. The enthalpies associated with these transitions are 7.83 and 35.50 $kJ.mol^{-1}$ respectively. The broad exothermic peak at 35.00 °C is due to the transition from the mesophase to a solid material.

The second heating trace of this complex shows two slightly broad peaks which may be due to the decomposition or thermal isomerisation of some of the complex. The enthalpy and entropy changes estimated from DSC thermograms are recorded in Table 4.5.

Micrograph 4.8 The focal-conic fan texture of mesophase formed on cooling of *7* at 136.4 °C.

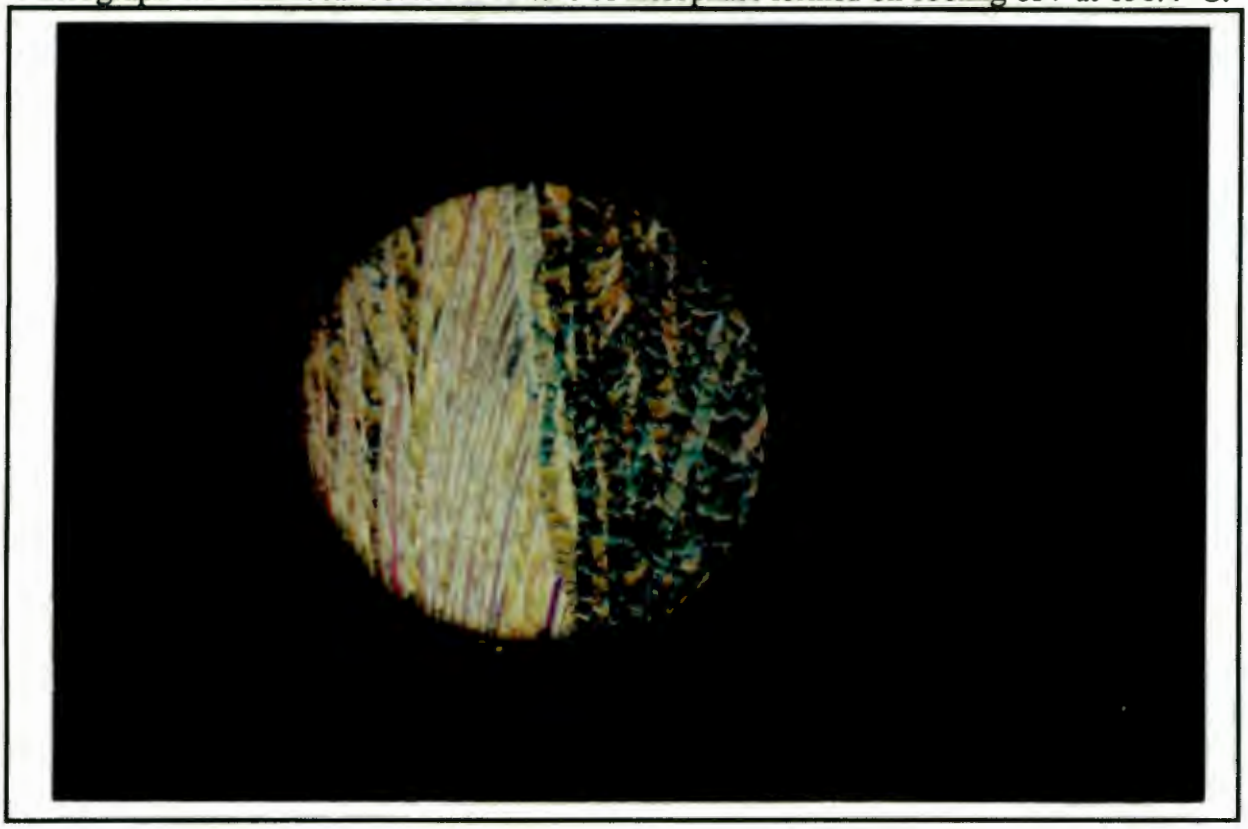

Micrograph 4.9 The other texture of mesophase formed on cooling of *7* at 132.5 °C.

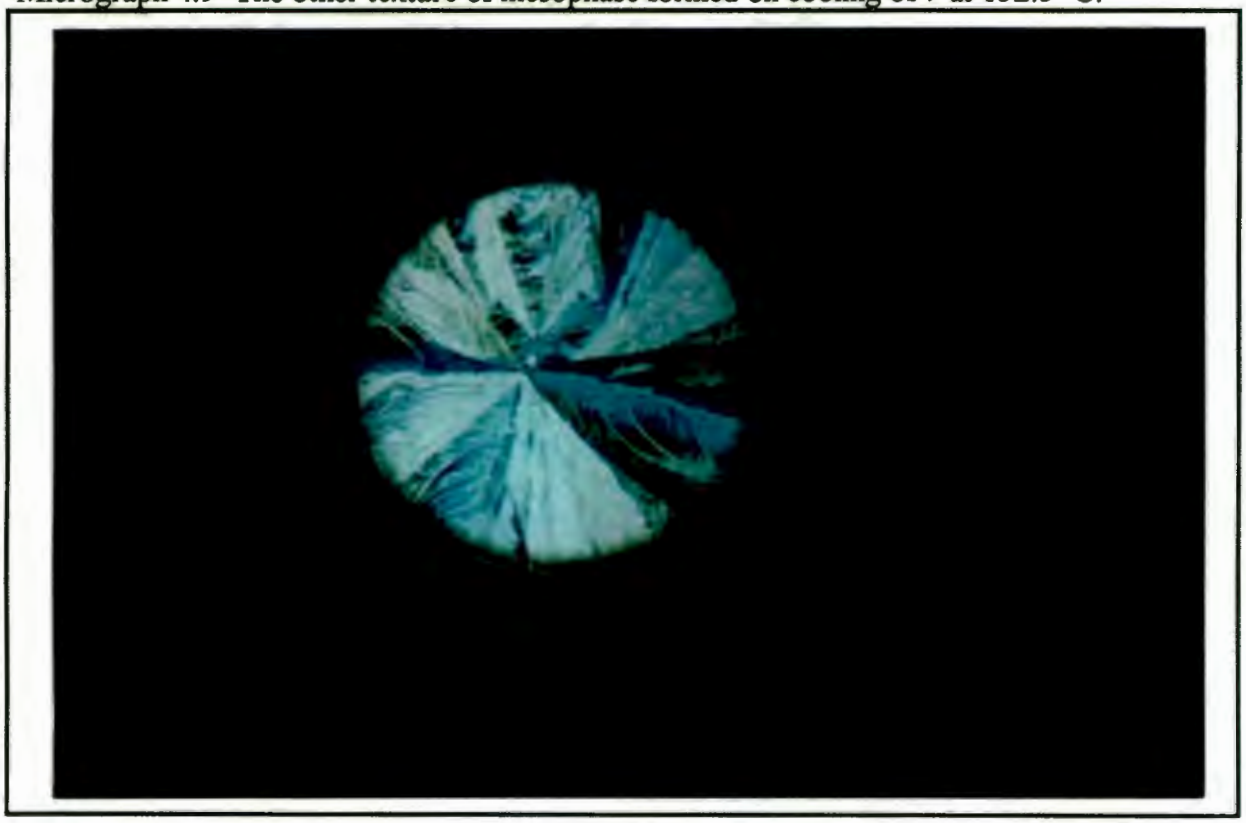

Figure 4.14 DSC heating and cooling traces of complex *7*.

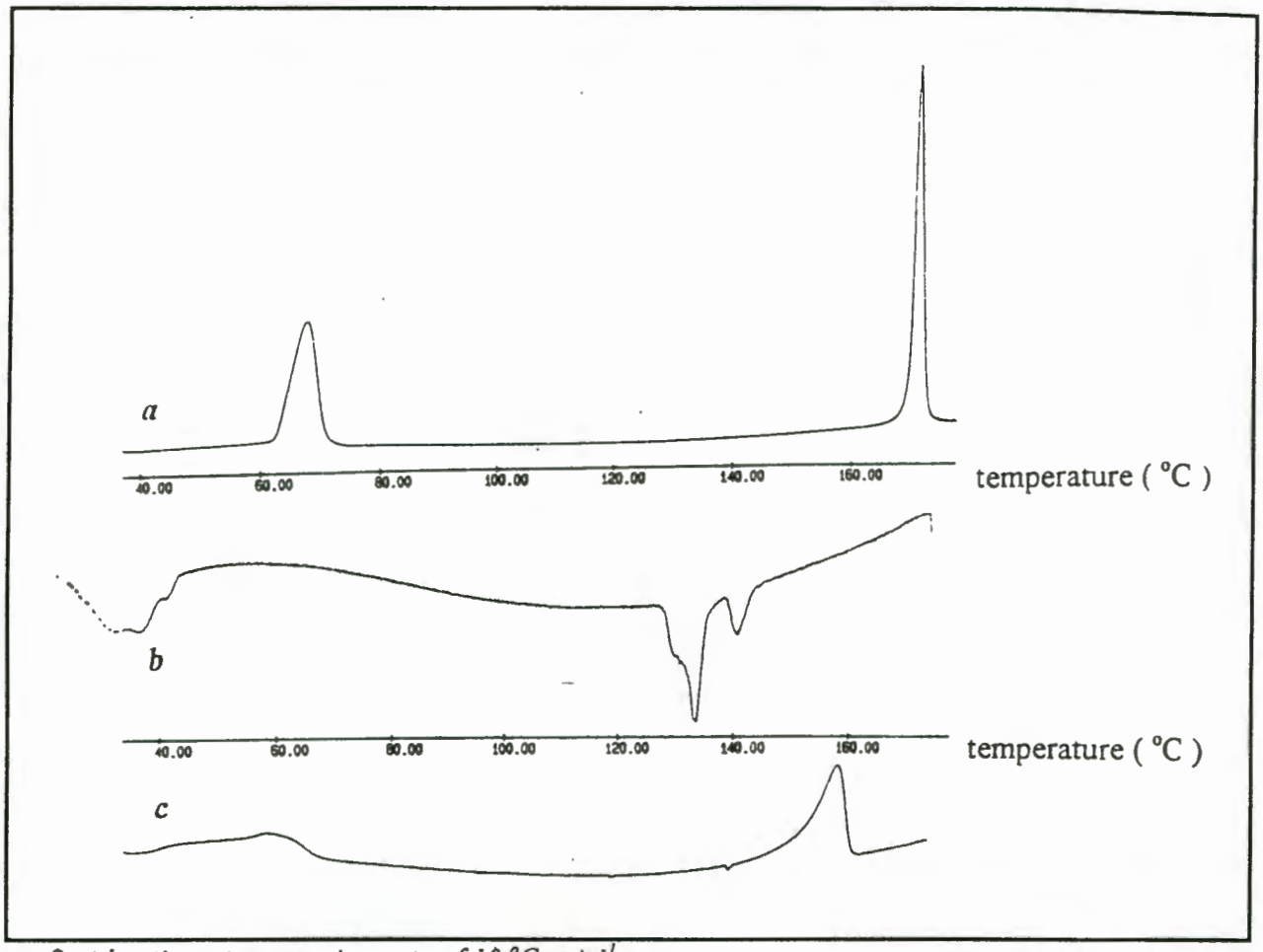

a. first heating at a scanning rate of 10 °C. min^{-1}.

b. cooling at a scanning rate of 2 °C. min^{-1}.

c. second heating at a scanning rate of 10 °C. min^{-1}.

Table 4.5 Transition temperatures, mesophase and thermodynamic data of *7*.

transition	T(°C)	ΔH (kJ.mol^{-1})	ΔS (J.K^{-1}.mol^{-1})
I → S	140.52	7.83	18.93
S → S	133.62	35.50	87.26
S → C	35.00	-	-

Transition temperatures, enthalpy and entropy values obtained from DSC trace at a cooling rate of 2 °C. min^{-1}.

To consider the results obtained, we have successfully synthesised and characterised ten diiodo platinum acylthiourea complexes in which four complexes have mesogenic properties. These metallomesogens form smectic phases (S) on either heating or

cooling. After the complexes reach melting, some decomposition or isomerisation of the samples might take place.

4.2.8 Characterisation of *trans*-bis(*N*-octyl-*N'*-(*p*-dodecyloxy)benzoylthiourea)dichloropalladium(II) (*8*)

Bruce *et al* have reported[12] that *trans*-$[PdCl_2L_2]$ (L = $RC_6H_4C_6H_4CN$, R = n-C_5H_{11}, n-C_8H_{17}, n-$C_9H_{19}O$; L = $R'C_6H_{10}C_6H_{10}CN$, R' = n-C_3H_7, n-C_5H_{11}) can display mesogenic character. In view of the fact that the Pt(II) complex *3*, *trans*-bis(*N*-octyl-*N'*-(*p*-dodecyloxy)-benzoylthiourea)diiodoplatinum(II), possesses mesogenic properties, we decided to ascertain whether the corresponding palladium complex also shows mesogenic behaviour. Unfortunately, the diiodo complexes of palladium could not be prepared according to our general synthetic method as described in chapter 3. Thus, *trans*-bis(*N*-octyl-*N'*-(*p*-dodecyloxy)benzoylthiourea)dichloropalladium(II) (*8*) (Figure 4.15) was prepared and characterised.

Figure 4.15 Schematic representation of complex *8*.

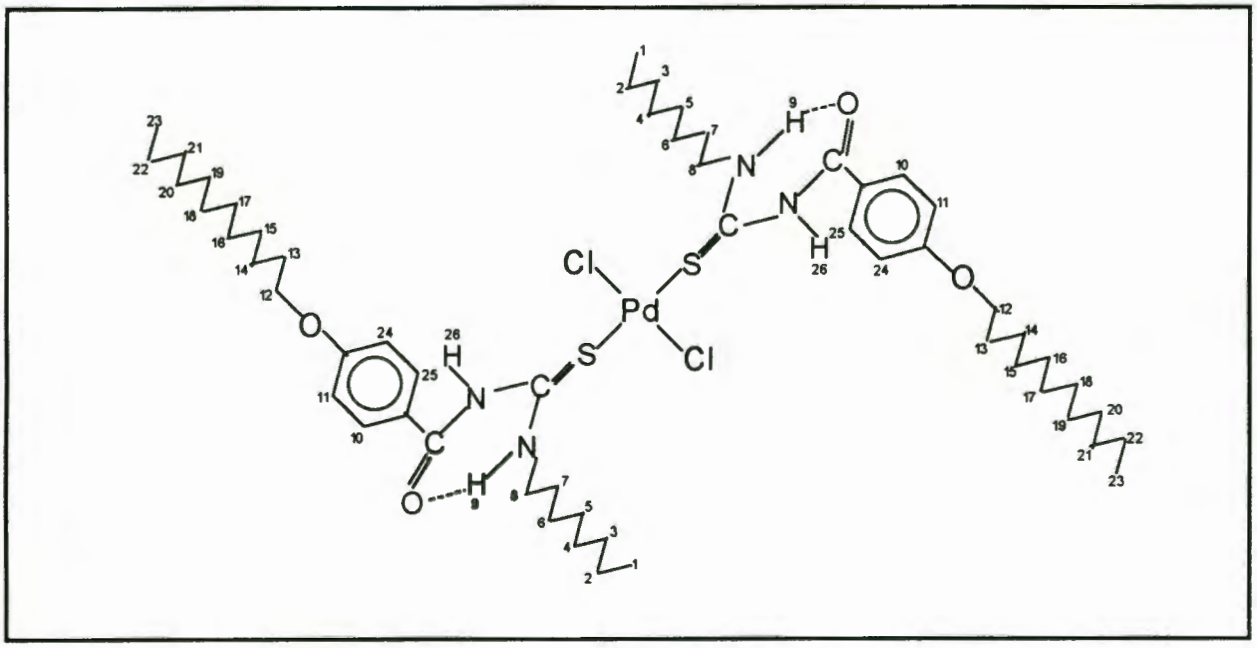

It is surprising that the complex *8* does not possess any mesogenic properties. It melts directly from the solid state into an isotropic liquid on heating at 94 - 95 °C. Slow

cooling of the isotropic liquid results in crystallisation of the complex, with no evidence of any mesogenic behaviour.

4.2.9 Characterisation of *trans*-bis(*N*-(*p*-alkyl(oxy))aniline-*N'*-(*p*-alkyl(oxy))benzoylthiourea)dibromopalladium(II) (*9-10*)

To consider the results that the Pt(II) complexes *6* (*trans*-bis(*N*-(*p*-pentyloxy)aniline-*N'*-(*p*-heptyloxy)benzoylthiourea)diiodoplatinum(II)) and *7* (*trans*-bis(*N*-(*p*-dodecyl)-aniline-*N'*-(*p*-hexyl)benzoylthiourea)diiodoplatinum(II)) exhibit mesogenic character, we decided to ascertain whether the corresponding *trans*- dibromo-palladium complexes possess liquid crystalline properties. Accordingly, *trans*-bis(*N*-(*p*-pentyloxy)aniline-*N'*-(*p*-heptyloxy)benzoylthiourea)dibromopalladium(II) (*9*) and *trans*-bis(*N*-(*p*-dodecyl)aniline-*N'*-(*p*-hexyl)benzoylthiourea)dibromopalladium(II) (*10*) were synthesised and studied (Figure 4.16). Unfortunately, these complexes also show no mesogenic properties. They melt directly from the solid material to the isotropic liquid on heating at 193-195 °C for *9*, and at 174-175 °C for *10*, and result in crystallisation from the isotropic phase on cooling.

From the results of the studies of complexes *8*, *9* and *10*, these Pd(II) complexes have not displayed any mesogenic properties. Considering the comparatively similar coordination chemistry of Pt(II) and Pd(II), it is interesting to note the marked differences in behaviour of the complexes with the same ligands. In this comparison it should be remembered that the Pt(II) complexes are the diiodo compounds, while the Pd(II) complexes are dichloro and dibromo. Thus it could be that the halide ion ligands substantially affect the mesogenic properties of these complexes.

Also, we could not synthesise the diiodo palladium complexes thus preventing comparison of the behaviour to the diiodo platinum complexes.

Figure 4.16 The schematic representation of complexes ***9*** and ***10***.

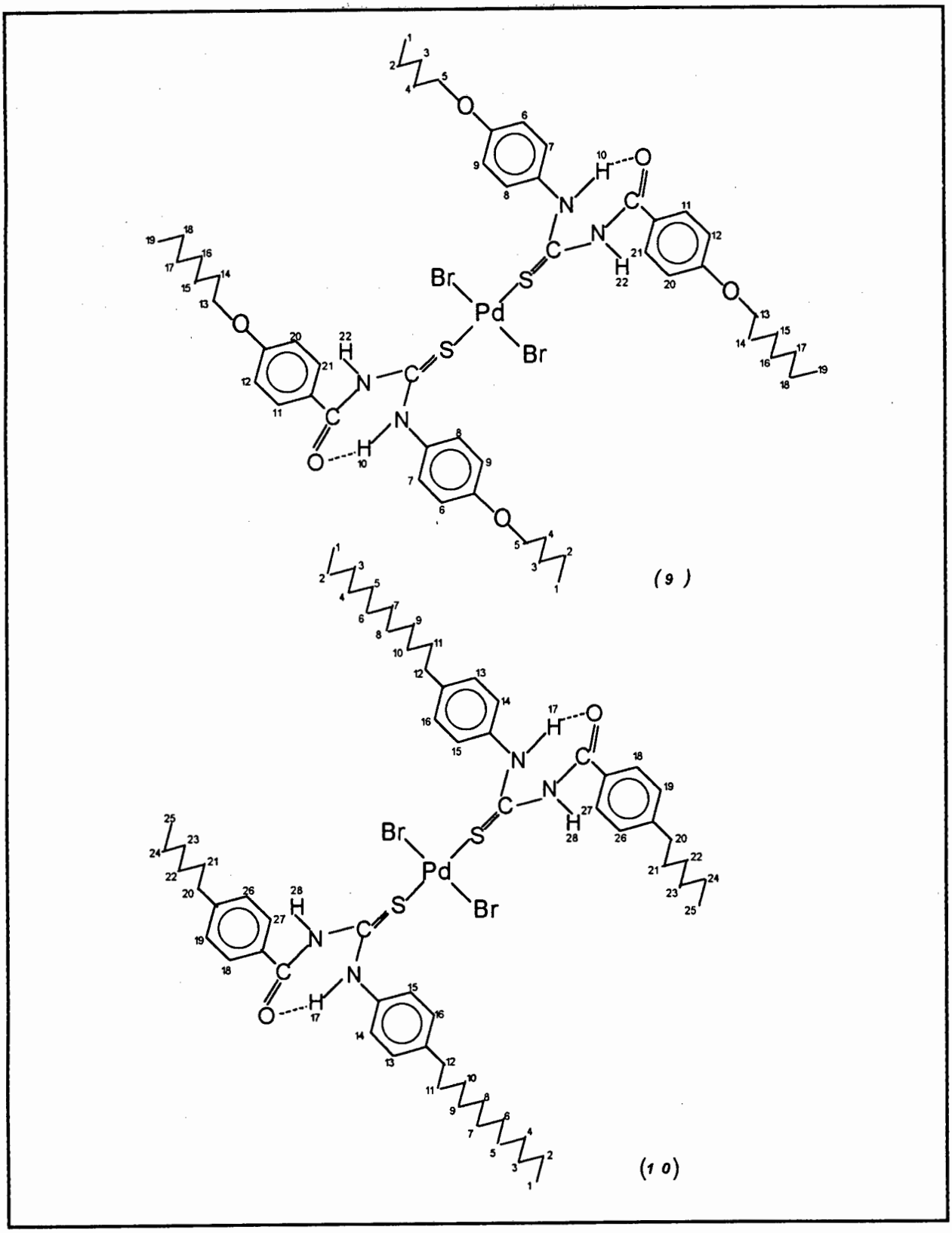

4.3 Conclusion

We have successfully synthesised and characterised a number of new *trans*- diiodo-platinum(II) and *trans*- dihalopalladium(II) complexes of modified *N*-acylthioureas. These complexes are easy to prepare in high yields and have low melting points. Some of the platinum(II) complexes (***3***, ***5b***, ***6*** and ***7***) have displayed mesogenic properties. These metallomesogens are thermotropics. The results of polarising optical microscopy and DSC indicate that the mesogenic phases produced are smectics. In contrast to platinum(II) complexes, palladium(II) complexes have shown no mesogenic properties.

Considering the molecular structures of all platinum(II) complexes prepared, we have been able to establish that one long alkyl chain (C_{12}) on the ligand is essential for the mesogenic behaviour of corresponding diiodo platinum complex; but when the alkyl chain is shorter (C_5-C_7), two alkyloxy chains become necessary. The number of phenyl groups in the molecule determines the type of thermotropic metallomesogens observed. The complex which involves a ligand having one phenyl group forms enantiotropics while the complex which involves a ligand having two phenyl groups forms monotropics.

The melting points of these complexes are influenced by the number of oxygen and phenyl groups in the ligands. The melting points are increased from one oxygen (or one phenyl ring) to two oxygens (or two phenyl rings). Some partial decomposition or thermal isomerisation of complexes might take place above the clearing points.

For these metallomesogens synthesised, the phase transitions in the first heating process cannot be repeated in the second heating process. This could be due to following possible reasons:

(1) partial crystallisation of the sample on cooling,

(2) some isomerisation might take place during the first heating process,

(3) some decomposition could take place.

In view of these facts, we would conclude that these complexes are not perfect metallomesogens and some modification might be useful to improve this.

One ideally would like to make the related *trans*-bis(*N,N*-dialkyl-*N'*-acylthiourea-to)M(II) (M=metal), but so far we have not investigated this. This way we could eliminate the *halide* effect.

4.4 Experimental

Commercially available chemicals were used. The ligands used in this chapter are contributed by Grimmbacher[4]. The general apparatus and analysis methods used are the same as those described in Chapter 2.

All melting points and mesophases are observed by using REICHERT THERMOVAR microscope. All DSC experiments have been performed by Dodds of the Chemistry Department of the University of Cape Town, on a Perkin-Elmer-PE7 DSC instrument. All photographs of mesogenic phases were obtained with a Nikon Optiphot-POL camera.

General procedure for the synthesis of $[M(H_2L)_2X_2]$ complexes

The $[M(H_2L)_2X_2]$ (M = Pt, Pd) complexes were synthesised according to the procedure as described in Chapter 3. A general procedure is given below:

A K_2PtCl_4 solution (10% HI / CH_3CN, v : v = 1 : 2~25) containing 25 fold molar NaI was stirred for 1 hr and then reacted with a ligand (same solvent) for 30 minutes at 50 °C. The precipitate formed was collected by filtration after adding 100 - 200 ml of cold water, and was washed with water and ether and dried under vacuum. The products were analysed by means of C, H and N elemental analysis and ^1H NMR spectroscopy. The characterisation results of the complexes are recorded in the following section.

trans*-bis(*N*-dodecyl-*N'*-benzoylthiourea)diiodoplatinum(II)** ***1a 78.6% yield, m.p. 121-122 °C. Calc. for $[Pt(C_{20}H_{32}N_2OS)_2I_2]$: C,41.93; H,5.63; N,4.89%. Obs. C,42.09; H,5.64; N,4.94%. $\delta^1H(CDCl_3)$: 10.99 (2H,s,H^{19}), 10.85 (2H,t,H^{13}), 8.14 (4H,d,H^{14}/H^{18}), 7.61 (2H,t,H^{16}), 7.50 (4H,t,H^{15}/H^{17}), 3.70 (4H,s,H^{12}), 1.77 (4H,q,H^{11}), 1.43-1.26 (44H,bm,H^{2-10}), 0.87 (6H,t,H^1) ppm.

trans*-bis(*N*-tetradecyl-*N'*-benzoylthiourea)diiodoplatinum(II)** ***1b 96.8% yield, m.p. 118-120 °C. Calc. for $[Pt(C_{22}H_{36}N_2OS)_2I_2]$: C,43.97; H,6.04; N,4.66%. Obs. C,44.06; H,6.12; N,4.66%. $\delta^1H(CDCl_3)$: 10.98 (2H,s,H^{21}), 10.86 (2H,t,H^{15}), 8.14 (4H,d,H^{16}/H^{20}), 7.61 (2H,t,H^{18}), 7.50 (4H,t,H^{17}/H^{19}), 3.71 (4H,s,H^{14}), 1.77 (4H,q,H^{13}), 1.43-1.26 (48H,bm,H^{2-12}), 0.87 (6H,t,H^1) ppm.

trans*-bis(*N*-hexadecyl-*N'*-benzoylthiourea)diiodoplatinum(II)** ***1c 87.3% yield, m.p. 122-124 °C. Calc. for $[Pt(C_{24}H_{40}N_2OS)_2I_2]$: C,45.83; H,6.41; N,4.45%. Obs. C,45.94; H,6.49; N,4.48%. $\delta^1H(CDCl_3)$: 10.99 (2H,s,H^{23}), 10.86 (2H,t,H^{17}), 8.14 (4H,d,H^{18}/H^{22}), 7.62 (2H,t,H^{20}), 7.50 (4H,t,H^{19}/H^{21}), 3.71 (4H,s,H^{16}), 1.77 (4H,q,H^{15}), 1.45-1.25 (52H,bm,H^{2-14}), 0.87 (6H,t,H^1) ppm.

trans*-bis(*N*-octcyl-*N'*-naphthoylthiourea)diiodoplatinum(II)** ***2 92.3% yield, m.p. 170-173 °C. Calc. for $[Pt(C_{20}H_{28}N_2OS)_2I_2]$: C,42.23; H,4.96; N,4.83%. Obs. C,42.42; H,4.59; N,4.96%. $\delta^1H(CDCl_3)$: 10.87 (2H,t,H^9), 10.84 (2H,s,H^{17}), 8.50 (2H,d,H^{16}), 8.36 (2H,d,H^{10}), 7.96 (2H,d,H^{12}), 7.84 (2H,d,H^{13}), 7.65 (2H,t,H^{11}), 7.57 (2H,t,H^{14}), 7.50 (2H,t,H^{15}), 3.70 (4H,s,H^8), 1.78 (4H,q,H^7), 1.44-1.28 (20H,bm,H^{2-6}), 0.89 (6H,t,H^1) ppm.

trans*-bis(*N*-octyl-*N'*-(*p*-dodecyloxy)benzoylthiourea)diiodoplatinum(II)** ***3 82.5% yield, m.p. 107-108 °C. Calc. for $[Pt(C_{28}H_{48}N_2O_2S)_2I_2]$: C,47.97; H,6.90; N,4.00%. Obs. C,48.60; H,7.14; N,4.09%. $\delta^1H(CDCl_3)$: 10.93 (2H,t,H^9), 10.87 (2H,s,H^{26}), 8.08 (4H,d,H^{10}/H^{25}), 6.93 (4H,d,H^{11}/H^{24}), 4.00 (4H,t,H^{12}), 3.68 (4H,s,H^8), 1.78 (8H,q,H^7/H^{13}), 1.44-1.26 (56H,bm,H^{2-6}/H^{14-22}), 0.87 (12H,t,H^1/H^{23}) ppm.

trans*-bis(*N*-(*p*-hexyloxy)aniline-*N'*-heptylbenzoylthiourea)diiodoplatinum(II)** ***4 96.6% yield, m.p. 166-168 °C. Calc. for $[Pt(C_{27}H_{38}N_2O_2S)_2I_2]$: C,47.76; H,5.64; N,4.13%. Obs. C,48.01; H,5.69; N,4.12%. $\delta^1H(CDCl_3)$: 12.41 (2H,s,H^{11}), 11.12 (2H,s,H^{23}), 8.08 (4H,d,H^{12}/H^{22}), 7.44 (4H,d,H^{13}/H^{21}), 7.30 (4H,d,H^8/H^9), 6.97 (4H,d,H^7/H^{10}), 3.99 (4H,t,H^6), 2.66 (4H,t,H^{14}), 1.80 (4H,q,H^5), 1.63 (4H,q,H^{15}), 1.48-1.29 (28H,bm,H^{2-4}/H^{16-19}), 0.89 (12H,t,H^1/H^{20}) ppm.

trans*-bis(*N*-(*p*-hexyl)aniline-*N'*-(*p*-heptyloxy)benzoylthiourea)diiodoplatinum(II)** ***5a 94.4% yield, m.p. 166-169 °C. Calc. for $[Pt(C_{27}H_{38}N_2O_2S)_2I_2]$: C,47.76; H,5.64; N,4.13%. Obs. C,47.94; H,5.69; N,4.04%. $\delta^1H(CDCl_3)$: 12.57 (2H,s,H^{11}), 11.05 (2H,s,H^{23}), 8.13 (4H,d,H^{12}/H^{22}), 7.45 (4H,d,H^7/H^{10}), 7.27 (4H,d,H^8/H^9), 6.95 (4H,d,H^{13}/H^{21}), 4.00 (4H,t,H^{14}), 2.64 (4H,t,H^6), 1.79 (4H,q,H^{15}), 1.60 (4H,q,H^5), 1.48 (4H,q,H^{16}), 1.37-1.29 (34H,bm,H^{2-4}/H^{17-19}), 0.91 (12H,t,H^1/H^{20}) ppm.

trans*-bis(*N*-(*p*-hexyl)aniline-*N'*-(*p*-*d*odecyloxy)benzoylthiourea)diiodo-platinum(II)** ***5b 95.8% yield, m.p. 169-171 °C. Calc. for $[Pt(C_{32}H_{48}N_2O_2S)_2I_2]$: C,51.30; H,6.46; N,3.74%. Obs. C,52.10; H,6.72; N,3.74%. $\delta^1H(CDCl_3)$: 12.57 (2H,s,H^{11}), 11.05 (2H,s,H^{28}), 8.13 (4H,d,H^{12}/H^{27}), 7.45 (4H,d,H^7/H^{10}), 7.27 (4H,d,H^8/H^9), 6.92 (4H,d,H^{13}/H^{26}), 4.01 (4H,t,H^{14}), 2.64 (4H,t,H^6), 1.80 (4H,q,H^{15}), 1.60 (4H,q,H^5), 1.48 (4H,q,H^{16}), 1.35-1.27 (44H,bm,H^{2-4}/H^{17-24}), 0.88 (12H,t,H^1/H^{25}) ppm.

trans*-bis(*N*-(*p*-pentyloxy)aniline-*N'*-(*p*-heptyloxy)benzoylthiourea)diiodo-platinum(II)** ***6 94.6% yield, m.p. 192-194 °C. Calc. for $[Pt(C_{26}H_{36}N_2O_3S)_2I_2]$: C,45.86; H,5.33; N,4.11%. Obs. C,46.46; H,5.46; N,3.88%. $\delta^1H(CDCl_3)$: 12.43 (2H,s,H^{10}), 11.04 (2H,s,H^{22}), 8.12 (4H,d,H^{11}/H^{21}), 7.43 (4H,d,H^7/H^8), 6.96 (4H,d,$H^{12}H^{20}$), 6.94 (4H,d,H^6/H^9), 4.02 (4H,t,H^{13}), 3.98 (4H,t,H^5), 1.81 (8H,q,H^4/H^{14}), 1.50-1.32 (24H,bm,H^{2-3}/H^{15-18}), 0.94 (12H,t,H^1/H^{19}) ppm.

trans*-bis(*N*-(*p*-dodecyl)aniline-*N'*-(*p*-hexyl)benzoylthiourea)diiodoplatinum(II)** ***7 96.5% yield, m.p. 168-171 °C. Calc. for $[Pt(C_{32}H_{48}N_2OS)_2I_2]$: C,52.42; H,6.60; N,3.82%. Obs. C,52.44; H,6.79; N,3.78%. $\delta^1H(CDCl_3)$: 12.54 (2H,s,H^{17}), 11.13

(2H,s,H^{28}), 8.09 (4H,d,H^{18}/H^{27}), 7.47 (4H,d,H^{19}/H^{26}), 7.31 (4H,d,H^{13}/H^{16}), 7.28 (4H,d,H^{14}/H^{15}), 2.66 (8H,s,H^{12}/H^{20}), 1.63 (8H,q,H^{11}/H^{21}), 1.32-1.24 (48H,bm,H^{2-10}/H^{22-24}), 0.87 (12H,t,H^{1}/H^{25}) ppm.

trans*-bis(*N*-octyl-*N'*-(*p*-dodecyloxy)benzoylthiourea)dichloropalladium(II)** ***8 88.0% yield, m.p. 94-95 °C. Calc. for [$Pd(C_{28}H_{48}N_2O_2S)_2Cl_2$]: C,59.49; H,8.56; N,4.96%. Obs. C,59.49; H,8.96; N,4.86%. δ^1H($CDCl_3$): 11.42-11.33 (4H,b,H^{9}/H^{26}), 8.10 (4H,b,H^{10}/H^{25}), 6.97 (4H,d,H^{11}/H^{24}), 4.00 (4H,t,H^{12}), 3.67 (4H,s,H^{8}), 1.80 (8H,q,H^{7}/H^{13}), 1.43-1.20 (56H,bm,H^{2-6}/H^{14-22}), 0.86 (12H,t,H^{1}/H^{23}) ppm.

trans*-bis(*N*-(*p*-pentyloxy)aniline-*N'*-(*p*-heptyloxy)benzoylthiourea)dibromo-palladium(II)** ***9 87.4% yield, m.p. 193-195 °C. Calc. for [$Pd(C_{26}H_{36}N_2O_3S)_2Br_2$]: C,52.96; H,6.15; N,4.75%. Obs. C,53.05; H,6.16; N,4.74%. δ^1H($CDCl_3$): 12.67 (2H,s,H^{22}), 11.14 (2H,s,H^{10}), 8.14 (4H,d,H^{11}/H^{21}), 7.39 (4H,d,H^{7}/H^{8}), 6.96 (4H,d,$H^{12}H^{20}$), 6.92 (4H,d,H^{6}/H^{9}), 4.02 (4H,t,H^{13}), 3.97 (4H,t,H^{5}), 1.80 (8H,q,H^{4}/H^{14}), 1.50-1.31 (24H,bm,H^{2-3}/H^{15-18}), 0.90 (12H,t,H^{1}/H^{19}) ppm.

trans*-bis(*N*-(*p*-dodecyl)aniline-*N'*-(*p*-hexyl)benzoylthiourea)dibromo-palladium(II)** ***10 97.7% yield, m.p. 174-175 °C. Calc. for [$Pd(C_{32}H_{48}N_2OS)_2Br_2$]: C,59.88; H,7.54; N,4.37%. Obs. C,60.63; H,7.82; N,4.06%. δ^1H($CDCl_3$): 12.75 (2H,s,H^{17}), 11.22 (2H,b,H^{28}), 8.10 (4H,b,H^{18}/H^{27}), 7.42 (4H,b,H^{19}/H^{26}), 7.33 (4H,d,H^{13}/H^{16}), 7.23 (4H,d,H^{14}/H^{15}), 2.65 (8H,q,H^{12}/H^{20}), 1.63 (8H,q,H^{11}/H^{21}), 1.35-1.18 (48H,bm,H^{2-10}/H^{22-24}), 0.89 (12H,t,H^{1}/H^{25}) ppm.

References

1. J. Szydlowska, W. Pyzuk, A. Krowczynski and I. Bikchantaev, *J. Mater. Chem.*, 1996, **6**(5), 733; and *references therein*.
2. A-M. Giroud-Godquin and P.M. Maitlis, *Angew. Chem. Int. Ed. Engl.* 1991, **30,** 375.
3. F. Neve, *Adv. Mater.* 1996, **8**(4), 277.
4. T. Grimmbacher, *Ph.D Thesis*, University of Cape Town, 1995.
5. K.R. Koch, unpublished results.
6. V. Prasad and B.K. Sadashiva, *Mol. Cryst. Liq. Cryst.*, 1994, **241**, 167.
7. J.M. Kroon, P.S. Schenkels, M.V. Dijk and E.J.R. Sudholter, *J. Mater. Chem.*, 1995, **5**(9), 1309.
8. M. Lee and N.K. Oh, *J. Mater. Chem.*, 1996, **6**(7), 1079.
9. P. Humberstone, G.J. Clarkson, N.B. McKeown and K.E. Treacher, *J. Mater. Chem.*, 1996, **6**(3), 315.
10. J. Andersch, S. Diele and C. Tschierske, *J. Mater. Chem.*, 1996, **6**(9), 1465.
11. J. Andersch, C. Tschierske, S. Diele and D. Lose, *J. Mater. Chem.*, 1996, **6**(8), 1297.
12. D.W. Bruce, E. Lalinde, P. Styring, D.A. Dunmur, and P.M. Maitlis, *J. Chem. Soc., Chem. Commun.*, 1986, 581.

CHAPTER 5

Crystal Structure Of *Trans*-$[Pd(H_2L^1)_2Br_2]$ (H_2L^1=*N*-(*n*-propyl)-*N*'-benzoylthiourea)

5.1 Introduction

The crystal structure[1] (Figure 5.1) of *cis*-$[Pt(H_2L^1)_2Cl_2]$ (H_2L^1 = *N*-(*n*-propyl)-*N'*-benzoylthiourea) shows the molecule to be locked into a planar six-membered O-C-N-C-N-H ring by means of an intramolecular N-H···O hydrogen bond. The crystal structure of *trans*-$[Pt(HL)_2I_2]$ (HL = *N,N*-dibutyl-*N'*-benzoylthiourea) has also been investigated and characterised by Koch[2]. It also has an intramolecular hydrogen bond as seen in the similar complex. Subsequently, the crystal structure of *trans*-$[Pd(H_2L^1)_2Br_2]$ (H_2L^1 = *N*-(*n*-propyl)-*N'*-benzoylthiourea) has been determined and investigated in this study by x-ray crystallography in order to compare with $[Pt(H_2L^1)_2Cl_2]$ and $[Pt(HL)_2I_2]$.

Figure 5.1 The crystal structure of *cis*-$[Pt(H_2L^1)_2Cl_2]$ complex.

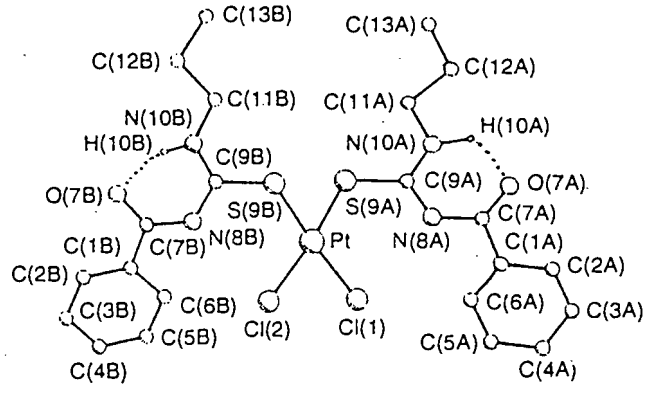

5.2 Results and discussion

The crystal system is triclinic and contains one molecule / unit cell. The complex *trans*-$[Pd(H_2L^1)_2Br_2]$ crystallised in the space group P $\bar{1}$, with Z = 1. It is located in a special position, with the Pd atom located on a center of symmetry. A perspective view of the molecule and the atom-labeling scheme are shown in Figure 5.2. A projection along c* is shown in Figure 3.3 to illustrate the packing in the unit cell. The crystal data and structure refinement are give in Table 4.1 of Appendix 4. The bond lengths and angles are found in Table 4.2 of Appendix 4.

Figure 5.2 Perspective view of the molecule *trans*-[$Pd(H_2L^1)_2Br_2$], with the numbering scheme. Only those hydrogen involved in hydrogen bonding are shown. The hydrogen bonds are indicated by dotted lines.

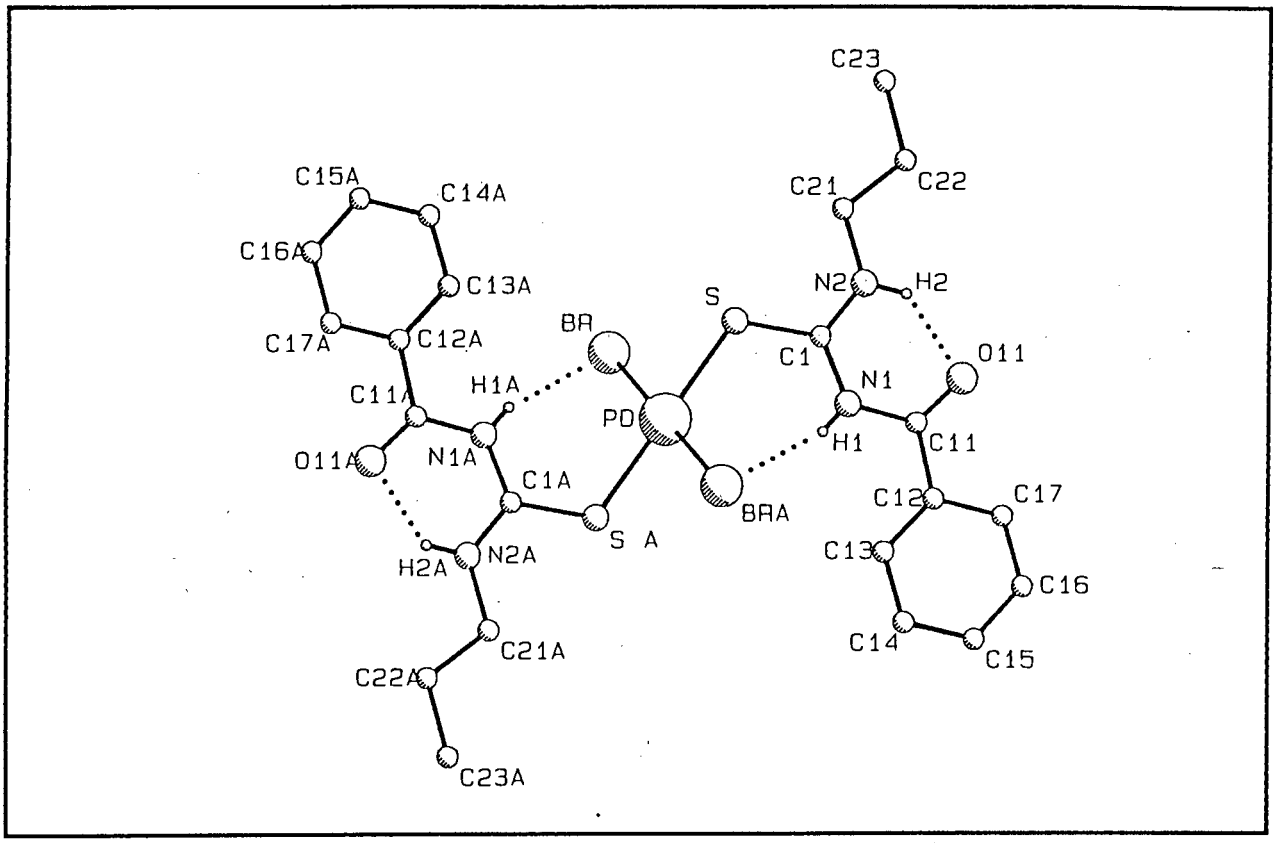

Figure 5.3 Packing diagram of *trans*-[$Pd(H_2L^1)_2Br_2$].

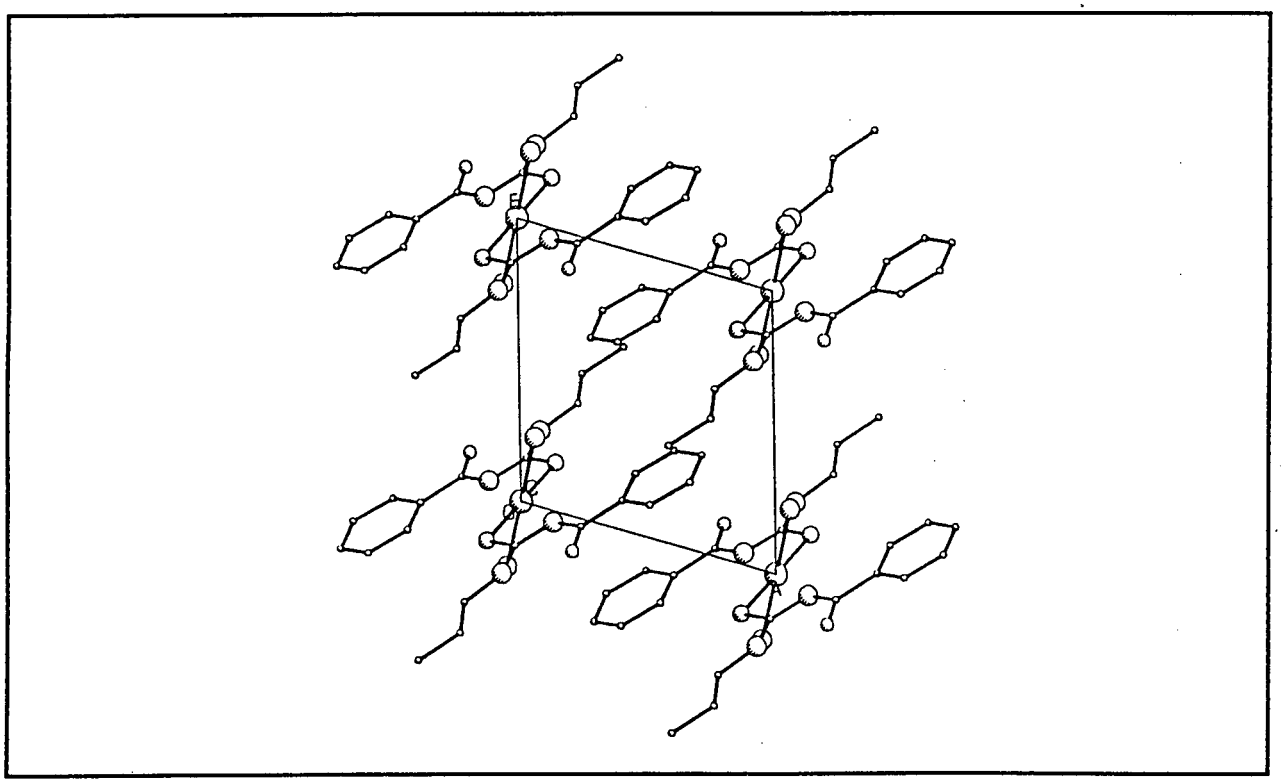

Description of the molecular structure

Square planar coordination is observed for the Pd atom in this structure (the molecule exists in *trans*- form), with bond length Pd-S = 2.316(1) Å and Pd-Br = 2.442(1) Å. The bond length of Pd-S is slightly longer than that of Pt-S in *cis*-$[Pt(H_2L^1)_2Cl_2]$ complex[1], but interestingly it is similar with the typical range of Pt-S (2.309-2.335 Å) observed for tetrakis(thiourea)platinum(II) cations[3, 4]. The bond angles S(A)-Pd-S and Br-Pd-Br(A) are 180.0 ° respectively, while S(A)-Pd-Br (94.54 °), S-Pd-Br (85.46°), S(A)-Pd-Br(A) (85.46°) and S-Pd-Br(A) (94.54 °) deviate from 90 °.

Two hydrogen bonds have been observed between N2 and O11 with d(N2···O11) = 2.601(4) Å, and between N1 and Br with d(N1···Br) = 3.294(4) Å. The H-bonded ring C1-N1-C11-O11-H2-N2 is tested for planarity, and the atoms are found to deviate by a RMS of 0.026 Å. The structure of the coordinated ligands is remarkably similar to that of the free ligand[5], and that of the coordinated ligands in similar square planar *cis*-$[Pt(H_2L^1)_2Cl_2]$ complex[1], the corresponding bond lengths involved in the C-N-C-O-H-N ring being comparable to the free ligand are given in Table 5.1.

Table 5.1 The comparing length data involved in the C-N-C-O-H-N ring for the free ligand, coordinated ligand in *cis*-$[Pt(H_2L^1)_2Cl_2]$ and in *trans*-$[Pd(H_2L^1)_2Br_2]$, respectively.

bond	**length (Å)**		
	H_2L^1	***cis*-$[Pt(H_2L^1)_2Cl_2]$**	***trans*-$[Pd(H_2L^1)_2Br_2]$**
S-C1	1.678(4)	1.699(23), 1.696(21)	1.689(4)
N1-C1	1.393(5)	1.366(26)	1.378(5)
N1-C11	1.383(4)	-	1.379(5)
N2-C1	1.332(7)	1.307(28), 1.273(25)	1.315(5)
C11-O11	1.226(5)	1.223(25), 1.259(23)	1.220(5)

The two symmetry related rings in the molecule are parallel to each other. The atoms are found to deviate by a RMS of 0.000 Å, which confirms that the phenyl rings are exactly planar in this molecule.

The determination of the crystal structure has confirmed the square planar coordination chemistry for Pd and the existence of a strong intramolecular hydrogen bond that allows for the formation of a planar six-membered ring. It also indicates an interesting rod-shaped molecular geometry.

5.3 Experimental

The crystal structure of *trans*-$[Pd(H_2L^1)_2Br_2]$ has been determined by Dr Anita Coetzee (Department of Crystallography, UCT).

The crystal was obtained by recrystallisation of crude product in chloroform/ethanol (1:1 volume) solution. It was dried under vacuum.

A single crystal of diffraction quality was mounted on a glass fibre. X-ray intensity data were collected on an Enraf-Nonius CAD4 diffractometer, using graphite-monochromated Mo Kα radiation (λ=0.7107) and the ω - 2θ mode. The unit cell was refined using the setting angles of 24 reflections in the θ range 16-17 °. Three reference reflections were monitored periodically for intensity and orientation control. A lorentz-polarisation correction was applied to the data, as well as an empirical absorption correction[6].

The non-hydrogen atoms were located by direct methods using SHELXS-86[7]. The remaining atoms were located in difference Fourier maps and refined using SHELXL-93[8]. All non-hydrogen atoms were treated anisotropically. The N-H amide hydrogen atoms were located in the difference electron density map and allowed to refine. All other hydrogen atoms were placed in geometrically calculated positions and linked to a common temperature factor for chemically equivalent groups.

References

1. S. Bourne and K.R. Koch, *J. Chem. Soc. Dalton Trans.*, 1993, 2071.
2. K.R. Koch, unpublished work.
3. R.L. Girling, K.K. Chatterjee and E.L. Amma, *Inorg. Chim. Acta*, 1976, **17**, 225.
4. F. Bachechi, L. Zambonelli and G. Marcotrigiano, *Inorg. Chim. Acta*, 1973, **7**, 557.
5. A. Drago, Yu. Shepelev, F. Fajardo, F. Alvarez and R. Pomes, *Acta Crystallogr., Sect. C*, 1989, **45**, 1192.
6. A.T.C. North, D.C. Phillips and F.S. Mathews, *Acta Crystallogr., Sect. A*, 1968, **24**, 351.
7. G.M. Sheldrick, SHELXS-86 in *Crystallographic Computing 3*, eds G.M. Sheldrick, C. Kruger, R. Goddard, Oxford University Press, 1985, 175.
8. G.M. Sheldrick in preparation.

Appendix 1

Figure 1.1 Least-square curves obtained from the ^{1}H NMR results for *cis-trans* isomerisation of $[Pt(H_2L^1)_2Cl_2]$ at an initial concentration of 0.00381M in chloroform-d_3 at 25 °C.

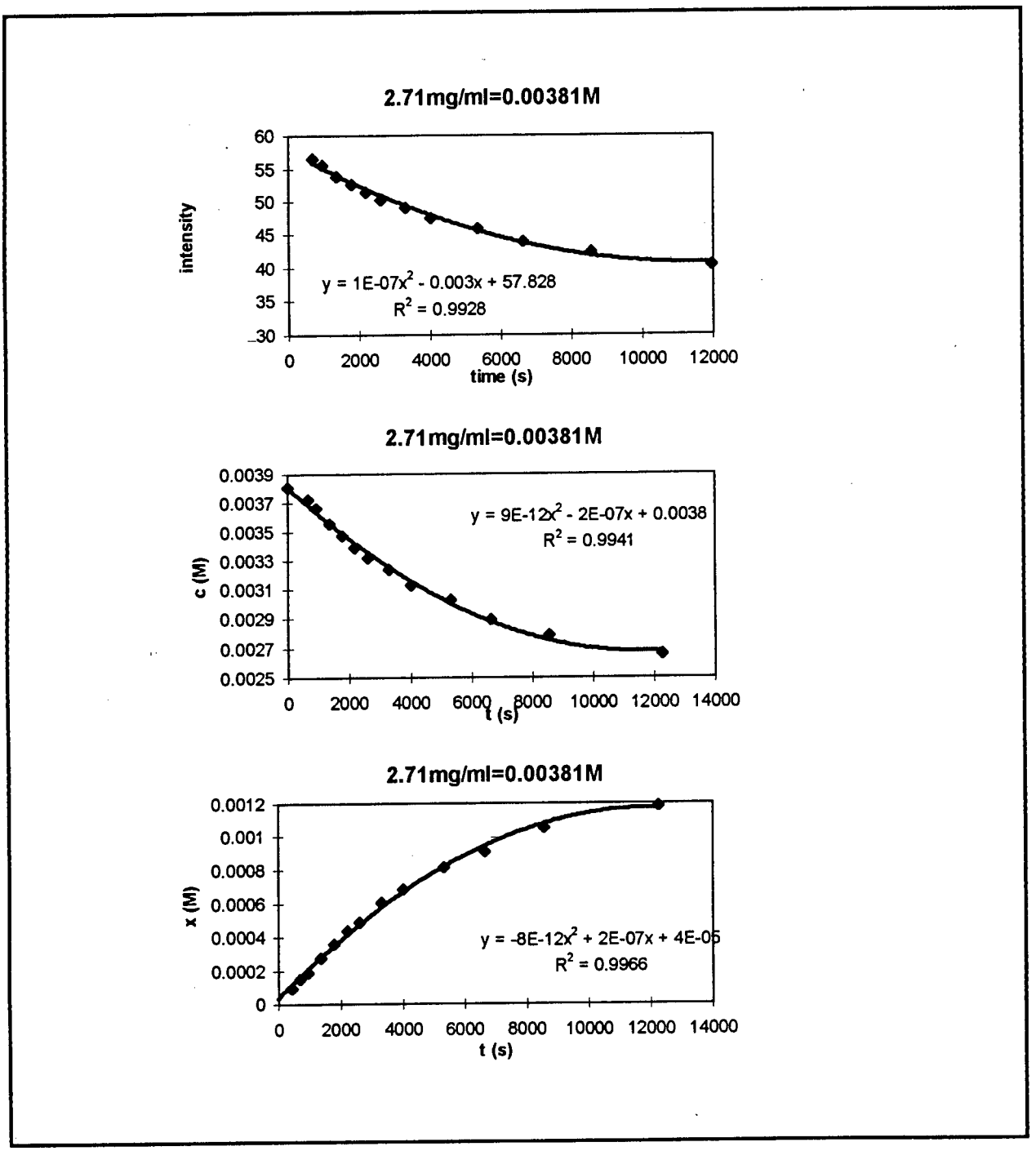

Appendix 1

Figure 1.2 Least-square curves obtained from the ^{1}H NMR results for *cis-trans* isomerisation of $[Pt(H_2L^1)_2Cl_2]$ at an initial concentration of 0.00420M in chloroform-d_3 at 25 °C.

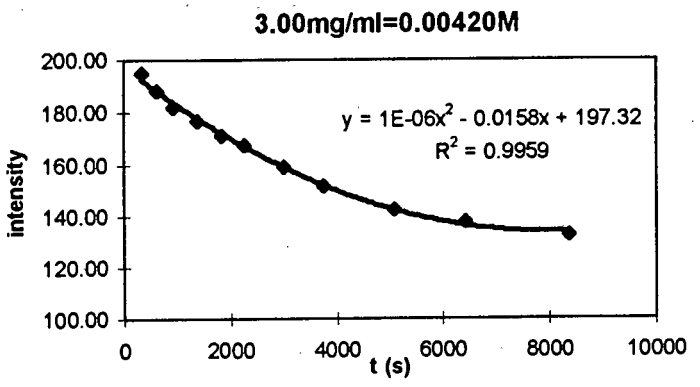

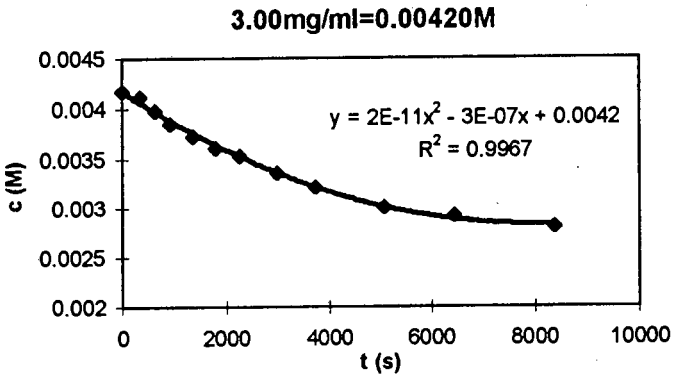

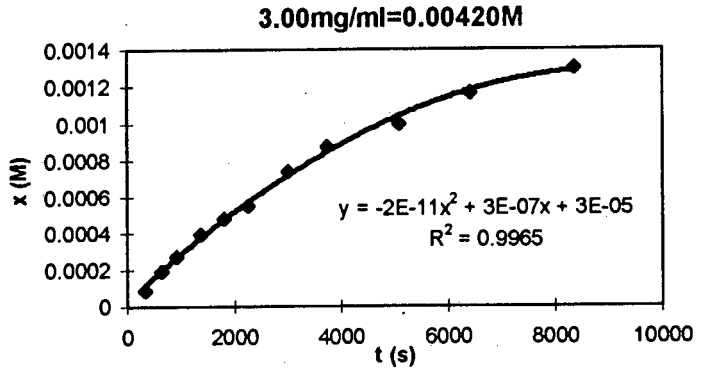

Appendix 1

Figure 1.3 Least-square curves obtained from the ^{1}H NMR results for *cis-trans* isomerisation of $[Pt(H_2L^1)_2Cl_2]$ at an initial concentration of 0.00660M in chloroform-d_3 at 25 °C.

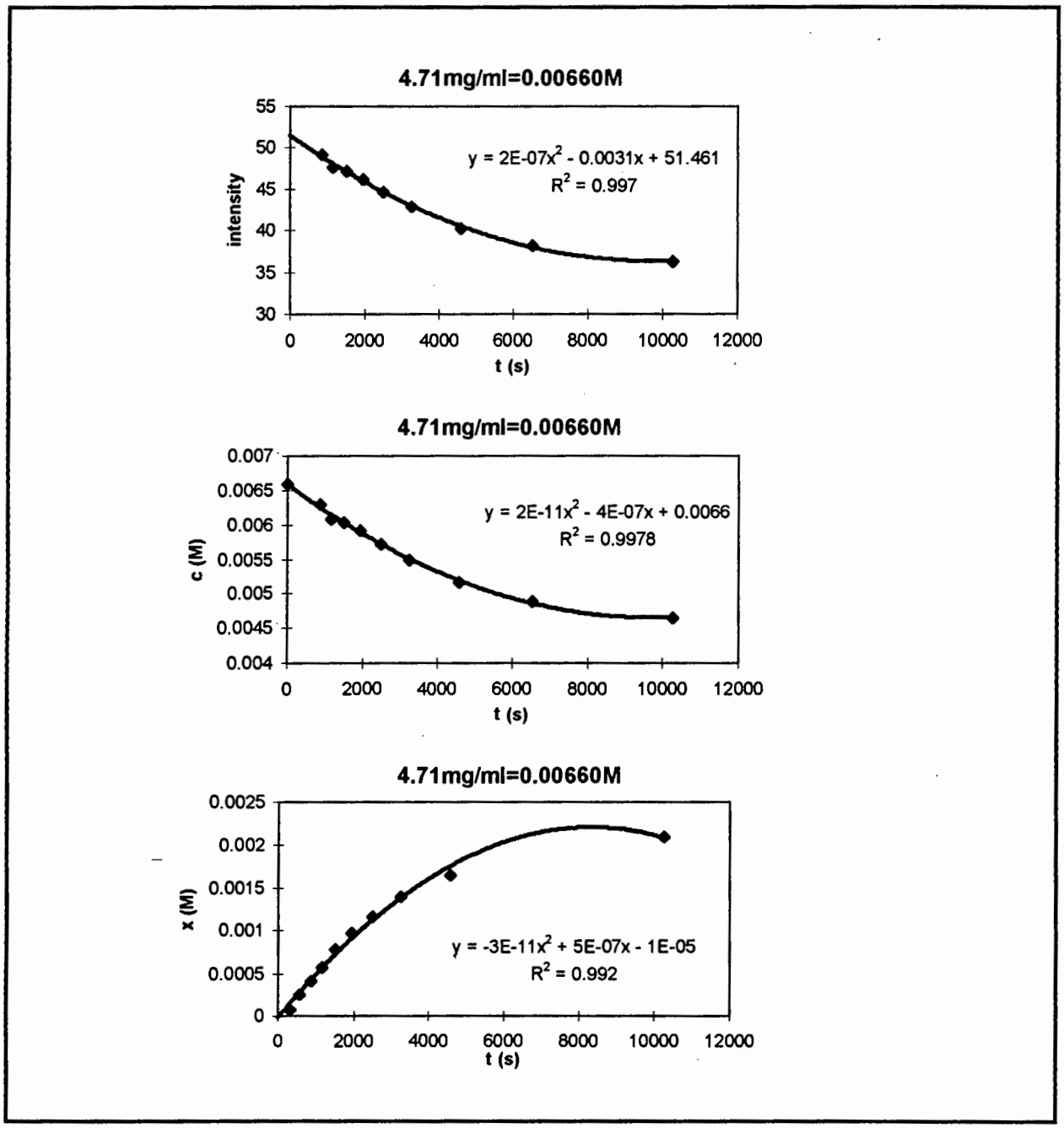

Appendix 1

Figure 1.4 Least-square curves obtained from the ^{1}H NMR results for *cis-trans* isomerisation of $[Pt(H_2L^1)_2Cl_2]$ at an initial concentration of 0.01065M in chloroform-d_3 at 25 °C.

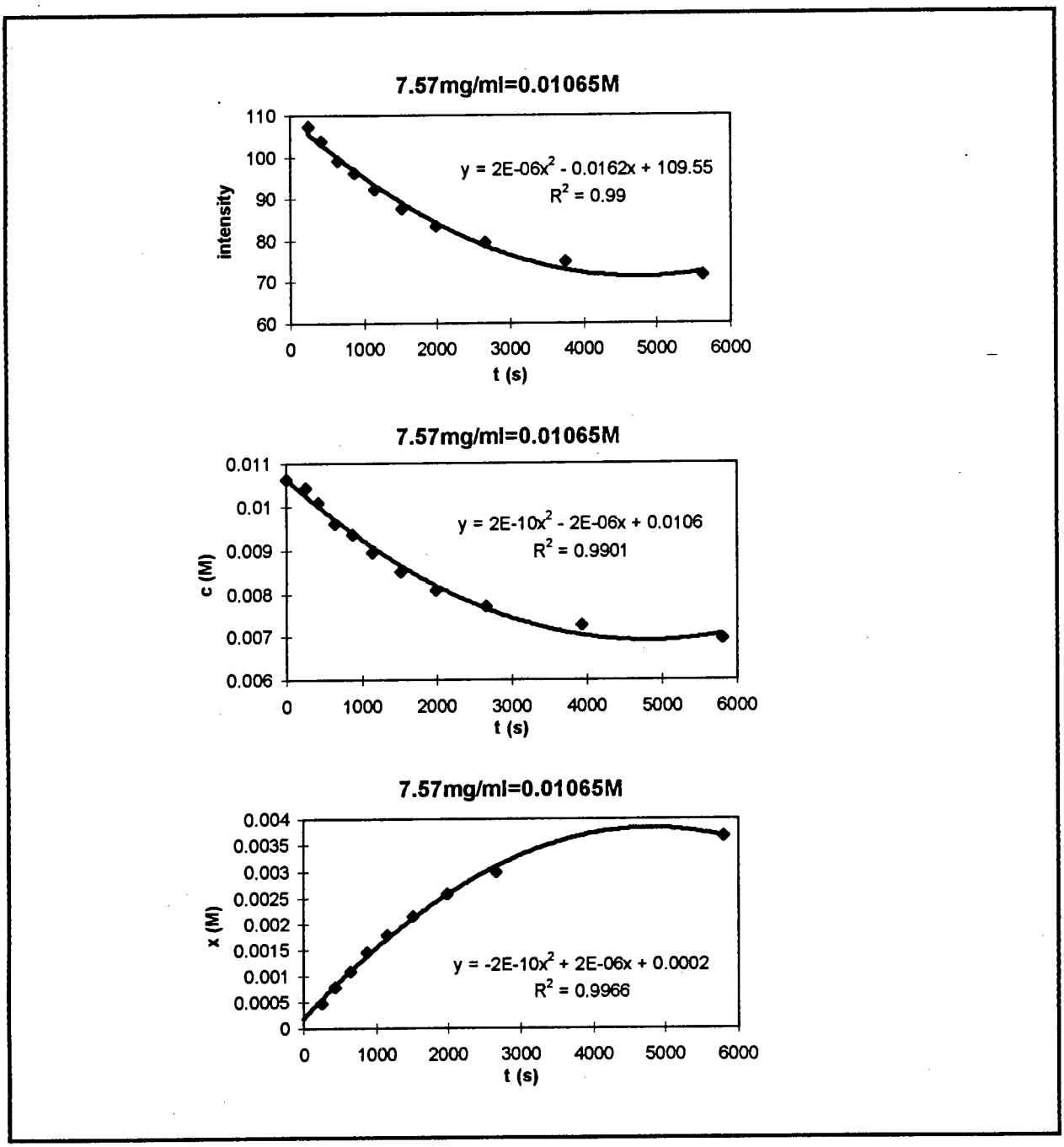

Appendix 1

Figure 1.5 Least-square curves obtained from the ^{1}H NMR results for *cis-trans* isomerisation of $[Pt(H_2L^1)_2Cl_2]$ at an initial concentration of 0.01628M in chloroform-d_3 at 25 °C.

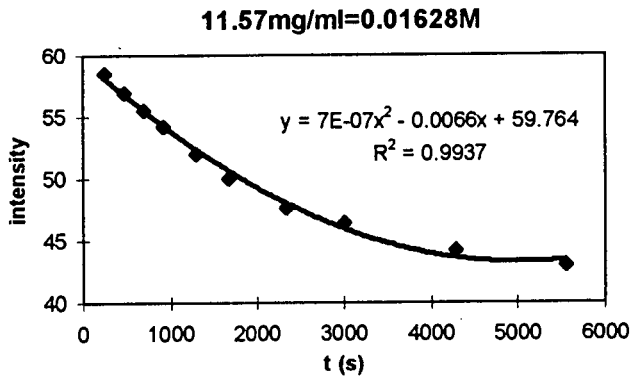

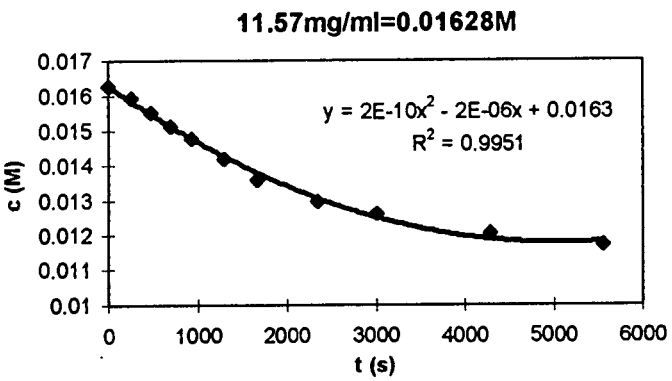

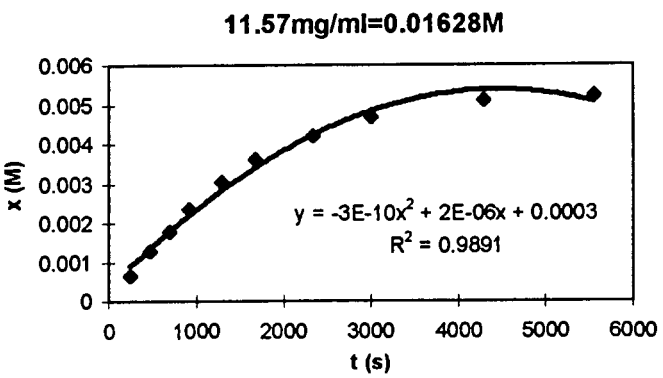

Appendix 1

Figure 1.6 Least-square curves obtained from the ^{1}H NMR results for *cis-trans* isomerisation of $[Pt(H_2L^1)_2Cl_2]$ at an initial concentration of 0.02774M in chloroform-d_3 at 25 °C.

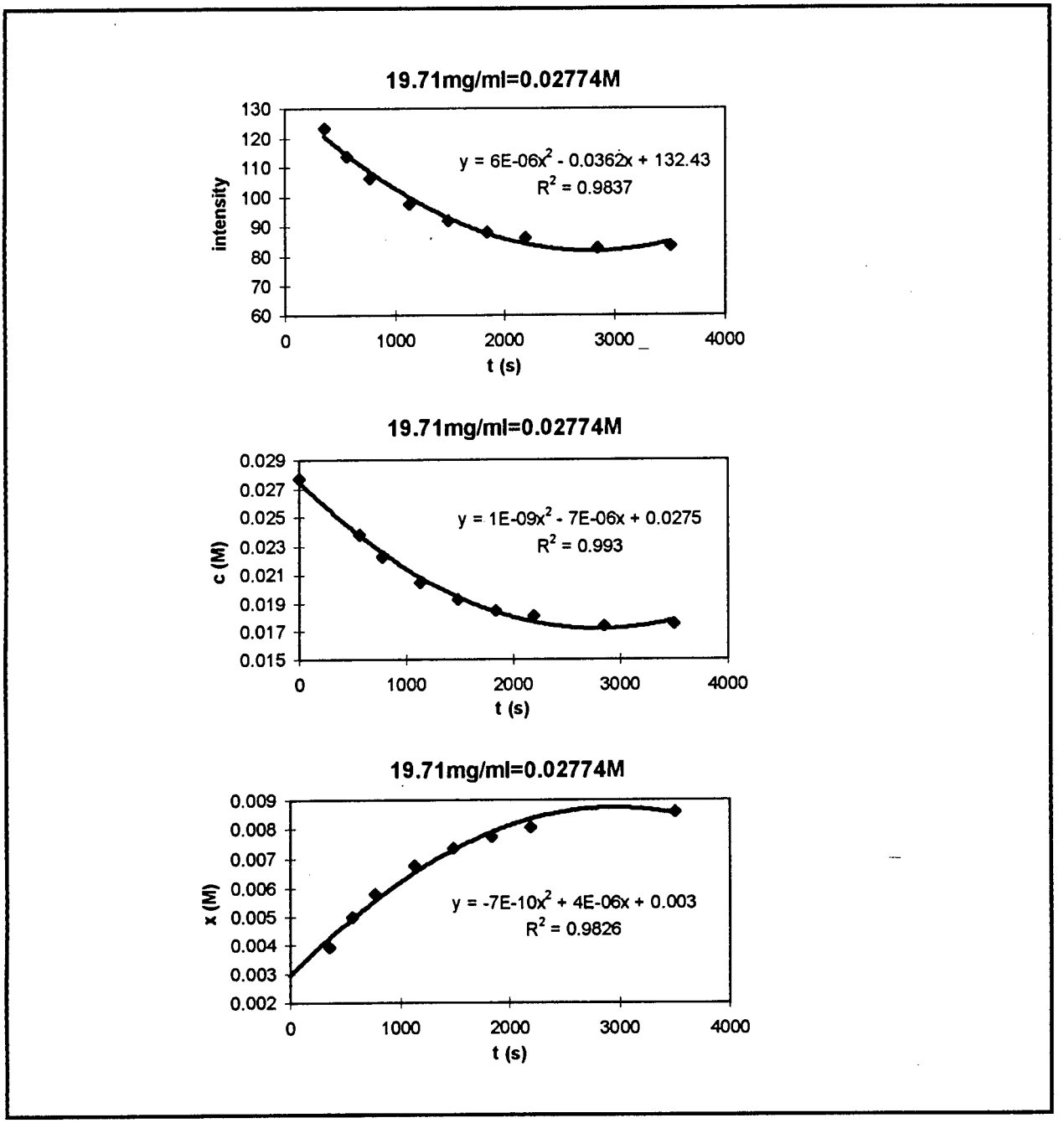

Appendix 1

Figure 1.7 Least-square curves obtained from the ^{1}H NMR results for *cis-trans* isomerisation of $[Pt(H_2L^1)_2Cl_2]$ at an initial concentration of 0.03116M in chloroform-d_3 at 25 °C.

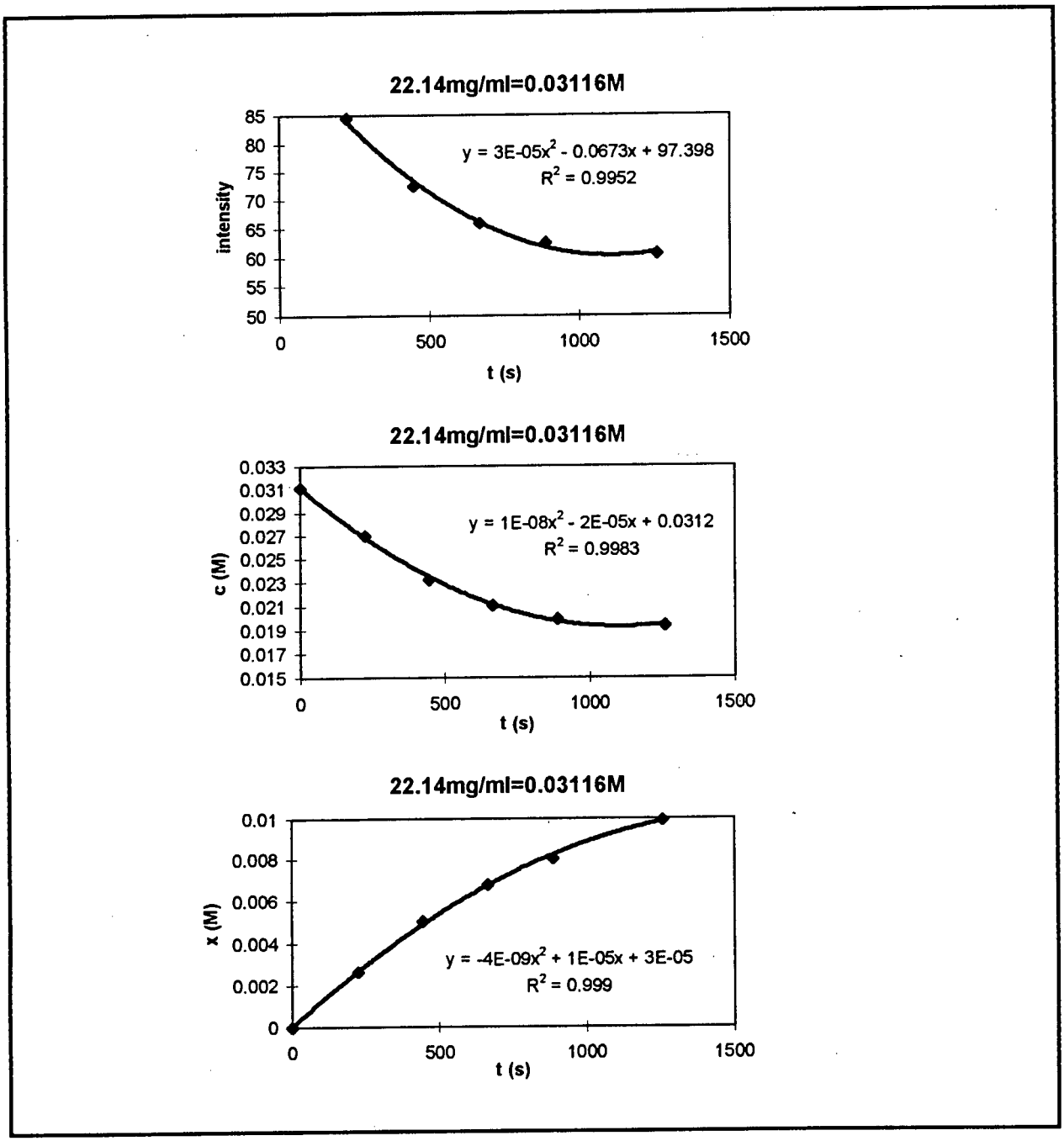

Appendix 1

Figure 1.8 Least-square curves obtained from the ^{1}H NMR results for *cis-trans* isomerisation of $[Pt(H_2L^1)_2Cl_2]$ at an initial concentration of 0.04080M in chloroform-d_3 at 25 °C.

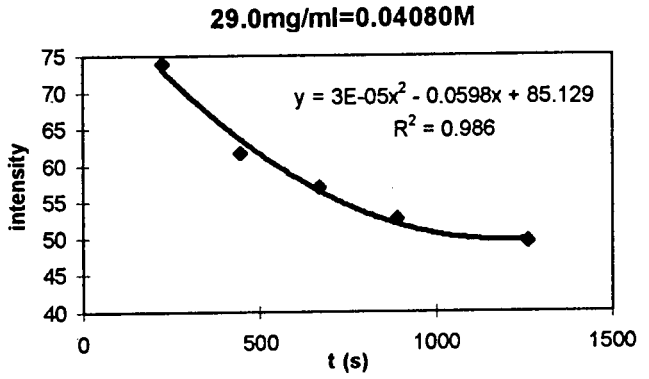

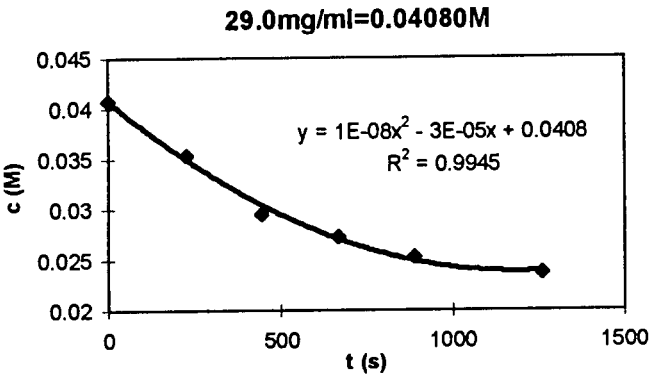

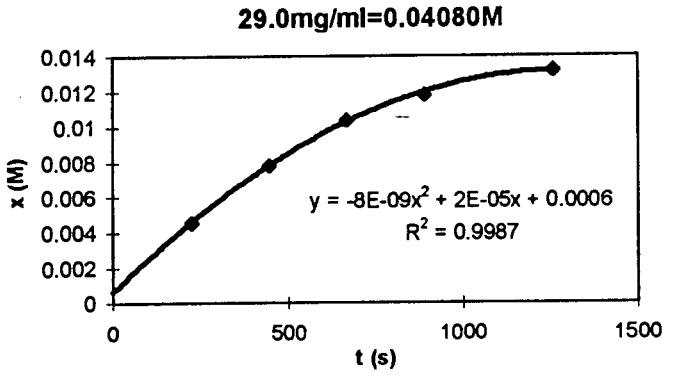

Appendix 1

Figure 1.9 Least-square curves obtained from the ^{1}H NMR results for *cis-trans* isomerisation of $[Pt(H_2L^1)_2Cl_2]$ at an initial concentration of 0.05350M in chloroform-d_3 at 25 °C.

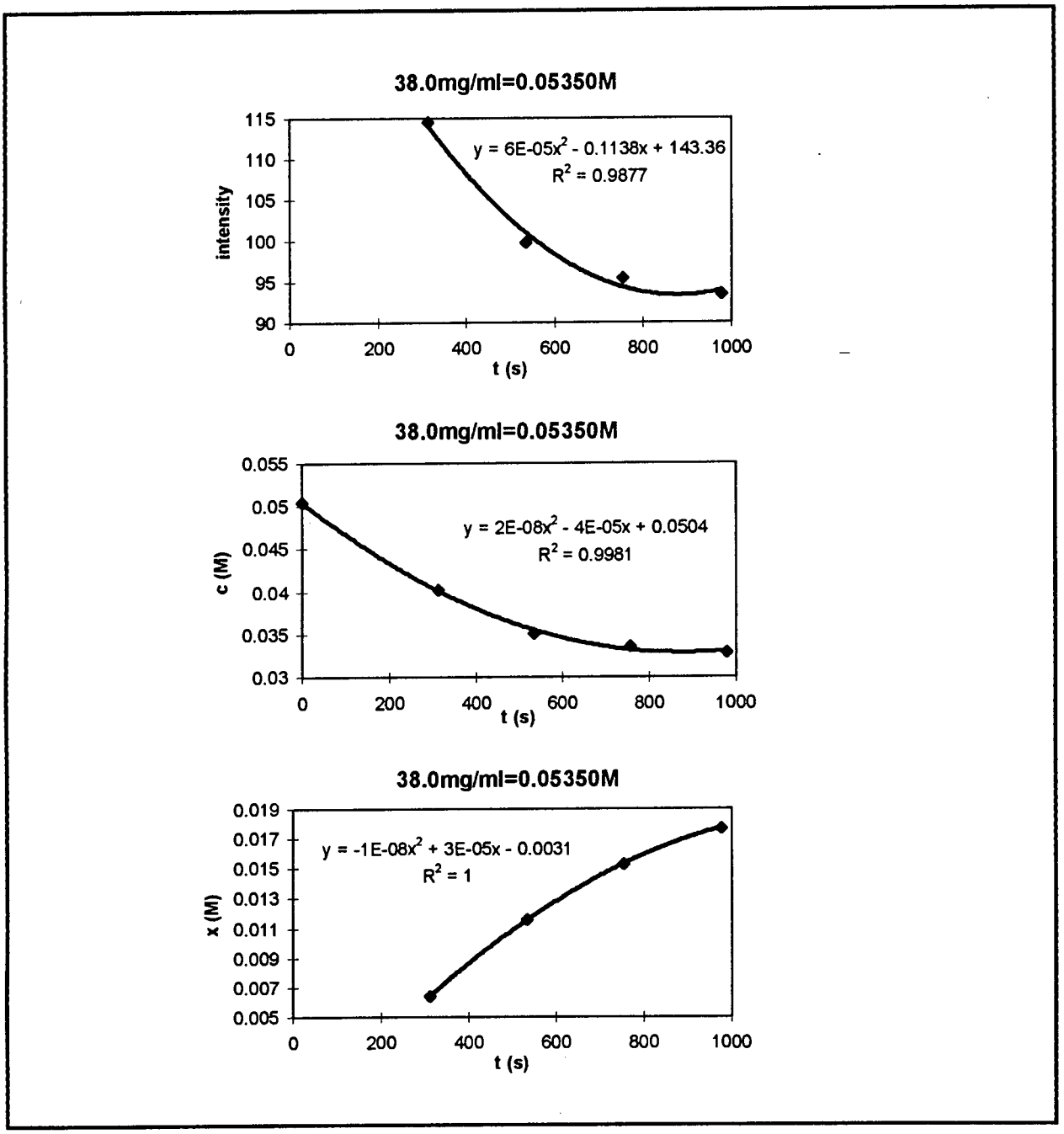

Appendix 1

Figure 1.10 Least-square curves obtained from the ^{1}H NMR results for *cis-trans* isomerisation of $[Pt(H_2L^1)_2Cl_2]$ at an initial concentration of 0.06230M in chloroform-d_3 at 25 °C.

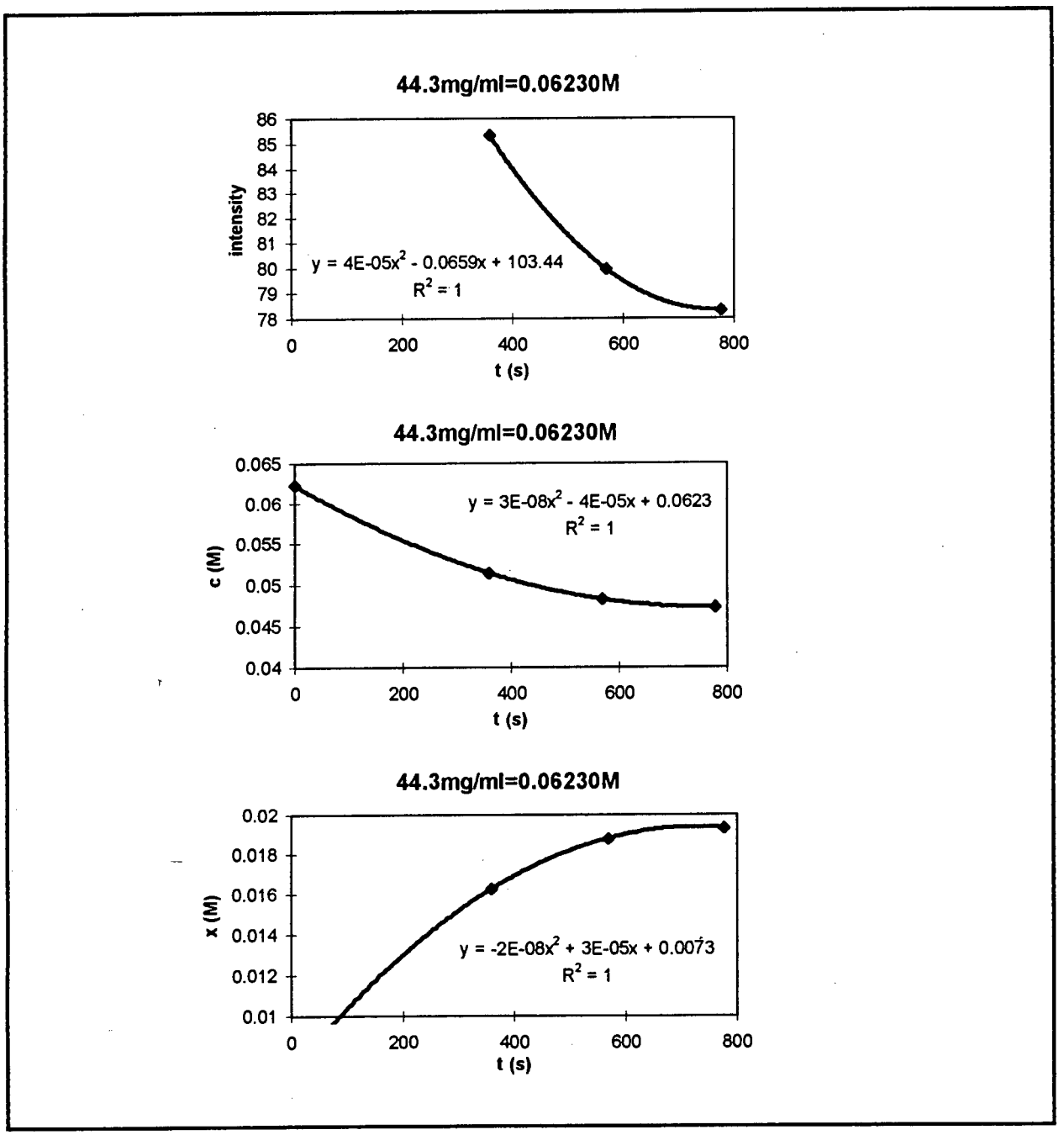

Appendix 2

One of the postulated mechanisms for the *cis-trans* isomerisation of $[Pt(H_2L^1)_2Cl_2]$ can be represented as follow:

$$\begin{cases} cis-[Pt(H_2L^1)_2Cl_2] + cis-[Pt(H_2L^1)_2Cl_2] \underset{k_2}{\overset{k_1}{\rightleftharpoons}} [dimer] + 2\,H_2L^1 & (1) \\ [dimer] + 2\,H_2L^1 \underset{k_4}{\overset{k_3}{\rightleftharpoons}} trans-[Pt(H_2L^1)_2Cl_2] + trans-[Pt(H_2L^1)_2Cl_2] & (2) \end{cases}$$

The product *trans*-$[Pt(H_2L^1)_2Cl_2]$ is produced by reaction (2) and its rate is

$$\frac{d\{trans-[Pt(H_2L^1)_2Cl_2]\}}{dt} = k_3[dimer][H_2L^1]^2 - k_4\{trans-[Pt(H_2L^1)_2Cl_2]\}^2 \qquad (3)$$

We can obtain an expression for $[dimer][H_2L^1]$ in terms of the concentration of the reactant, *cis*-$[Pt(H_2L^1)_2Cl_2]$. Differential equation may be written down for the net rates of appearance of dimer, as follows:

$$\frac{d\{[dimer]\}}{dt} = k_1\{cis-[Pt(H_2L^1)_2Cl_2]\}^2 - k_2[dimer][H_2L^1]^2 + k_3[dimer][H_2L^1]^2 + k_4\{trans-[Pt(H_2L^1)_2Cl_2]\}^2 \qquad (4)$$

If the steady-state assumption is made equation (4) becomes:

$$k_1\{cis-[Pt(H_2L^1)_2Cl_2]\}^2 - k_2[dimer][H_2L^1]^2 + k_3[dimer][H_2L^1]^2 + k_4\{trans-[Pt(H_2L^1)_2Cl_2]\}^2 = 0 \qquad (5)$$

Appendix 2

its solution is:

$$[\text{dimer}][H_2L^1]^2 = \frac{k_1\{cis-[Pt(H_2L^1)_2Cl_2]\}^2 + k_4\{trans-[Pt(H_2L^1)_2Cl_2]\}^2}{k_2 + k_3} \quad (6)$$

From the equation (3) and (6), the rate of the reaction is found to be:

$$\frac{d\{trans-[Pt(H_2L^1)_2Cl_2]\}}{dt} = \frac{k_1k_3}{k_2 + k_3}\{cis-[Pt(H_2L^1)_2Cl_2]\}^2 - \frac{k_2k_4}{k_2 + k_3}\{trans-[Pt(H_2L^1)_2Cl_2]\}^2 \quad (7)$$

i.e.

$$-\frac{d\{cis-[Pt(H_2L^1)_2Cl_2]\}}{dt} = \frac{k_1k_3}{k_2 + k_3}\{cis-[Pt(H_2L^1)_2Cl_2]\}^2 - \frac{k_2k_4}{k_2 + k_3}\{trans-[Pt(H_2L^1)_2Cl_2]\}^2 \quad (8)$$

In another case (chloride ion is lost), the calculation steps of the rate of the reaction are similar to that described above and thus will not be presented here.

Appendix 3

Figure 3.1 Least-square curves of temperature dependence for *cis-trans* isomerisation of $[Pt(H_2L^1)_2Cl_2]$ in benzene and DMF solutions.

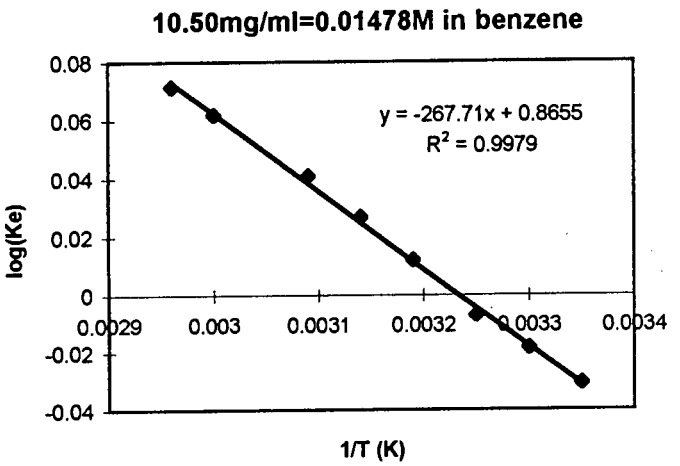

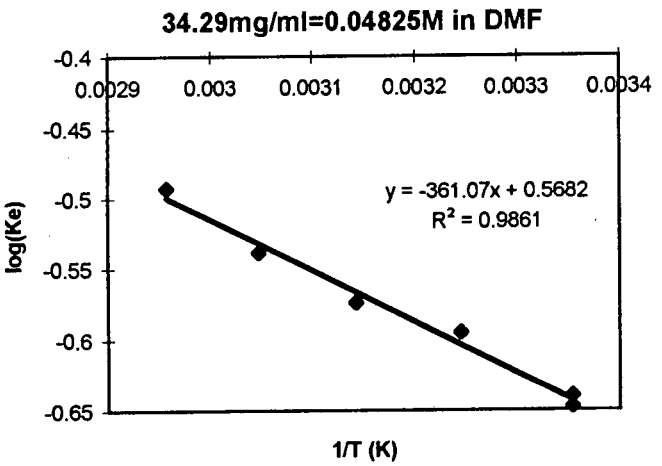

Appendix 4

Table 4.1 Crystal data and structure refinement for *trans*-$[Pd(H_2L^1)_2Br_2]$.

empirical formula	$C_{22}H_{28}Br_2N_4O_2PdS_2$
formula weight	710.84
temperature	293 (2) K
wavelength	0.71069 Å
crystal system	triclinic
space group	P $\bar{1}$
unit cell dimensions	a = 8.768 (1) Å α = 104.034 (8) °
	b = 8.9525 (9) Å β = 113.016 (8) °
	c = 9.8668 (8) Å γ = 99.226 (9) °
volume	662.7 (1) $Å^3$
z	1
density (calculated)	1.781 g/cm^{-3}
absorption coefficient	3.849 mm^{-1}
F (000)	348
crystal size	0.30 × 0.25 × 0.25 mm
theta range for data collection	2.38 to 22.54 deg.
index ranges	-9<=h<=9, -9<=k<=9, -10<=l<=10
reflections collected	1867
independent reflections	1744 [R (int) = 0.0137]
refinement method	full-matrix least-squares on F^2
data / restrains /parameters	1744 / 0 / 163
goodness-of-fit on F^2	1.093
final R indices [I>2sigma (I)]	R1 = 0.0254, wR2 = 0.0724
R indices (all data)	R1 = 0.0306, wR2 = 0.0739
largest diff. peak and hole	0.492 and -0.605 e. $Å^{-3}$

Appendix 4

Table 4.2 Atomic coordinates ($\times 10^4$) and equivalent isotropic displacement parameters ($Å^2 \times 10^3$) for *trans*-[$Pd(H_2L^1)_2Br_2$]. U (eq) is defined as one third of the trace of the orthogonalized uUij tensor.

	x	y	z	U (eq)
Pd	0	0	0	39 (1)
Br	583 (1)	2409 (1)	2139 (1)	55 (1)
S	1394 (1)	1720 (1)	-842 (1)	58 (1)
N(1)	-1267 (4)	410 (4)	-3727 (4)	42 (1)
N(2)	793 (4)	2694 (4)	-3236 (4)	44 (1)
C(1)	247 (5)	1608 (4)	-2712 (4)	40 (1)
C(11)	-2376 (5)	284 (4)	-5225 (4)	40 (1)
C(12)	-4019 (5)	-1052 (4)	-6068 (4)	40 (1)
C(13)	-4533 (5)	-2132 (5)	-5422 (5)	49 (1)
C(14)	-6083 (6)	-3331 (5)	-6298 (5)	58 (1)
C(15)	-7134 (5)	-3441 (6)	-7797 (5)	60 (1)
C(16)	-6648 (6)	-2359 (6)	-8429 (5)	59 (1)
C(17)	-5089 (5)	-1167 (5)	-7582 (5)	52 (1)
O(11)	-2026 (4)	1237 (4)	-5831 (3)	58 (1)
C(21)	2327 (5)	4070 (5)	-2272 (5)	48 (1)
C(22)	2496 (5)	5168 (5)	-3172 (5)	49 (1)
C(23)	4150 (6)	6544 (5)	-2229 (6)	63 (1)

Appendix 4

Table 4.3 Bond lengths (Å) and angles (°) for *trans*-[$Pd(H_2L^1)_2Br_2$].

	bond lengths (Å)		bond angles (°)
Pd-S(A)	2.3164 (10)	S(A)-Pd-S	180.0
Pd-S	2.3164 (10)	S(A)- Pd-Br	94.54 (3)
Pd-Br	2.4415 (5)	S-Pd-Br	85.46 (3)
Pd-Br(A)	2.4415 (5)	S(A)-Pd-Br(A)	85.46 (3)
S-C(1)	1.689 (4)	S-Pd-Br(A)	94.54 (3)
N(1)-C(1)	1.378 (5)	Br-Pd-Br(A)	180.0
N(1)-C(11)	1.379 (5)	C(1)-S-Pd	114.83 (13)
N(2)-C(1)	1.315 (5)	C(1)-N(1)-C(11)	126.9 (3)
N(2)-C(21)	1.460 (5)	C(1)-N(2)-C(21)	123.9 (3)
C(11)-O(11)	1.220 (5)	N(2)-C(1)-N(1)	118.0 (3)
C(11)-C(12)	1.492 (5)	N(2)-C(1)-S	119.8 (3)
C(12)-C(17)	1.386 (5)	N(1)-C(1)-S	122.2 (3)
C(12)-C(13)	1.388 (6)	O(11)-C(11)-N(1)	121.0 (3)
C(13)-C(14)	1.382 (6)	O(11)-C(11)-C(12)	121.4 (3)
C(14)-C(15)	1.371 (6)	N(1)-C(11)-C(12)	117.6 (3)
C(15)-C(16)	1.370 (7)	C(17)-C(12)-C(13)	119.5 (4)
C(16)-C(17)	1.383 (6)	C(17)-C(12)-C(11)	116.2 (4)
C(21)-C(22)	1.502 (6)	C(13)-C(12)-C(11)	124.3 (3)
C(22)-C(23)	1.517 (6)	C(14)-C(13)-C(12)	120.1 (4)
		C(15)-C(14)-C(13)	120.2 (4)
		C(16)-C(15)-C(14)	119.9 (4)
		C(15)-C(16)-C(17)	120.8 (4)
		C(16)-C(17)-C(12)	119.5 (4)
		N(2)-C(21)-C(22)	110.7 (3)
		C(21)-C(22)-C(23)	111.5 (4)

Symmetry transformations used to generate equivalent atoms: A -x, -y, -z